Role of pax7 in the development and regeneration of muscle satellite cells in Xenopus laevis

Chen, Ying

Award date:
2007

Awarding institution:
University of Bath

Role of pax7 in the Development and Regeneration of Muscle Satellite Cells in *Xenopus laevis*

Ying CHEN

A thesis submitted for the degree of Doctor of Philosophy

University of Bath

Department of Biology and Biochemistry

December 2007

Copyright

ProQuest LLC
789 East Eisenhower Parkway
P.O. Box 1346
Ann Arbor, MI 48106-1346

Table of Contents

List of Tables and Figures

Acknowledgements

I gratefully acknowledge my supervisor, Professor Jonathan Slack, for his able guidance throughout my PhD study. His suggestions and encouragement were indispensable to the completion of my thesis.

I am indebted to Dr. Bea Christen, Dr. Ian Jones, Mrs Ursula Potter, Dr. James Dutton, Dr. Wan-Chun Li, and Dr. Jimmy Susanto for their discussions and technical support during my study. Thanks to the rest of the people in Room 0.62 who create a convivial place to work. I also would like to thank Dr. Momna Hejmadi who has given me valuable advice during my demonstration work and Chris Apark for husbandry of *Xenopus laevis*.

My special gratitude goes to my parents and my husband, who have been giving me love and support throughout my life. I know it would impossible to finish my PhD study without their encouragement and understanding.

Lastly, I would like to thank the Department of Biology and Biochemistry in the University of Bath for providing my studentship throughout my PhD study.

List of Abbreviations

CMV	Cytomegalovirus
CSF	Crude Cytostatic Factor
DSHB	Developmental Studies Hybridoma Bank
EnR	Engrailed Repression domain
GFP	Green Fluorescent Protein
hCG	human Chorionic Gonadotropin
HGEM	Heat-shock Green-Eyed Monster
HGF	Hepatocyte Growth Factor
HSPG	Heparan Sulfate Proteoglycan
IEM	Immuno-Electron Microscopy
IRF	Interferon Regulatory Factor
MAB	Maleic Acid Buffer
MMR	Marc's Modified Ringers
MRF	Myogenic Regulatory Factor
NAM	Normal Amphibian Medium
NCAM	Neural Cell Adhesion Molecule
NF	Nieuwkoop and Faber
NPB	Nuclear Preparation Buffer
nucGFP	nuclear Green Fluorescent Protein
Pax	Paired-box
PBSA	Phosphate Buffered Saline Dulbecco A
PMSG	Pregnant Mare Serum Gonadotropin
RDA	Rhodamine Dextran Amine

REMI	Restriction Enzyme Mediated Integration
TGFbeta	Transforming Growth Factor beta
TNF	Tumor Necrosis Factor
VCAM	Vascular Cell Adhesion Molecule
WISH	Whole-mount In Situ Hybridization
XB	Extraction Buffer

Abstract

Muscle satellite cells are a population of undifferentiated mononuclear myogenic progenitor cells. The aim of this study was to explore the developmental origin of satellite cells in *Xenopus laevis* embryos and identify the function of *Xenopus* pax7, a reliable marker of *Xenopus* satellite cells, in satellite cell development and muscle regeneration.

By orthotopic grafting and transgenic technique, we found that a region of mesoderm about 100 μm wide, located 100 μm lateral to the dorsal midline of a stage15 embryo, could give rise to muscle satellite cells. Moreover, *pax7* mRNA was expressed in this zone at stage 15.

To test whether pax7 is able to specify the muscle satellite cell lineage, we over-expressed *pax7* and inhibited pax7 function using *pax7EnR* (encoding a dominant negative form of pax7). This was done by RNA injection of 32-cell stage embryos. The results showed that *pax7* was able ectopically to induce expression of *myf5* and *pax3*. But injection of *pax7* or *pax7EnR* did not affect the number of muscle satellite in tadpole tails. So pax7 alone is not sufficient to specify the lineage of muscle satellite cells in *Xenopus laevis*.

The tails of *Xenopus* tadpole will regenerate after amputation. To gain insight of the function of pax7 in *Xenopus* tadpole tail regeneration, we generated transgenic tadpoles containing *pax7EnR* driven by a heat-inducible promoter. When induced, it reduced the number of muscle satellite cells formed in the regenerates by increasing their rate of cell death. A second amputation of the resulting tails yielded second regenerates containing spinal cord and

notochord but little or no muscle. These results demonstrated that pax7 was required for the survival of the proliferating satellite cells in muscle and hence the formation of new muscle during regeneration.

I. Introduction

I.1 *Xenopus* as a laboratory model system

The African clawed frog, *Xenopus laevis*, is a gentle, freshwater anuran amphibian. Used as a model organism for several decades, it has many advantages for experimental work. The female adult *Xenopus* can be induced to spawn repeatedly by simple hormone injection. By means of *in vitro* fertilization, we can easily obtain hundreds of *Xenopus laevis* embryos of synchronized developmental stage, which are then able to develop normally *in vitro*. Thus we can easily get access to embryos at all developmental stages. *Xenopus* embryos are comparatively large (about 1.4 mm in diameter) and robust. Biologists take advantage of these features to manipulate the embryos, for instances, by microinjecting genes of interest or grafting a small piece of tissue, at a very early stage and observing the consequences at later stages.

Another advantage of working with *Xenopus laevis* is that we have a complete fate map of the embryo (Dale and Slack, 1987; Lane and Sheets, 2002; Moody, 1987). Based on this fate map, we can target a particular tissue or region by injecting materials of interest to a specific blastomere in the early embryo, while leaving the other parts of the body unaffected. This flexibility helps us identify a gene's function in a tissue specific context.

Due to its ease of access and microsurgical manipulation, *Xenopus laevis* has been a standard laboratory model organism for studying early developmental events, such as dorsal-ventral patterning and mesoderm induction (Slack,

2006). In this system, we now have a set of fully developed gene delivery techniques, an inventory of cDNA libraries of different stages, a pool of gene probes and an increasing number of transgenic *Xenopus* lines.

However, *Xenopus laevis* is pseudotetraploid, which means it is not suitable for gene mutation screens or gene knockout analysis. Fortunately, this can be overcome by using *Xenopus tropicalis*. *Xenopus tropicalis* is a diploid with complete genome sequence available. Moreover, most of the normal techniques work with *Xenopus tropicalis* and the sequence divergence between the two species is low enough to enable us to use a probe from one species to hybridize with its homologue gene from the other species. Therefore, we can flexibly use these two species for different purposes.

I.2 *Xenopus* tadpole as a model for regeneration research

Recently, *Xenopus* tadpoles have emerged as a popular laboratory model for regeneration research. *Xenopus* tadpoles can fully restore their missing tails with three main axial structures, the spinal cord, the notochord and the myotomes (Slack et al., 2007). Regeneration never occurs when the main bodies of tadpoles are transected, although they contain the same axial structures as their tails do. Tadpole limb buds will regenerate nicely after amputation at the early stages and then this ability is lost at later stages (Dent, 1962). Although these regeneration behaviours are not new to scientists, only in the last few years that the *Xenopus* tadpole model has re-attracted scientists' attention.

This is mainly because of the development of transgenic techniques in *Xenopus*, which enables scientists to investigate regeneration at molecular levels (Amaya and Kroll, 1999). This gene delivery method is especially useful to study the function of a transgene at later stages, as the transgene is integrated so, unlike injected mRNA, it will not disappear at the tadpole stage. To avoid possible developmental defects in early transgenic embryos, Beck et.al have used a heat shock promoter to induce expression of transgenes only during tail regeneration (Beck et al., 2003). Cre-lox and Gal4 systems have also been adapted to *Xenopus* system, which allows us to activate a transgene in a tissue specific context during regeneration (Gargioli and Slack, 2004; Hartley et al., 2002; Ryffel et al., 2003). As a result, more and more *Xenopus* transgenic lines are available. Using the transgenic lines, we can further investigate gene activities or signalling pathways required in regeneration.

Another advantage of using this regeneration model is that we have already had a profound knowledge of the early developmental progress of *Xenopus* embryos. Regeneration has long been believed to recapitulate the process of embryonic development. Therefore, we can take advantage of the available knowledge regarding *Xenopus* early development to further understand cellular and molecular mechanisms of regeneration.

Our lab has been studying regeneration using *Xenopus* tadpoles for several years. We now know a couple of signals involved in the tadpole tail regeneration and cellular sources of main axial structures in regenerated tails.

My project is based on these findings to study muscle regeneration in regenerating tadpole tails.

I.3 Tails of *Xenopus laevis* tadpoles

The tail is defined as a region posterior to the proctodeum (the caudal opening of the digestive tract). It is a major part of the body in most vertebrates. Tails of *Xenopus* tadpoles, like all the other tails of vertebrates at embryonic stages, consist a caudal extension of the main axial structures: spinal cord, notochord, muscle, dorsal aorta and caudal vein. As water-dwelling tadpoles, they need their tails for locomotion.

I.3.1 Tail development in *Xenopus laevis* embryos

A fate map study shows that the *Xenopus* tadpole tail arises from a tail-forming region in neurula stage embryos (Tucker and Slack, 1995). The tail-forming region is a rectangle 700 μm wide by 600 μm long, 100 μm anterior to the base of the proctodeum at the mid-late neurula stage. This 'standard rectangle' extends as the embryo develops and eventually makes up the whole of the axial component of the tail of a stage 40 embryo. The fate map study altered a longstanding conception that vertebrate tails are derived only from the tail bud, which is a region of undifferentiated cells at the posterior extreme of embryos (Griffith et al., 1992; Holmdahl, 1939). Actually about the anterior two thirds of the *Xenopus* tadpole tail is derived from the posterior trunk tissue as a result of an anterior movement of the proctodeum during body extension. Only the distal one third of the tail arises from the tail bud (Tucker and Slack, 1995). Those trunk cells constitute most of the tail-forming region. So it is tempting to know why the trunk cells in the tadpole tails can

regenerate, whereas those in main body region cannot.

I.3.2 Tail regeneration of *Xenopus* tadpoles

After amputation, the *Xenopus* tadpole tail will regenerate within three weeks. Like other regeneration process, the tadpole tail regeneration proceeds in three phases.

The first phase, within 24 hours after tail amputation, is a wound healing process in which the amputated surface is covered by a specialised wound epithelium that lacks an underlying dermis and basement membrane (Neufeld and Day, 1996; Tschumi, 1957). Following wound healing, cell proliferation and migration dominate in the second phase of tail regeneration. As a result of the cell divisions and continuous cell migration to the wound site, a bud is noticeable growing from the amputated surface. In terms of nomenclature, we call this structure a regeneration bud, rather than a blastema which refers to a region of undifferentiated cells typically present in limb regeneration. The final phase is growth of the regeneration bud. At this stage, the new tail grows much faster than normal, and then form a well-structured tail similar to its original.

I.3.3 Cell lineage tracing in tadpole tail regeneration

Understanding the cellular origin of each regenerating appendage in amphibian tails is of great importance in gaining insight into cell therapies of damaged tissues of human beings. Studies on urodele tail and limb regeneration show evidence of cell de-differentiation and metaplasia which means a conversion of a differentiated cell type to another regardless of

pathway or mechanism (Echeverri et al., 2001; Echeverri and Tanaka, 2002; Lo et al., 1993; Tosh and Slack, 2002). During limb regeneration in newts, multinucleated myotubes or myofibres de-differentiate, re-enter cell cycle, and then undergo conversion to mononucleated cells (Brockes and Kumar, 2002). These cells entered the undifferentiated blastema of the limb and some can even differentiate into other tissue types, such as cartilage (Kumar et al., 2000; Lo et al., 1993). Another example of metaplasia was observed in axolotl tail regeneration. During regeneration, radial glial cells of the axolotl spinal cord were able to give rise to cell types of both ectodermal and mesodermal origin (Echeverri and Tanaka, 2002).

However, neither of these processes occurs in the tail regeneration of the anuran *Xenopus* tadpoles. A cell lineage tracing study in the tadpole tail regeneration showed that each of the three main tissues (the spinal cord, the notochord and the myofibres) behaves independently, which means they regenerate from their respective specialised cell types (Gargioli and Slack, 2004).

Three days after tail amputation, the regeneration bud is clearly visible. Its sagittal sections show that the original spinal cord closes off and forms a neural ampulla (Fig.1.1A and B)(Stefanelli, 1951). The notochord terminates with a bullet-shaped mass of cells in continuity with the sheath of the more proximal tissue (Fig.1.1A and C). Myofibres in the vicinity of the cut surface appear to degenerate with large amounts of cellular debris (Fig.1.1A). In addition, a mass of undifferentiated cells accumulates in a ring around the neural ampulla and notochord tip, which is called as a 'blastema'.

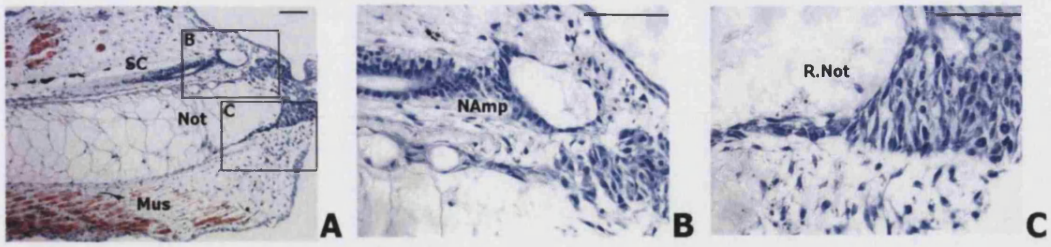

Figure 1.1 Morphology of a 3-day regenerating tail in *Xenopus* tadpoles

(A) Longitudinal section immunostained with 12/101 mAb (pink) and conterstained with Haematoxylin (blue). (B) Enlarged view of boxed area in A, showing details of the neural ampulla. (C) Enlarged view showing the regenerating notochord. Not: notochord, Mus: muscle, NAmp: neural ampulla, R. Not: regenerating notochord. Scale bar: 100μm. (Reprint from Gargioli and Slack 2004, with permission).

Cesare Gargioli, a previous student in our lab, labelled the three different types of tissues (the spinal cord, the notochord and the muscle) within the tail by grafting explants of either neural plate, or notochord, or presomitic mesoderm, from CMV-GFP transgenic neurulae, into the presumptive tail region of wild type host embryos (Gargioli and Slack, 2004). The resulting host tail will have one tissue type labelled with GFP. The CMV promoter remains active in all the tissue types of tails, so after the tail is amputated through the graft, a labelled cell should still express GFP even if it de-differentiates or re-differentiates into the same or a different tissue type.

Five days after tail amputation, the GFP expression was observed solely within the reforming spinal cord and notochord in each tissue specific type of grafting (Gargioli and Slack, 2004). The blastema and other tissue types are all negative for GFP expression until the tail fully regenerated.

Since the labelled cells are restricted to the ventral part of the spinal cord, Lin

et.al conducted a whole spinal cord grafting at tadpole stage to find what happens to all the cells of the spinal cord, especially cells on the dorsal side, during regeneration. This showed that about 0.5mm of the CMV-GFP labelled spinal cord populates the whole reforming spinal cord, and that the regenerated spinal cord stems from the spinal tissue within this extent. The regenerated spinal cord contains both neural fibre tracts and neurons, of both motor and sensory types. But it lacks the dorsal root ganglias which are normally situated in a ventrolateral position of the spinal cord and contains sensory neurons and glial cells. Most importantly, no labelled cells within the spinal cords were observed in other tissue type until the tails fully regenerate (Lin et al., 2007). Thus, these evidences demonstrate that the two major tissues of tail, the spinal cord and the notochord, regenerate from their own tissue types.

The presomitic mesoderm grafting performed by Cesare Gargioli could label a subset of myofibres within the tail rather than whole myotomes. He found that unlike the situations in the spinal cord and notochord regeneration, myofibres in the regenerates were rarely labelled with GFP. As we explained before, a labelled cell should still express GFP even if it de-differentiates or re-differentiates into the same or a different tissue type. However, in many cases, GFP are not expressed at all in regenerated tails. It was found that the presence of GFP labelled myofibres in the regenerates relies on the grafts from specific position of presomitic mesoderm. If the grafts are taken from a more lateral region of presomitic mesoderm, the regenerating tails are more likely to contain GFP labelled myofibres.

This experiment firstly suggests that no de-differentiation takes places in *Xenopus* muscle regeneration; otherwise we would observe GFP expression in newly formed myofibres from amputations through regions containing labeled myofibres. Secondly, it indicates that some other type of cells rather than myofibres must be the precursor cells for the regenerated muscle in the tadpole tail regeneration.

In principle three possibilities have been proposed for the origin of regenerated muscle: de-differentiation of myofibres, muscle satellite cells and various of non-muscle stem cells such as bone marrow cells and side population (SP) cells. During regeneration of the limbs of urodele amphibians (newts and salamanders) it has been well documented that the striated muscle fibres can de-differentiate (Echeverri et al., 2001; Kumar et al., 2000; Lo et al., 1993; Namenwirth, 1974). In this process the nuclei of the myofibres re-enter S-phase and the fibres break apart to become mononuclear cells. These cells then participate in the regeneration blastema, proliferate, and eventually become re-differentiated, mostly as new myofibres, but also as some other tissue types. However, the results described above indicate that de-differentiation of myofibres does not occur in anuran tail regeneration (Gargioli and Slack, 2004). In postnatal mammals there is no regeneration of appendages such as limbs or tails. However striated muscle does have some ability to repair itself following tissue damage. In this process the new fibres are generally considered to be derived from muscle satellite cells: a population of small mononuclear cells located beneath the basement membrane of the myofibres (Seale and Rudnicki, 2000). Muscle satellite cells

can be considered as a type of adult stem cell as they are able both to reproduce themselves and to produce myoblasts, which can differentiate to form new myofibres. However, this idea has been challenged because in skeletal muscle, there also exist some putative non-muscle stem cells. The exact typology of these cells is unclear but some are probably bone marrow-derived, some are described as mesoangioblasts which are vessel-associated stem cells, and some are the CD45 positive side population (SP) cells that can be recognized by exclusion of a DNA-binding Hoechst (33342) dye (Gussoni et al., 1999; Jackson et al., 1999; Seale et al., 2001). All these cells have also been shown under certain circumstances to be able to adopt the myogenic lineage and to participate in muscle repair.

On the basis of the labelling patterns from different types of the presomitic mesoderm graft, it was conjectured that satellite cells might be the precursors of the striated muscle of the regenerate (Gargioli and Slack, 2004).

I.4 Muscle satellite cells

I.4.1 Identification of muscle satellite cells

Muscle satellite cells are a population of undifferentiated mononuclear myogenic progenitor cells. They were actually first discovered in frogs, visualised by electron microscopy as mononucleated cells wedged between the basement membrane and the plasma membrane of myofibres (Fig.1.2) (Mauro, 1961). Later on the muscle satellite cells were also found in skeletal muscles of mammals and birds (Campion et al., 1981a; Campion et al., 1981b; Gamble et al., 1978; Hartley et al., 1992). Morphologically, the satellite cell is characterized by an increased nuclear-to-cytoplasmic ratio and reduced

organelle content. Its nucleus contains abundant heterochromatin that is shown by the black nuclear staining under electron microscope (Fig.1.2). These characteristics are consistent with the fact that the satellite cells are mitotically quiescent and transcriptionally less active than myonuclei (Schultz et al., 1978; Snow, 1983).

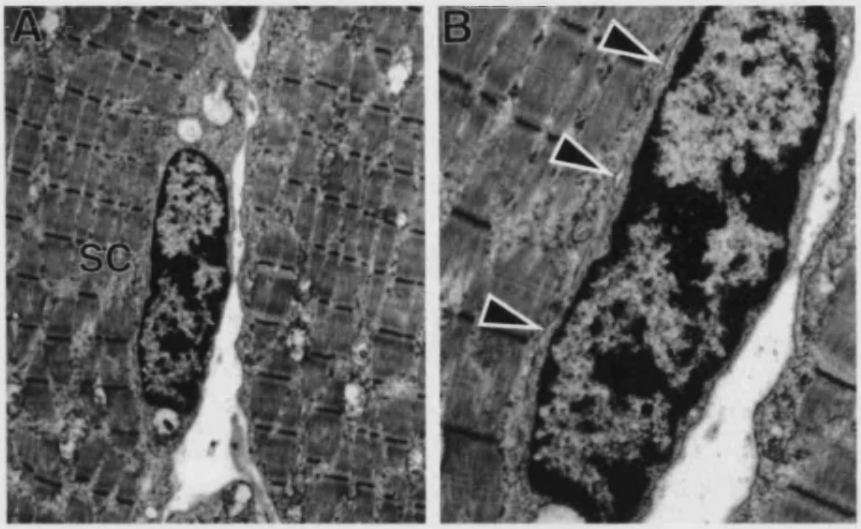

Figure 1.2 Transmission electron micrograph of a muscle satellite cell.

(A) A satellite cell at 7500X magnification. (B) High magnification of A shows the plasma membrane (black arrowheads) separating the satellite cell from its adjacent myofire, the continuous basal lamina surrounding the satellite cell and myofibre, and the heterochromatic appearance of the nucleus (20,000X). (Reprint from Seale et. al., 2000, with copyright license number 1852781345660).

However, these features disappear following the activation and proliferation of the satellite cells in response to muscle growth or regeneration. The activated satellite cells will swell on the myofibre, followed by an increase in the cytoplasmic volume. In addition, the amount of heterochromatin decreases and organelles, such as the Golgi, endoplasmic reticulum, ribosomes, and

mitochondria become apparent (Schultz and McCormick, 1994). These morphological criteria enable us to distinguish the quiescent satellite cells and the activated ones.

I.4.2 Role of muscle satellite cells

Since the discovery of the satellite cell in 1960s, scientists have long been studying its role during development. At a conference on regeneration of striated muscle and myogenesis in 1969, Milhorat associated the satellite cells with the myogenic progenitor cells for the first time (Milhorat, 1970). He concluded from several studies that the satellite cells represent reserve myoblasts that could fuse to form multinucleated muscle fibres. However, the role of satellite cells as myogenic precursor cells was still not appreciated at that time. Most scientists thought that myofibres themselves could fragment into undifferentiated blastema cells and then re-form a new myofibre. Even now, there is still controversy about the cellular origin of regenerated muscle in urodele amphibians, in which de-differentiated myofibres re-forming new fibres or the satellite cells constituting newly formed muscle are both observed (Carlson, 2003; Morrison et al., 2006).

In 1970s, Charles Leblond's group showed by a time-course study that satellite cells were the only cell type incorporated [^{3}H]-thymidine in growing rat muscle (Moss and Leblond, 1970; Moss and Leblond, 1971). Because the differentiated myonuclei are not capable of dividing, it ruled out the possibility that the myonuclei give rise to the increasing number of new myonuclei during mammalian muscle growth. Since then, the role of muscle satellite cells has

been established to be as myogenic precursor cells that proliferate and fuse to form new skeletal muscle fibres.

This finding is of much scientific and clinical interest. The muscle satellite cells are thought to be a major cell source of postnatal growth and regeneration of skeletal muscle. During postnatal muscle growth, the satellite cells proliferate and contribute to the expansion of myofibres. In mature muscles, satellite cells are normally quiescent, but they can be activated as needed following subtle or massive muscle trauma. Once activated, the quiescent satellite cells re-enter the cell cycle. During muscle regeneration, if muscle damage is minimal, progeny of the satellite cells will fuse to existing damaged fibres. Upon massive damage, they align with each other and fuse to form new myofibres (Cooper et al., 1999; Cornelison and Wold, 1997).

I.4.3 Molecular markers of muscle satellite cells

Studying cellular and molecular regulation of muscle satellite cells during regeneration requires an easy identification method of this population *in vivo*. However, the traditional method using electron microscopy hindered studies of this population because it involves a lot of of preparation work and it is often incompatible with other techniques. Therefore, in the past decade scientists have identified many molecular markers specific to muscle satellite cells in muscles and also developed various specific antibodies. Based on the antibody staining signals, we can easily observe muscle satellite cells under the light microscope, which greatly streamlines the detection procedure. Moreover, these identified molecular markers provide us with some clues of possible pathways regulating satellite cell behaviour during muscle

regeneration.

We may classify these molecules into two types: the transcription factor markers and the cell surface markers. The transcription factors include MNF(Myocyte Nuclear Factor), myf5, pax3, and pax7 (Beauchamp et al., 2000; Cornelison and Wold, 1997; Garry et al., 1997; Relaix et al., 2005; Seale et al., 2000). The surface markers are CD34, c-met, m-cadherin, NCAM (Neural Cell Adhesion Molecule), syndecan-3, syndecan-4,VCAM-1(Vascular Cell adhesion Molecule-1) and Glycoprotein Leu-19 (Beauchamp et al., 2000; Cornelison et al., 2001; Cornelison and Wold, 1997; Illa et al., 1992; Maier and Bornemann, 2004; Rosen et al., 1992; Schubert et al., 1989; Tatsumi et al., 1998). Almost all of these molecules were discovered in mammalian systems. Some of their homologues are also found specific in avian muscle satellite cells, such as pax3 and pax7 (Otto et al., 2006).

I.4.3.1 MNF

MNF (Myocyte nuclear factor), a member of the *forkhead* wingled helix transcription factor family, has two isoforms that display reciprocal expression profiles in muscle satellite cells (Garry et al., 1997). MNF-alpha is expressed in activated muscle satellite cells, whereas MNF-beta predominates in quiescent satellite cells and is downregulated upon activation. Studies with mice lacking both isoforms reveal that they are not required for correct patterning of skeletal muscle during embryonic and fetal stages. But the function of muscle satellite cells during muscle regeneration is disturbed in regard to the timing of expression of myogenic regulatory genes and cell cycle genes, which result in impairment of skeletal muscle regeneration (Garry et

al., 2000). The distinct functions of the two isoforms have not been identified. Yang et.al reported that MNF-beta can form a transcriptionally repressive complex with a mammalian sin3 family member (Yang et al., 2000). The reciprocal expression pattern of MNF-alpha and MNF-beta suggests that they may coordinate the timing of their expression by repressing each other at different stages. A detailed functional study of these two isoforms may provide insight into the molecular regulation of satellite cell activation and subsequent self-renewal process.

I.4.3.2 pax3 and pax7

Pax7, a paired box transcription factor, was isolated as a gene expressed both in quiescent and activated satellite cells by representational difference analysis (Seale et al., 2000). In addition, pax7 expression is not detectable in non-myogenic cell lineages of mouse adults (Seale et al., 2000). Because of its unique expression pattern, pax7 has become the most widely used satellite cell marker among all the identified ones. Recently, pax3, a paralogue of pax7, which is essential for the delamination and migration of the somitic muscle progenitor cells to the limb bud, was also found to be expressed in quiescent satellite cells (Relaix et al., 2005). However, unlike pax7, pax3 expression in satellite cells is mostly down-regulated before birth, although a subset of satellite cells appear to express pax3 (Kassar-Duchossoy et al., 2005; Montarras et al., 2005; Relaix et al., 2005). Moreover, some pax3 expressing cells were identified locating in interstitial environment outside the basal lamina of muscle fibres (Kuang et al., 2006). Given these, pax7 is more suitable to label adult satellite cell lineage than pax3.

I.4.3.3 CD34 and VCAM-1

CD34 is a highly O-glycosylated transmembrane sialomucin, which is often clinically used as a marker of adult hematopoietic stem cells and early blood progenitors (Gangenahalli et al., 2006). Intriguingly, *CD34* transcripts were detectable in skeletal muscle at the stage when the satellite cells appear and recently its expression in the satellite cells was confirmed by antibody staining(Beauchamp et al., 2000; Cossu et al., 1983). But not all of the satellite cells are CD34 positive, suggesting that the muscle satellite cell at least has two subpopulations, CD34 positive and CD34 negative. Moreover, its expression in satellite cells is associated with quiescent and activated states, which means CD34 transcripts are not detectable once myogenic cells differentiate (Beauchamp et al., 2000). It is also not expressed in somites during primary myogenesis, demonstrating the myogenic lineage commitment is CD34 independent. Given these, scientists speculate that some of the satellite cells may come from primordial endothelial cells that maintain CD34 expression and incorporate into skeletal muscle via blood circulation. Interestingly, VCAM-1, another vascular-endothelial marker, is expressed in the muscle satellite cells as well.

VCAM-1 is a member of the immunoglobulin gene superfamily (Osborn et al., 1989). Apart from its expression on the cell surface of endothelial cells, VCAM-1, like CD34, is expressed on the cell surface of quiescent and activated satellite cells *in vivo* (Jesse et al., 1998). An *in vitro* cell culture study shows that VCAM-1 is able to mediate cell-cell interactions by binding to its ligand, alpha4beta1 or IRF-2 (Jesse et al., 1998). One feature of muscle

regeneration is the influx of a large amount of alpha4beta1 or IRF-2 positive leukocytes into injury site in response to muscle damage. So it is highly possible that the interaction of VCAM-1 positive satellite cells and infiltrating leukocytes triggers recruitment of cytokines that are required for satellite cell activation and proliferation.

I.4.3.4 c-met

The *c-met* gene encodes the receptor tyrosine kinase of hepatocyte growth factor (HGF), which is an important factor involved in organ regeneration through its mitogenic and motogenic properties(Conway et al., 2006). A single cell PCR assay first demonstrated that c-met is expressed in quiescent satellite cells regardless of muscle type (Cornelison and Wold, 1997). But its expression is not restricted to the quiescent population. High levels of c-met expression are found in mononuclear cells surrounding necrotic myofibres during the early phase of muscle regeneration, showing that it is also required for activation and proliferation of muscle satellite cells(Gille et al., 1998). In addition, c-met has been implicated in mediating satellite cell migration to the site of muscle injury (Suzuki et al., 2000).

I.4.3.5 syndecan-3 and syndecan-4

Syndecans are cell surface transmembrane heparan sulfate proteoglycans (HSPGs) (Rapraeger, 2000). The syndecan family contains four members (syndecan-1–4) in mammals, which are highly conserved at the protein level in the transmembrane and intracellular domains but divergent in their extracellular domains. Among these, only syndecan-3 and syndecan-4 are

expressed in adult muscle satellite cells (Cornelison et al., 2001). They act as co-receptors to transduce FGF or HGF signalling by forming a ternary complex of syndecan, FGFr/c-met and FGF/HGF (Rapraeger, 2000). A closer examination demonstrates that their expression overlaps with expression of c-met both in quiescent and activated satellite cells. But syndecan-3 and syndecan-4 have separate roles in satellite cells. *Syndecan-3* null satellite cells resemble wild type but there is a greatly increased number of satellite cells and myonuclei in *syndecan-3* -/-mice, indicating a potential inhibitory role in regulating the number of the activated satellite cells and differentiated muscle. However, *syndecan-4* null satellite cells are much more severely impaired than the *syndecan-3* null cells, since the *syndecan-4* null satellite cells are deficient in activation, proliferation and differentiation during muscle regeneration (Cornelison et al., 2004). The different behavior of *syndecan-3* -/- and *syndecan-4* -/- satellite cells shows that individual syndecans are differentially required for binding and transducing different growth factor *in vivo*. Further identification of specific ligands and receptors binding individual syndecans will provide insight into the singalling pathways that are integral to satellite cell activation and proliferation.

I.4.3.6 NCAM

Neural Cell Adhesion Molecule (NCAM), a calcium-independent adhesion molecule of the immunoglobulin superfamily, is expressed on the surface of neurons, glia, skeletal muscle and natural killer cells(Peck and Walsh, 1993). During muscle development, NCAM plays important role in mediating myotube formation, muscle innervation and muscle-nerve interaction in the

early stages and disappears as development proceeds(Rutishauser and Landmesser, 1991; Suzuki et al., 2003). However, a closer examination of NCAM expression during muscle regeneration shows that it is expressed on the cell surface of adult muscle satellite cells (Illa et al., 1992). It may modulate the interaction of satellite cells with the extracellular matrix and enhance muscle fibre repair.

I.4.4 Distribution of muscle satellite cells

With the ease of identifying satellite cells *in vivo* by muscle satellite cell markers, we now have a complete knowledge of its distribution in muscle. The satellite cells are present in all skeletal muscle, albeit with unequal distribution between different muscle fibre types and muscle groups (Chargé and Rudnicki, 2004). Even along individual fibre, the satellite cells are found more likely to be located in close proximity to neuromuscular junctions as well as to adjacent capillaries (Schmalbruch and Hellhammer, 1977; Wokke et al., 1989). In general, slow muscle fibres host more satellite cells than fast muscle fibres do, which might be because the slow oxidative fibres lie within a higher density of capillaries and motor innervation compared with the fast glycolytic myofibres (Gibson and Schultz, 1982). So an increased number of satellite cells populate muscles containing abundant slow fibres, such as the slow soleus muscle.

Currently we are not clear about the underlying mechanism of this phenomenon. The distribution of the satellite cells is possibly also associated with the source of their progenitor cells. Endothelial cells have been considered as progenitors of muscle satellite cells (Chargé and Rudnicki,

2004), so the satellite cells near capillaries may possibly be derived from the endothelial cells. Alternatively, some factors released from the neuromuscular junction or adjacent capillaries may attract nearby satellite cells, homing and maintaining the satellite cells.

The percentage of quiescent satellite cells in the sublaminar region of myofibres also varies with age. For example, the satellite cells account for about 20-30% of muscle nuclei in mice at birth. As postnatal muscle grows, the satellite cells fuse to their residing myofibres and accordingly increase in the myonucleus number. Due to this, the percentage of quiescent satellite cells declines to less than 5% (Snow, 1977). The number of satellite cells gradually falls with age in both fast and slow myofibres because of their incomplete replenishment during routine muscle growth or repair. In senile mice only about 2% of sublaminar nuclei represent quiescent satellite cells (Snow, 1977). As a result, the ability of muscle growth and regeneration continuously declines with age. This trend happens in human skeletal muscle as well.

I.4.5 Self-renewal of muscle satellite cells

Since subtle muscle injuries routinely occur during normal muscle activity, there is a continuous demand for functional satellite cells throughout life. However, as we mentioned above, a continuous shrinkage of the satellite cell pool takes place with age. It is because of this, rather than deterioration of myogenic potential of the satellite cells, that the ability of muscle regeneration falls in aged mammals (Shefer et al., 2006).

The replenishment of the satellite cell pool after routine usage occurs by a self-renewal process. After proliferation, most of the progeny of satellite cells will differentiate to muscle, while a minority of the cells return to a quiescent state to maintain a pool of satellite cells. This is an important feature of muscle satellite cells, which enables them to be classified as a typical adult stem cell population for maintaining the integrity of skeletal muscle throughout the lifespan. Direct evidence for satellite cell self-renewal comes from an elegant grafting experiment. Collins et.al grafted single isolated myofibres, in which satellite cells are present in their endogenous anatomical position beneath the basal lamina and from which other cell types were excluded. It was shown that the grafted satellite cells proliferated and generated both differentiated muscle tissue and a population of new satellite cells, identified by their anatomical position, by expression of the satellite cell marker pax7, and by an ability to mediate further regeneration after experimental injury of the engrafted muscle (Collins et al., 2005).

In addition, Zammit et.al studied the self-renewal process during muscle regeneration by observing cultured myofibres (Fig.1.3). They found that the activated satellite cells synchronously co-expressed the transcription factors pax7 and myoD. After several rounds of proliferation, most of the cells down-regulated pax7, and differentiate. In contrast, other cells retaining pax7 but losing myoD expression withdrew from cell cycle, thus returning to a quiescent state (Zammit et al., 2004). This result shows different cell fates of the progeny of satellite cells and also suggests a potential role of pax7 in maintaining the satellite cell pool.

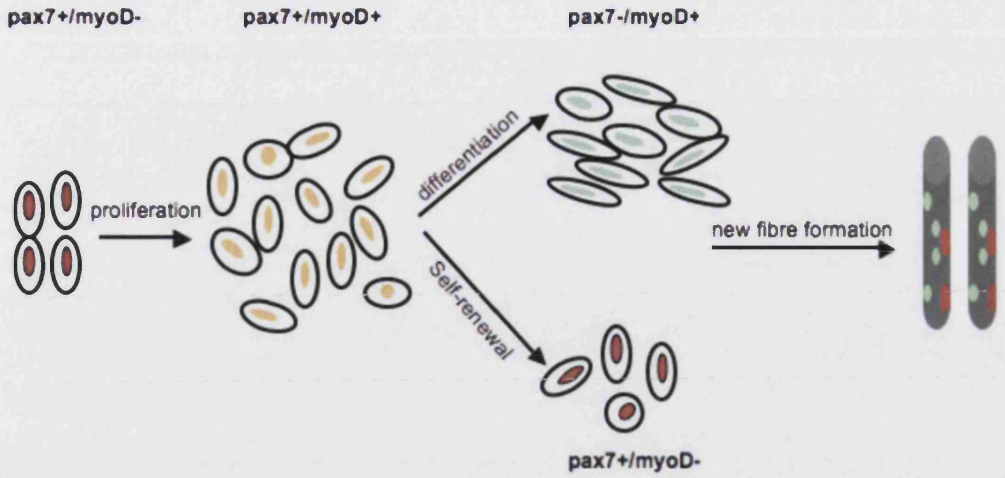

Figure: 1.3 Model of satellite cell self-renewal

Upon activation, quiescent satellite cells (pax7+, red) co-express pax7 and myoD (pax7+/myoD+, yellow). After several rounds of cell division, most of the cells down-regulate pax7 but maintain myoD (pax7-/myoD+, green), and differentiate to form new fibres. A small portion of cells retains pax7 expression but loses myoD expression (red). These cells return to a quiescent state and attach to newly formed myofibres, thus the satellite cell pool is self-renewed.

Although we know that the replenishment of satellite cells throughout lifespan is via a self-renewal process, we are still not clear about its molecular mechanism. Many scientists now favor an "asymmetric division of satellite cells" model to explain the self-renewal process. In this model, asymmetric cell division may happen in the first round of satellite cell proliferation after activation, in which one daughter cell forms a new quiescent satellite cell and the other undergoes further symmetric divisions to generate a pool of myoblasts for regenerated muscle.

The asymmetric model was first proposed based on an asymmetric

distribution of Numb, an inhibitor of Notch signalling, in dividing satellite cells. Daughters with high level of Numb protein were found to undergo muscle differentiation, while those without Numb maintained an undifferentiated state (Conboy and Rando, 2002). This phenomenon was further examined by an *in vivo* label retention assay in which Shinin et.al use pulse-chase labelling with BrdU to trace DNA in slowly dividing muscle satellite cells (Shinin et al., 2006). The idea comes from the immortal DNA strand hypothesis proposed by John Cairns as a mechanism to minimize mutations in genome (Cairns, 1975). Cairns thought that adult stem cells would retain parental DNA strands in the daughter destined to be the self-renewed one in each cell division, while pass mutations arising from errors in DNA replication on to non-stem cell daughters. Consistent with this hypothesis, Shinin et.al showed that in activated muscle satellite cells template and newly synthesized DNA strands do segregate selectively to ensure consistent retention of the original template strand by the stem cell daughter. This finding provides direct evidence of the asymmetric DNA division in activated satellite cells *in vivo*. In addition, pax7 was found to be specifically expressed in the daughter cells with template DNA, further indicating a role in self-renewal of satellite cells.

More recently, Kuang et.al reported that activated satellite cells divide through a basal-apical orientation, which fits a standard division pattern for asymmetric cell division model (Kuang et al., 2007). Using a *myf5-Cre* knockin allele and a ROSA-YFP Cre reporter, they found that activated muscle satellite cell population is composed of apical pax7+/myf5+ and basal pax7+/myf5- subpopulations, the latter of which is able to maintain a reservoir

of satellite cells. This novel finding not only further supports the concept of asymmetric division of satellite cells taking place during muscle growth and regeneration, but also provides some insight into the nature of the stem cell niche regulating the identity of activated satellite cells.

So far, we are clear that the muscle satellite cell, like many other types of stem cell, such as intestinal epithelial stem cells and neural stem cells, is capable of self-renewal via asymmetric cell divisions (Molofsky et al., 2004; Potten et al., 2002). But our understanding about the molecular regulation of this process and the maintenance of this ability is still limited. With these questions in mind, scientists are endeavoring to look for signalling pathways required for the maintenance of muscle satellite cell pool and some important factors preferentially expressed in quiescent or activated satellite cells.

I.4.7 Role of pax7 in muscle satellite cells

Pax7 is a widely used satellite cell marker because of its exclusive expression in satellite cell lineage in adult mice. It is potentially a key factor for self-renewal of satellite cells indicated by the Zammit group's work on cell fates of activated satellite cells(Zammit et al., 2004). However, pax7 functions in a way more complex than what we expected. It was initially proposed to be able to specify the lineage of muscle satellite cells based on the following evidence: 1. The muscle satellite cells are absent in *pax7-/-* mutant mice and the mice died postnatally; 2. Primary cultured muscle cells or myofibres from the *pax7-/-* mice fail to produce any myoblasts; 3. Muscle stem cells from *pax7-/-* mice readily differentiate to haematopoietic cells rather than myogenic cells if cultured in the medium suitable both for the growth of muscle and

haematopoietic colonies(Seale et al., 2000). These findings support the idea that pax7 is required for the specification of the muscle satellite cells by restricting developmental potential.

Moreover, pax7 is shown to be necessary and sufficient for the myogenic specification of $CD45^+$:$Sca1^+$ adult stem cells isolated from regenerating muscle(Seale et al., 2004). $CD45^+$ and $Sca1^+$ are two cell surface markers used to isolate adult stem cells, other than the satellite cells, from skeletal muscle. $CD45^+$:$Sca1^+$ stem cells from injured muscle with pax7 expression are able to give rise to myogenic lineage. Therefore, these stem cells are valued as potential source of the muscle progenitor cells for the treatment of neuromuscular disease. But this capacity was lost if the cells were isolated from *pax7-/-* mice. When the *pax7* deficient muscle was infected with viral pax7, the newly isolated $CD45^+$:$Sca1^+$ stem cells regained their capacity to give rise to myoblasts. These experiments further support the notion that pax7 has an ability to specify the myogenic lineage. However, these data still can not exclude the possibility that pax7 maintains survival of those $CD45^+$:$Sca1^+$ progenitor cells that are already competent to enter the myogenic lineage.

In fact, recent findings suggest that pax7 has new functions other than lineage specification in muscle development. This idea first comes from the surprising observation from Braun's lab that *pax7-/-* mice in a mixed C57/BL/Sv129 genetic background do have muscle satellite cells, albeit at a greatly reduced number compared to wild type mice (Oustanina et al., 2004). This finding was confirmed by Rudnicki's lab using viable *pax7-/-* mutants in 129Sv/J genetic

background (Kuang et al., 2006). They also found that the number of satellite cell was severely reduced during postnatal development in *pax7-/-* mutants.

Although the *pax7-/-* adult mice posses fewer satellite cells, these *pax7* null satellite cells are functional, namely being capable of expanding and completing partial regeneration of damaged muscle (Oustanina et al., 2004). In spite of this, the number of satellite cells in the mutants continuously declines postnatally. This result suggests a role for pax7 in the renewal and propagation of the satellite cells. The idea is supported by works from Zammit's lab. Upon muscle injury, quiescent satellite cells became activated and synchronously co-express myoD and pax7. They found most of these satellite cells proliferated, down-regulated pax7 and then went on to differentiation. However, a small proportion of the cells maintained their expression of pax7, down-regulated myoD and left the cell cycle. They returned to a quiescent state and accordingly replenished the pool of muscle satellite cells (Zammit et al., 2004). These data demonstrate that pax7 is responsible for self-renewal or other function rather than the specification of satellite cells.

Rudnicki's group agreed that muscle satellite cells exist in the *pax7-/-* mice in 129Sv/J background. However, they showed that their pax7 null muscle satellite cells were negative for satellite cell markers and failed to give rise to myogenic lineage if cultured *in vitro* (Kuang et al., 2006). This observation is in disagreement with the result from Braun' lab that the remaining satellite cells are still functional. Rudinick's group attributed the defects to the absence of functions of satellite cells in the *pax7-/-* mutants. Therefore, they

summarized that pax7 is essential for the formation of functional myogenic lineage from the satellite cells.

Another possible interpretation concerning pax7 function is that it acts as a cell survival signal. In the absence of pax7, certain cell populations might initiate an apoptotic pathway. Relaix et.al have shown that activated caspase3 was immediately detectable in postnatal muscle of *pax7-/-* mutant mice. They demonstrated that pax7 has an anti-apoptotic function that could not be replaced by pax3 in normal muscle growth (Relaix et al., 2006).

Taken together, pax7 seems to act at several points in muscle development and regeneration. We need more evidence to decipher its exact and comprehensive functions during development and regeneration. Hopefully such knowledge will inform the development of methods to cure muscle disorders via cell therapy and/or gene therapy.

I.4.8 Activation and differentiation of muscle satellite cells

Muscle injury itself is able to simulate satellite cell activation. But to restore functional muscle architecture, activation and differentiation of muscle satellite cells require a timely and highly controlled regulation of the myogenic regulatory factors. Several signals have been implicated in this process.

I.4.8.1 Cytokine signals

Upon injury, macrophages rapidly invade damaged muscle and remove cellular debris. Meanwhile macrophage secreted proteins are able to stimulate muscle progenitor cell proliferation. The proteins we known so far are the cytokines IL-6, leukemia inhibitory factor (LIF) and tumor necrosis factor

(TNF-alpha) that can stimulate the muscle progenitor proliferation and inhibit their differentiation in culture (Austin et al., 1992; Jo et al., 2005; Kurek et al., 1996).

In vivo, addition of LIF to the injury site promotes muscle regeneration by increasing proliferation of the activated satellite cells without affecting their differentiation and fusion(Austin et al., 2000; Barnard et al., 1994). Moreover, *LIF-/-* mice display impaired muscle regeneration and this deficiency could be rescued by over-expression of LIF (Kurek et al., 1997). Although IL-6, like LIF is highly up-regulated after muscle damage, its knock out mice do not show any muscle regeneration defect (Warren et al., 2002).

The *in vivo* role of TNF-alpha in muscle repair is complex. Mice treated with neutralizing anti- TNF-alpha antibody show defects in expression of muscle differentiation markers and in formation of new muscle fibres (Chen et al., 2005). But over-expression of TNF-alpha *in vivo* still inhibits muscle regeneration (Coletti et al., 2005). These data suggest that muscle regeneration needs a fine tuning of TNF-alpha signals.

I.4.8.2 HGF and FGF signals

Hepatocyte growth factor (HGF), the ligand of the c-met receptor, is the key regulator of satellite cell activity during regeneration. It appears to directly activate satellite cells to enter the cell cycle (Tatsumi et al., 1998). The role of HGF in muscle regeneration is crucial during the early stage, not only because it increases satellite cell proliferation, but also because it is able to promote migration of satellite cells to the site of injury (Suzuki et al., 2000).

Among members of the FGF family, FGF1, FGF2, FGF4, FGF6 and FGF9 have been shown to be capable of promoting myoblast proliferation and inhibiting differentiation *in vitro* (Chargé and Rudnicki, 2004). This effect is enhanced by addition of HGF (Sheehan and Allen, 1999). FGFr-1 and FGFr-4 are the most abundant receptor transcripts in satellite cells. However, the relationship between the FGF ligands and receptors in activated satellite cells has not been identified yet.

Apart from their receptors, the FGF and HGF signals both require heparan sulfate proteoglycans (HSPGs) to facilitate receptor binding and intracellular signalling transduction to activate satellite cells (Rapraeger, 2000). Syndecan-3 and syndecan-4 are the well known HSPGs present on the membrane of quiescent and activated satellite cells (Cornelison et al., 2001). The interaction of HSPGs with FGF/HGF and their receptors is via the heparan sulfate (HS) chains of HSPGs. Recently, Langsdorf et.al reported that extracellular HS 6-O-endosulfatase (Sulfs) is able to repress FGF2-mediated inhibition of myogenic differentiation during muscle regeneration by controlling HS 6-O-desulfation in activated satellite cells. The negative role of Sulfs in forming a tertiary complex of FGF, receptor and HSPG suggests that Sulfs act as a switch to initiate muscle differentiation during regeneration (Langsdorf et al., 2007).

I.4.8.3 TGF-beta signals

Role of TGF-beta signals in muscle regeneration is complex. Here we focus on describing the role of myostatin, a member of the TGF-beta superfamily, in regulating activation and differentiation of the satellite cells. Myostatin is

uniquely expressed in skeletal muscle and is well known as an endogenous inhibitor of muscle growth (Lee, 2004; McPherron et al., 1997). Functional analyses of myostatin shows that it maintains a quiescent state of satellite cells by regulating p21 activity to inhibit the G1-to-S progression (McCroskery et al., 2003). So myostatin deficient muscle displays an increased number of activated satellite cells *in vivo* (McCroskery et al., 2003). Consistent with this result, high levels of myostatin within damaged fibres are detectable at a time when degeneration occurs and activated satellite cell number is low. With the progression of muscle regeneration, myostatin is down-regulated when the satellite cells are proliferating and is then restored to a normal expression level in more mature regenerated muscle (Mendler et al., 2000). So muscle regeneration is enhanced in *myostatin* mutant mice (McCroskery et al., 2005). Thus, myostatin is a negative regulator of muscle regeneration.

The identification of these signals and molecules has expanded the range of possible applications to regenerative medicine. Using small molecules to augment muscle regeneration is likely to be more feasible for treating muscular disorders than cell transplantation or other surgical interventions. Scientists are now exploring the effect of these known signals applied in combination during muscle regeneration.

I.4.9 Developmental origin of muscle satellite cells

Since the discovery of muscle satellite cells, a large body of experimental work has been rapidly accumulating on the activation, the self-renewal and differentiation of muscle satellite cells. Nevertheless, the field of developmental origin of muscle satellite cells is less explored. Based on

limited evidences from mouse and chick system, the satellite cells are believed to constitute a myogenic lineage distinct from embryonic and fetal myoblast lineage. However, due to imperfect labelling techniques, scientists are still not able to provide a unanimous conclusion about its embryonic origin.

Before we review several studies on the origin of satellite cell, it is useful to know about their mode of formation in embryonic development. The formation of the satellite cell is believed to be closely relevant to the progression of myogenesis. Skeletal muscle of the vertebrate derives from the somites, transient embryonic segments established through the segmentation of presomitic mesoderm. In mammals and birds, the ventromedial somite becomes a mesenchymal mass of sclerotome, while the dorsal lateral part becomes an epithelial sheet named the dermomyotome. This structure is then subdivided into the dermatome and the myotome which gives rise to all skeletal muscle except head muscle (Shi and Garry, 2006). It is noteworthy that *Xenopus* somites, unlike those in mammals and birds, mostly contain myotomes, the dermatome and sclerotome being very small (Chanoine and Hardy, 2003).

Vertebrate embryonic myogenesis starts with the specification of muscle progenitors in the myotome. Once specified, the myogenic precursor cells proliferate to become myoblasts, most of which then undergo terminal differentiation to form myocytes. In most vertebrate myogenesis, the fully differentiated myoblasts aggregate and fuse each other to form multinucleated myofibres (primary myofibres) (Pownall et al., 2002). But the cell fusion does

not occur in *Xenopus* embryonic (primary) myogenesis. In *Xenopus*, the terminally differentiated myofibres are initially mononuclear and lie parallel to the A-P axis with each myofibre spanning the whole length of a somite (Chanoine and Hardy, 2003). With the formation of myofibres, a mononucleated satellite cell will attach to the plasma membrane of a myofibre. After this, a basal lamina begins to form around each myofibre. It is only after this stage that we could identify the cells that are lying between the fibre plasma membrane and the basal lamina as the muscle satellite cells (Cossu and Biressi, 2005). The process of satellite cell formation suggests that they are derived from the same progenitors of myogenic cells, or at least from the cells physically close to muscle precursors in embryonic development.

Therefore, one proposed origin of satellite cell is the somite which is also the cell source of skeletal muscle. Kieny's group first reported that the satellite cells are derived from somites by quail-chick somite transplantation (Armand et al., 1983). They found that grafted somitic cells of quail origin finally appear in the satellite cell population in chick hosts, which is based on morphological observation of quail heterochromatin. However, in their assay, they did not show that all of the satellite cells are of somitic origin. They also did not address whether the satellite cell lineage is already separated from embryonic myoblasts in the somite by the time of grafting, or the lineage is only committed by local signals emanating from adjacent primary myofibres, at a time point, for example, after somite grafting.

These uncertainties raise a possibility that the satellite cells do not originate exclusively from somites. This hypothesis is supported by a novel finding that progenitor cells in the dorsal aorta could give rise to muscle satellite cells (De Angelis et al., 1999). *In vitro* cultured cells isolated from embryonic dorsal aorta display the same morphology as muscle satellite cells derived from adult skeletal muscle. In addition, these cells express myogenic and endothelial markers similar to those of adult satellite cells. Interestingly, myogenic clones could even be derived from the limb buds of *pax3-/-* or *c-met-/-* mice that are devoid of appendicular musculature due to lack of migratory muscle of somite origin, but maintain normal vasculature. Furthermore, De Angelis et. al tested regeneration ability of these myogenic cells derived from dorsal aorta by transplantation. Their result shows that the injected cells could incorporate into the newly regenerated myofibres, the same cell behaviour as the satellite cell has. All together, these data support an alternative origin of the muscle satellite cells from endothelial cells.

Most recently, thanks to a breakthrough of labelling techniques, several lines of evidence have re-confirmed the somitic origin of the satellite cells. Combining *in vivo* electroporation labelling with a modified quail-chick grafting technique, Gros et al. clearly demonstrated that most of the chick satèllite cells present in skeletal muscles of the trunk originate from the central region of the dermomyotome, the common origin of skeletal muscle (Gros et al., 2005). Relaix et al. used genetic labelling method to trace the fate of pax3/pax7 expressing cells in the central dermomyotome region of mouse embryos (Relaix et al., 2005). In agreement with Gros et al.'s observation,

they found this cell population represents the progenitors of embryonic and fetal myoblasts and muscle satellite cells. Another lineage analysis further identified that the satellite cells residing in limbs of mouse and chick are derived from pax3 expressing cells in the somites (Schienda et al., 2006). Here we must point out that although all these studies confirm that the progenitors of satellite cells originate from the somite, they do not tell us that all of the satellite cells came from this location, nor whether the satellite cell progenitors come from the same region of the early mesoderm as the myofibres.

Thus, evidence for a somitic origin of satellite cells does not rule out an endothelial origin. The two origins of satellite cells are not mutually exclusive, since the somite and endothelial cells are both of mesoderm origin. The endothelial cells in the roof and lateral wall of the dorsal aorta originate from the dorsal paraxial mesoderm, which is a part of the future somites (Jaffredo et al., 1998). Given this, it would be worth finding out the real origin of the muscle satellite cells in an earlier stage than that of fully formed somites.

I.5 Aims

1. To locate the progenitor region for muscle satellite cells by grafting different parts of the neurula mesoderm from transgenic labelled donors to the presomite plate region, and identifying satellite cells derived from the graft.

2. To demonstrate, using electron microscopy, that the pax7 positive cells in *Xenopus* tadpole muscle are, in fact, satellite cells.

3. To confirm using BrdU labelling and electron microscopy that the satellite cells are active in DNA synthesis while the myofibre nuclei are not.

4. To find how many of the molecular markers of satellite cells in mammals are present in *Xenopus* satellite cells.

5. To study the expression pattern of *pax7* and pax7 during development.

6. To make and test, by RNA injection, a dominant negative version of pax7, pax7EnR.

7. To find, by RNA injection, whether overexpression of *pax7*, or expression of *pax7EnR*, in the early embryo mesoderm will increase or decrease the number of satellite cells formed.

8. To find whether transgenic *pax7EnR*, induced using a heat shock promoter, will inhibit formation of new muscle in the regenerating tail.

II. Materials and Methods

This chapter describes general techniques used throughout my PhD study. Techniques used for specific experiments are listed in their respective chapters.

II.1 Plasmid construction

II.1.1 *pax7*-pGEMT

Xenopus pax7 (Xpax7) gene was isolated from cDNA of stage 25 embryos by RT-PCR. The primers were designed according to the sequence submitted by the laboratory of Dr Richard Harland (NCBI: AF725267): Sense- 5'-CAA CTT GTG AGG ACT CTT CTA GGC T-3'; Antisense- 5' – TTT TCA CCA AGT GGC AGA CAT-3'. A 2kb DNA fragment contains pax7 was amplified and ligated to pGEM-Teasy vector (Promega). This construct was then sequenced.

II.1.2 *pax7*-pSL1180

pax7 gene was excised from *pax7*-pGEMT plasmid by *Spe*I and *Apa*I (Promega) and cloned into the same sites of pSL1180 vector (Amershan). This construct is used for subsequent cloning.

II.1.3 *pax7*-HGEM

pax7 gene was excised from *pax7*-pSL1180 with *Hin*dIII and *Eco*RI (Promega), and cloned into the same sites of HGEM transgenic vector (Heat shock Green-Eyed Monster) (Beck et al., 2003). The HGEM plasmid was constructed by Caroline Beck and contains a GFP gene driven by γ-crystallin

promoter. This makes the lens of the tadpole green, hence "green eyed monster". *pax7*-HGEM was linearized with *Xmn*I (Promega) before use in transgenesis.

II.1.4 *pax7*-pcDNA3

To generate the construct for RNA injection, *pax7* gene was excised from *pax7*-HGEM with *Hin*dIII and *Eco*RI, and cloned into the same sites of pcDNA3 (Invtrogen). Capped *Pax7* RNA was transcribed *in vitro* with T7 messenger machine kit (Ambion) after linearization with *Tth111*I (Promega).

II.1.5 *pax7EnR*

pax7EnR is a dominant negative form of pax7. It was made by fusing the N-terminal of *pax7* gene (1-245 amino acids) to the transcriptional repression domain of Drosophila *engrailed* gene (Lagna and Hemmati-Brivanlou, 1998). The N-terminal of *pax7* was excised from *pax7*-pSL1180 with *Hin*dIII and *Sma*I (Promega), and then cloned into *Hin*dIII and *Cla*I (blunt filled) sites of ENR-N-pCS2+ vector (kind gift of Dan Kessler).

II.1.6 *pax7EnR*-pcDNA3

For RNA injection, the sequence of *pax7EnR* was cloned into pcDNA3 with *Hin*dIII and *Xba*I (Promega) to generate *pax7EnR*-pcDNA3. This plasmid was then linearized with *Sma*I and transcribed *in vitro* with T7 messenger machine kit (Ambion).

II.1.7 *pax7EnR*-HGEM

A *pax7EnR* plasmid suitable for transgenesis was made by excising the sequence of *pax7EnR* from *pax7EnR*-pcDNA3 with *Hin*dIII and *Xba*I (blunt filled), and then cloning into *Hin*dIII and *Sma*I sites of HGEM. The *pax7EnR*-HGEM was linearized with *Xmn*I before use in transgenesis.

II.2 RT- PCR

To detect gene expression in regenerating tails by RT-PCR, ten regenerating tails of each experimental group were collected for RNA isolation. Total RNA was prepared using Trizol reagent (Invitrogen). DNaseI (Invitrogen) treatment is necessary to completely remove residual DNA in total RNA preparations before they were reversely transcribed into cDNAs with the Superscript III Reverse Transcriptase system (Invitrogen). Primers and annealing temperatures (Ta) used are listed in table 2.1:

Table 2.1 PCR primer sequence and annealing temperature of target genes

Gene	Forward primer (5'-3')	Reverse primer (5'-3')	Ta (°C)
ODC	ACACGGCATTGATCCTACAG	AGCTCCTTCGGTGTAATGAC	55
pax7	TCAATAATGGTCTCTCCCCGC	TTGCCAGGTAATCAACAGCGG	57
pax7EnR	GCTCTGTCCCCTCAGGTTTAGT	GGTGGTGTGCGTCTGATTGTG	53
pax6	GCAACCTGGCGAGCGATAAGC	CCTGCCGTCTCTGGTTCCGTAGTT	55

II.3 Embryos and tadpoles

Xenopus laevis embryos were obtained by *in vitro* fertilization and staged according to the Nieuwkoop and Faber (NF) table (Nieuwkoop and Faber, 1967). Embryos were dejelled with 2% (w/v) cysteine HCl (Sigma) at pH 7.8,

and then cultured in NAM/10 (Normal Amphibian Medium: 110 mM NaCl, 2 mM KCl, 1 mM $Ca(NO_3)_2$, 1 mM $MgSO_4$, 0.1 mM Na_2EDTA) at 22°C. From stage 46, they were transferred to a recirculating aquarium and fed on tadpole diet (Blades Biological, Redbridge, UK).

II.4 Transgenesis

Transgenic *Xenopus laevis* tadpoles were made mainly according to the REMI (Restriction Enzyme Mediated Integration) procedure developed by Kroll and Amaya (Kroll and Amaya, 1996). Restriction enzyme was omitted from the reaction because it will lower the survival of transgenic tadpoles.

Sperm nuclei preparation and *Xenopus* egg extract were prepared before starting transgenesis.

II.4.1 Sperm nuclei preparation

To get better sperm quality, each male frog was primed with 50 units of PMSG (Pregnant Mare Serum Gonadotropin, Calbiochem 367222) two days before hCG (human Chorionic Gonadotropin, Intervet) injection. The frogs were injected with 500 units of hCG 12-14 hours before sperm nuclei preparation. Testes were freshly isolated from the male frog and placed in a clean Petri dish containing cold 1X MMR (Marc's modified Ringers: 1M NaCl, 20 mM KCl, 20 mM $MgSO_4$, 20 mM $CaCl_2$, 5 mM Hepes, 1 mM EDTA pH 7.8). The testes were gently rinsed with ice cold 1X NPB (Nuclear Preparation Buffer: 250 mM sucrose, 15 mM Hepes, 1 mM EDTA, 0.25 mM spermidine [Roche], 0.1 mM spermine [Roche], 0.5 mM DTT). Then they were transferred to a dry Petri dish and macerated thoroughly with a pair of forceps. This

macerate was resuspended in 2 ml of 1X NPB by gently pipetting the solution with a cut yellow tip (3 mm in diameter). The sperm suspension is then squirted through four layers of cheesecloth placed into a 12 ml round bottom centrifuge tube and then centrifuged at 3,000 rpm for 10 min at 4°C. The pellet was resuspended in 1 ml of 1X NPB with a cut off micropipette tip. Once the suspension was warmed to room temperature, 50 µl of 10 mg/ml lysolecithin (Sigma L-alpha-Lysophosphatidylcholine from egg yolk) was added and incubated for 5 minutes. The lysolecithin is used to permeablize the sperm plasma membrane and maintain the membrane of sperm nuclei. To stop the lysolecithin reaction, 10 ml of cold 1X NPB containing 3% (w/v) BSA was added to the suspension. The suspension was then centrifuged at 3.000 rpm for 10 min at 4°C. The supernatant was decanted and the pellet was resuspended in 5 ml of cold 1X NPB containing 0.3%BSA (w/v) and centrifuged again as before. The final pellet was carefully resuspended in 500 µl of Sperm Storage Buffer (1X NPB + 0.3% (w/v) BSA + 30% (w/v) glycerol).

Before storage, the density of sperm nuclei was determined with a haemocytometer. 1 µl of sperm nuclei was diluted in 100 µl of sperm storage buffer containing Hoechst dye and sperm nuclei were counted under a fluorescence microscope. Typically, the sperm preparation was diluted to 1-2 $X10^5$ nuclei/µl as stock. This fresh stock could be kept at 4°C overnight to allow the penetration of glycerol. The next day, the stock was aliquoted (10µl) and fast frozen in liquid nitrogen. All the aliquots were than transferred to a -80° freezer.

II.4.2 High speed egg extract preparation

High speed egg extract is able to promote swelling of sperm nuclei and decondensation of chromatin. But it will not promote DNA replication. Replication of sperm DNA occurs after transplantation of the nucleus into the egg rather than in the egg extract.

Eight healthy female adult *Xenopus leavis* frogs were chosen for egg extract preparation. Each frog was primed by injecting 40 units of PMSG two days before hCG injection. The evening before egg extract preparation, the frogs were injected with hCG (500 units per frog) and kept in pairs in tanks containing 2 litres of 1XMMR. They were placed at 16°C overnight.

The next morning, the egg quality was screened before starting preparation. Only the intact and even-pigmented eggs were chosen and manually transferred with a wide mouth 20 ml pipette from each tank into a large beaker containing 1X MMR. After as much 1X MMR as possible was removed, the eggs were dejellyed in 2% cysteine (w/v) in XB salts (0.1 M KCl, 1 mM $MgCl_2$, 0.1 mM $CaCl_2$, pH 7.7) and washed in XB (Extract Buffer: 0.1 M KCl, 1 mM $MgCl_2$, 0.1 mM $CaCl_2$, 50 mM Sucrose, 10 mM Hepes, pH 7.7) for four times. Any broken eggs were removed with a wide-bore Pasteur pipette during washing. After last XB washing, the eggs were washed in CSF-XB (Crude Cytostatic Factor-XB: XB + 5 mM EGTA, pH 7.7) with protease inhibitors (10 μg/ml of leupeptin, chymostatin and pepstatin, Roche) twice. Using a wide-bore Pasteur pipette, the eggs were transferred into a Beckman ultraclear tube. CSF-XB was removed as much as possible and replaced with 1ml of Versilube F50. The eggs were packed by centrifuging for 60 seconds at

1000rpm and then 30 seconds at 2000 rpm. An inverted meniscus between the Versilube F50 and displaced CSF-XB should be easily visible at this stage. Any excess of CSF-XB was removed as much as possible.

The eggs were then crushed by centrifuging at 10.000 rpm for 10 minutes at 2°C, in a swinging bucket rotor. Three distinct layers were separated after centrifuge: lipid (top), cytoplasm (centre) and yolk (bottom). The cytoplasmic layer was collected with an 18-gauge needle by inserting the needle at the base of cytoplamic layer and withdrawing slowly, and transferred to a fresh Beckman tube on ice. A second spin is needed if the suspension is greyish rather than golden. Protease inhibitors (leupeptin and pepstatin) were added to the isolated cytoplasm and it was centrifuged for an additional 10 minutes at 10.000 rpm in a swinging bucket rotor to clarify. The clarified cytoplasm was collected as before and exact volume measured. Then $1/20^{th}$ volume of ATP-regenerating system (Energy Mix: 150 mM creatine phosphate (Roche), 20 mM ATP (Roche), 20 mM $MgCl_2$) was added and the clarified cytoplasm was transferred into TL100.3 tubes (Beckman thick wall polycarbonate tubes). $CaCl_2$ was added to a final concentration of 0.4 mM (to inactivate CSF and push the extract into interphase) and incubated for 15 minutes at room temperature.

After incubation, the cytoplasm was centrifuged in an ultracentrifuge (Beckman TL-100) at 70.000 rpm for 90 minutes at 4°C. The cytoplasm was fractionated into four layers. From top to bottom, they are: lipid, cytosol, membranes/mitochondria and glycogen/ribosomes). The cytosol layer was removed by inserting a syringe into the top of the tube through the lipid layer

and transferred to a fresh TL-100 tube and spun again at 70.000 rpm for 20 minutes at 4°C. The supernatant was transferred to a 0.5 ml microcentrifuge tube in 10 µl aliquots, quickly frozen in liquid nitrogen and stored at –80°C.

II.4.3 Preparation of transplantation needles and injection dishes

Transplantation needles and agar-coated dishes need to be prepared before starting nuclear transplantation.

The needles were made with borosilicate glass capillaries of 400 µm in diameter (Clark Electromedical Instruments). A glass capillary was pulled by a Flaming/Brown Micropipette Puller (Sutter Instrument P-97) with a setting of P=50, V=100 and T=5. Then it was clipped with a forceps to produce a bevelled tip of 60-80 µm in diameter (using a dissecting microscope micrometer for measurement).

To make agar-coated injection dishes, 8 ml of 1.5% (w/v) Agar (DIFCO) in NAM/10 was poured into a 35 mm Petri dish and then a square weighing boat was put onto it to create a rectangular cavity for the eggs. Once the agar solidified, the weighing boat was removed and the agar-coated injection dishes were ready to use. For embryo culture, 3 ml of 1.5% (w/v) Agar in NAM/10 was poured into each dish. These agar-coated dishes could be stored at 4°C until use.

II.4.4 Transgenesis by sperm nuclear transplantation into unfertilized eggs

Four female frogs were primed with PMSG (40 units per frog) two days before transgenesis. The evening before transplantation, they were injected with hCG (500 units per frog) and kept at 16°C overnight.

The next morning, injection apparatus (Harvard Apparatus Syringe Pump Series Model "22") was switched on first to stabilize the flow before injection. Then the transgenic reaction mix was set up: 2 µl of sperm nuclei stock (2-4X10^5 nuclei), linearized DNA (150-200ng) and 3 µl MSDB (Modified Sperm Diluent Buffer: 250 mM sucrose, 75 mM KCl, 0.25 mM spermidine, 0.25 mM spermine) were mixed by gentle pipetting (using a cut micropipette to avoid shearing the DNA). The mixture was incubated for 5 minutes at room temperature. After incubation, 5 µl of high speed egg extract and 13 µl of MSDB was added to the reaction mixture, which was incubated for another 15 minutes at room temperature. Then 10 µl of this mixture was diluted 25-50 fold in MSDB to obtain about 300 sperm/µl suspension. A piece of Tygon tube was attached to a yellow clipped tip and the tip was filled with the diluted sperm suspension. The suspension was then backfilled to a transplantation needle via the Tygon tube. The blunt end of the needle was then attached to the Tygon tube connected with the pump of the injection apparatus for the transplantation of the sperm nuclei into the unfertilized eggs.

It usually takes 20 minutes to finish the transgenic reaction. During this incubation, eggs were freshly squeezed, dejellied in 2% (w/v) Cysteine-HCl in 1 X MMR and washed in 1 X MMR. Any broken eggs were removed by using

a wide-bore Pasteur pipette before being transferred to an injection dish filled with NAM/2 + 6% (w/v) Ficoll (Sigma Ficoll 400). Ficoll is used to suppress the leakage that would come out of the hole of injected embryos.

A flow of 10 nl/sec (average 3 sperm/sec) was used to carry out the injection. The injection was performed by moving the needle to pierce the plasma membrane of eggs with right hand and driving the dish with left hand to let the tip of the needle target the plasma membrane of each egg. Usually, the transplantation would be finished within 30 minutes following which the injected eggs were kept at 16°C.

When the fertilized eggs reached the 4-cell stage, they were gently separated from uncleaved ones and transferred with a wide-bore Pasteur pipette into a new culture dish filled with NAM/10 + 3% Ficoll. The embryos were kept in this solution at 16°C until they finish gastrulation. Thereafter, the embryos could be cultured in NAM/10 at 20°C.

II.5 Whole-mount *in situ* hybridization (WISH)

II.5.1 Preparation of RNA probes

DIG labelled, single-stranded RNA probes were generated by *in vitro* transcription. Before probe synthesis, the DNA plasmid was linearized with an appropriate restriction enzyme. Table 2.2 shows restriction enzyme and RNA polymerases used in each RNA probe preparation. After linearization, DNA was purified with Promega SV PCR and Gel clean up system. A 50 µl volume of probe synthesis reaction was set up by mixing the following reagents in a RNase free eppendorf tube at room temperature:

Reagent	**Volume (µl)**
5x transcription buffer (Promega)	10
100 mM DTT (Promega)	5
10x DIG-NTP mix (Roche)	2.5
RNaseOut (Invitrogen)	2
Linear DNA template	2.5 µg
RNA polymerase (Promega)	2
DEPC water	to 50 µl

Then the probe was allowed to be synthesized at 37°C for 2 hours. After that, the DNA template was removed by adding 2 µl DNaseI (Invitrogen) for 20 minutes at 37°C. This step is optional, since the unlabelled DNA template will not affect *in situ* result. But probe purification is necessary. Otherwise the free DIG-labelled dUTP might increase staining background. The resulting RNA probe was cleaned up by a G50 Sephadex column (Amersham Bioscience). After purification, 2 µl of the probe was run on a 1% agarose gel to check its quality. Typically, good probe synthesis should yield a sharp band on the gel. The concentration of each probe was measured by a spectophotometer (Beckman DU530). The probes was stored at -20°C.

Table 2.2 Restriction enzymes and RNA polymerase used in RNA probe synthesis

Plasmid	**Restriction enzyme**	**RNA polymerase**
myf5-pSP73	*Sac*II	*SP6*
myoD-pSP73	*Bam*HI	*SP6*
pax3-pCS2+	*Sac*I	*T7*
pax7-pGEMT	*Pst*I	*T7*
nuclacZ-pcDNA3	*Apa*I	*T7*

II.5.2 Specimen preparation

Xenopus laevis embryos or tadpoles (younger than stage 43) were fixed in MEMFA (0.1 M MOPS, 2 mM EGTA, 1 mM MgSO4 and 4% (v/v) formaldehyde, pH 7.4) for 90 minutes at room temperature. After fixation the specimens were washed for 10 minutes in 100% EtOH and then placed in fresh 100% EtOH and stored at -20°C. The fixed specimens can be stored in this manner for up to 1 year.

II 5.3 *in situ* hybridization

Whole mount *in situ* hybidization (WISH) was performed according to the standard protocol (Harland, 1991). On the first day, the fixed specimens were taken out from a freezer and warmed up to room temperature. The specimens were first rehydrated through a series of rehydration washes on a nutator: 75% EtOH in PBSAT (Oxoid, Phosphate Buffered Saline Dulbecco A + 0.1% Tween 20, Sigma) for 10 minutes, 50% EtOH in PBSAT for 10 minutes and three 10-minute washes in PBSAT. Once rehydrated the specimens were treated with Proteinase K (20 µg/ml in PBSAT) for 10-20 minutes, depending on the specimen size, to help with permeability. For this step the specimens should be kept still, otherwise it will result in excessive damage. After Proteinase K treatment the specimens were washed twice in 3 ml of triethanolamine (0.1 M, pH 7.8) for 5 minutes each on nutator. In the second wash, 5 µl of acetic anhydride was added to each vial. At the end of the second wash, another 5 µl of acetic anhydride was added and incubated for a further 5 minutes. The acetic anhydride, which introduces uncharged groups, is used to acetylate and neutralizes free amines and help to prevent

electrostatic interaction between the probe and basic proteins. The specimens were then washed twice for 10 minutes each in PBSAT, re-fixed with 4% (v/v) formaldehyde in PBSAT for 20 minutes. After fixation they are washed again with PBSAT 5 times for 5 minutes each to remove traces of formaldehyde. At the end of the fifth wash the vials were filled with 1 ml of PBSAT + 250 µl of hybridization buffer (50% Formamide, 5X SSC, 1 mg/ml yeast RNA, 100 µg/ml heparin, 1X Denhardt's, 0.1% Tween 20, 0.1% CHAPS and 10 mM EDTA (pH8.0)). After the specimens settled, the buffer was replaced with 1 ml of hybridization buffer and the glass vial was put in a water bath at 60°C for 10 minutes. After this, the hybridization buffer is replaced with fresh hybridization buffer pre-warmed to 60°C. The specimens were incubated for a further 2-4 hours at 60°C in a shaking oven to pre-hybridize. After pre-hybridization, DIG-RNA probe prepared at 1 µg/ml concentration in hybridisation buffer was added to the specimens. Probes were allowed to hybridize with endogenous message RNA for 14-18 hours at 60°C.

On the second day of WISH, the DIG-RNA probes were removed. The specimens were washed in fresh warm hybridization buffer for 10 minutes, followed by three times washes in 2X SSC + 0.1% Tween 20 for 20 minutes each, and twice in 0.2X SSC + 0.1% Tween 20 for 30 minutes each. These buffer exchange were performed in a 60°C water bath and between each wash the specimens were still incubated in the 60°C oven with shaking. After the last wash in 0.2X SSC + 0.1% Tween 20, specimens were washed at room temperature three times in MABT (Maleic acid buffer, 100 mM Maleic acid, 150 mM NaCl, 0.1% Tween 20, pH 7.8) for 15 minutes each. This is

followed by blocking step for two hours in the blocking buffer (MABT+ 2% Boehringer Mannheim Blocking reagent (Roche) + 20% heat-inactivated sheep serum (Sigma)). After blocking, the specimens were incubated at 4°C overnight with anti-Digoxigenin antibody (Roche) at 1:2000 dilution in the blocking buffer.

On the third day of WISH, the antibody was removed from the specimens and the specimens were washed in MABT at room temperature, three times for 15 minutes each, and another six times for 30 minutes each. At the end of the washes the solution was replaced with AP buffer (Alkaline Phosphatase Buffer: 100 mM Tris Cl pH 9.5, 50 mM $MgCl_2$, 100 mM NaCl, 0.1% Tween 20), for three times, 10 minutes each. Levamisole (final concentration: 5 mM, Sigma) could be added to the last AP buffer wash. This helps to inhibit endogenous alkaline phosphatase activity. The AP buffer was then replaced with BM purple solution (Roche). The specimens were left undisturbed in the dark for colour development. Once the staining was done, the colour reaction was stopped by washing the specimens in PBSA several times and fixing in 4% (v/v) formaldehyde for 30 minutes. The stained specimen were stored in formaldehyde.

II.6 Immunohistochemistry

II.6.1 Tissue preparation

Immunohistochemistry is usually performed on tissue sections. Embryos or tadpoles were fixed in Zamboni's fixative (40 mM NaH_2PO4, 120 mM Na_2HPO4, 2% PFA, 0.1% saturated picric acid) at room temperature for 2

hours. After fixation, the specimens were washed three times in PBSA for 15 minutes each.

For paraffin section, the specimens were then dehydrated and embedded in paraffin with an automated tissue processor system (LEICATP 1020). For cryosectioning, the specimens were incubated in 30% sucrose in PBSA at 4°C overnight. Then they were embedded in OCT (Sigma). The specimens were frozen in dry ice and could be stored at -80°C for up to 1 month.

Paraffin sections were cut at 10 µm with a microtome (LEICA JUNG BIOCUT 2035) and mounted on polysine slides (Fisher). To avoid loss of tissue, the slides need to be dried on a thermostat at 37°C overnight before staining. Cryosections were cut in 10-20 µm with a cryostat (LEICA CM 1850) and mounted on polysine slides (Fisher). The cryosections should be dried at room temperature for about 1 hour before stain processing.

II.6.2 Immunostaining on sections

Paraffin sections were first de-waxed by immersing twice in Histo-clear (National diagonostics) for 10 minutes each. Then they were rehydrated in 100% EtOH, 90% EtOH, 70% EtOH, 50% EtOH and Milli-Q water for 5 minutes each. Cryosections were incubated in PBSA for 10 minutes to remove the OCT.

The sections were washed in PBSA twice for 10 minutes each. This was followed by permeabilization in PBST (PBSA+1% Triton X-100, Sigma) for 30 minutes. Then the sections were incubated in 2% BB (Boehringher Blocking Buffer) in PBSA for 1 hour to block non-specific antigen. After blocking,

sections were incubated at 4°C overnight with a primary antibody in 2% BB with an appropriate dilution. For double-immunostaining, two antibodies that are generated from different species could be added at the same time. Table 2.3 shows the information of the primary antibodies used in this study.

Table 2.3 list of primary antibodies used in immunohistochemistry studies

Primary antibody name	Host species	Catalogue number	Dilution
BrdU monoclonal	mouse	RNP 20 (Amersham)	1:100
GFP polyclonal	rabbit	Ab290 (Abcam)	1:500
Laminin monoclonal	rabbit	L9393 (Sigma)	1:100
MyoD monoclonal	mouse	Gift from John Gurdon	1:4
NCAM polyclonal	rabbit	AB5032 (Chemicon)	1:100
Pax7 monoclonal	mouse	Pax7 (DSHB)	1:300
PCNA monoclonal	mouse	M0879 (Dako cytomation)	1:100
12/101 monoclonal	mouse	Grown in the lab, cells originally gift from Liz Jones.	1:100

The following day, the primary antibody was removed and the sections were washed in PBSA four times for 15 minutes each. The specimens were then blocked in 2% BB for 1 hour. After blocking, the secondary antibody was added. Table 2.4 lists the secondary antibody in the assay. Again for double-immunostaining, two different secondary antibodies could be added at the same time. The sections were incubated at room temperature for 1 hour. After incubation, the slides were washed three times in PBSA, 15 minutes each.

In the cases of BrdU and Pax7 antibody staining, the ABC method was used after secondary antibody incubation to increase the intensity of labelling

signal. But the ABC method will promote the background staining as well. To avoid this, the specimens were treated in 0.3 M Glycine (Sigma) in PBSA for 30 minutes after permeabiization. Once the secondary antibody was washed away, the sections were incubated in ABC reagent (Dako Cytomation) for 30 minutes. The sections were washed in PBSA three times for 10 minutes each and followed by colour development using a DAB kit (Vector Labs).

Table 2.4 list of secondary antibodies used in immunohistochemistry studies

Secondary antibody name	Host species	Catalogue number	Antibody dilution
Alkaline Phosphatase Anti-Mouse IgG (H+L)	Horse	AP-2000 (Vector Labs)	1:1000
Biotinylated Anti-Mouse IgG (H+L)	horse	BA-2000 (Vector Labs)	1:500
Fluorescein Anti-Rabbit IgG (H+L)	goat	FI-1000 (Vector Labs)	1:200
Alexa Fluor® 594 F(ab')2 fragment anti-mouse IgG (H+L)	rabbit	A21205 (Invitrogen)	1:200

II.6.3 Counterstaining and slide mounting

If a fluorescence method was used, the nuclei were counterstained by incubation in PBSA containing 1 µg/ml of DAPI (Sigma) for 5 minutes. The sections were washed in PBSA before mounting in Gel mount medium (Biomeda). If the ABC staining method was used, the nuclei were counterstained in 0.5% Methyl Green solution (Fluka) for 10 minutes. Then they were washed in 90% EtOH once for 1 minutes, 100% EtOH twice for 5 minutes each and Histo-clear twice for 5 minutes each. After dehydration, the sections were mounted in Depex (BDH).

II.6.4 Whole mount immunostaining

Embryos and tadpole tails were fixed as previously described. After fixation, they were washed twice in PBSA and incubated with 0.1 M $K_2Cr_2O_7$ in 5% acetic acid for 30 minutes to inactivate endogenous phosphatase. The specimens were washed in PBSA three times for 10 minutes each. After washing, a bleaching step was performed by adding a final concentration of 5% (w/v) H_2O_2 (Sigma) in PBSA and incubating for 1 hour under the light. After the incubation they were washed four times in PBSA, twice in BBT (PBSA + 1% (w/v) BSA (Bovine Serum Albumin, Sigma) + 0.1% (w/v) Triton X-100) and once in BBT + 5% (w/v) horse serum (Sigma) for blocking. Then the primary antibody was added at a suitable dilution and incubated overnight at 4°C on a shaker. The second day the solution with antibody was removed and the samples were washed six times in BBT for 30 minutes each, and once in BBT + 5% horse serum for 1 hour. Then alkaline phosphatase conjugated secondary antibody was added and incubated overnight at 4°C on shaker. The third day the solution with the antibody was removed and the samples were washed once in BBT for 15 minutes and six times in PBT (PBSA + 0.1% Tween 20) for 30 minutes each. At the end of last wash, PBT wash replaced with AP buffer three times for 5 minutes each. It was followed by BM purple staining overnight at 4°C in the dark. The staining reaction was stopped by replacing BM purple solution with fresh PBSA. The specimens were washed in PBSA three times and, if not observed directly after, can be re-fixed in 4% (v/v) formaldehyde and stored in formaldehyde at room temperature for future observation.

II.7 Photography and microscopy

GFP or RDA was observed in live embryos or tadpoles under anaesthesia as described above, using a Leica Fluo III fluorescent dissecting microscope with a GFP2 or RFP filter set. Stained sections were visualized with a Leica DMRB microscope. Images were captured using a SPOT RT camera (Diagnostic instruments) and processed with Photoshop software (Adobe).

III. Origin of satellite cells in *Xenopus laevis*

III.1 Introduction

Muscle satellite cells are adult myogenic stem cells that are responsible for postnatal muscle growth and regeneration. Due to this nature, the satellite cell is becoming a potential cell therapy source of muscle progenitor cells for treating muscular diseases. Therefore, understanding the origin and specification of satellite cells lineage during embryonic development will benefit clinical researchers by enabling them to generate more satellite cells for treatment.

In *Xenopus laevis* embryos, presomitic mesoderm is specified at the onset of gastrulation, earlier than that in mammals and birds. A cell lineage tracing study on regenerated tadpole tails has shown that the satellite cells participating in muscle regeneration could be labelled in presomitic mesoderm. It also suggests a regional specification of satellite cell population has already taken place in the presomitic mesoderm of *Xenopus* embryos (Gargioli and Slack, 2004).

Thus this study aims to trace the origin of the satellite cells in *Xenopus* embryos in a period after gastrulation and before somitogenesis. During this period, the mesoderm of *Xenopus* embryo can be easily isolated and subdivided into different zones (type I-III according to the position of the mesoderm related to the midline). We labelled three different zones of posterior mesoderm by orthotopic grafting mesoderm from CMV-nucGFP transgenic donor embryos and identify the satellite cells within the grafts. The

findings from the labelling experiment could then help us to more accurately target the progenitors of satellite cells and identify the molecular mechanism of specifying the satellite cell lineage.

III.2 Materials and Methods

III.2.1 Neurula-stage mesoderm grafting

The grafting we did was an orthotopic one, which involves moving the posterior mesoderm of one side from a CMV nuclear GFP (nucGFP) labelled transgenic embryo to the same position of a wild type host embryo. Posterior mesoderm was grafted from three different dorsoventral positions; with each graft about 220 µm long and 100 µm wide. From dorsal midline to lateral, these are: 1) type I, mesoderm of 100 µm wide next to notochord; 2) type II, mesoderm of 100 µm wide next to type I mesoderm; 3) type III, mesoderm of 100 µm wide next to type II mesoderm (Fig. 3.1).

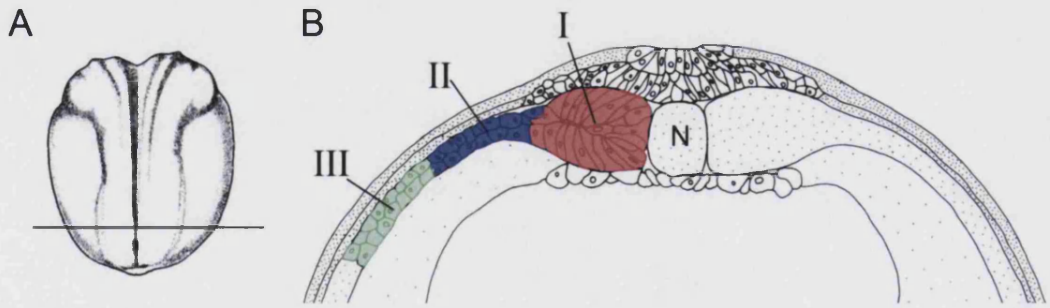

Figure 3.1 Diagrams illustrating the Neurula-stage mesoderm grafting types

(A) A dorsal view of a stage 15 embryo. Anterior is up. The line indicates the position of the cross section shown in B. (B) The mesoderm shown in red, blue and green stand for the mesoderm grafted in type I, II and III respectively. Abbreviations: I, type I grafting; II, type II grafting; III, type III grafting; N, notochord.

Before grafting, nucGFP transgenic embryos were sorted out under a fluorescent dissecting microscope with a GFP2 filter. nucGFP in pcDNA3 vector is usually visible after stage 13. The vitelline membrane of both donor and host embryos of the same stage were removed manually with a pair of sharp forceps. The demembranated host embryos were then transferred to an agar-coated Petri dish containing NAM/2+10 µg/ml of trypsin (Sigma). Trypsin is used to promote separation of the three germ layers. One of the donor embryos was transferred to the same dish. It was incised using an eye-brow needle in the posterior region next to the blastopore, at the level of the presumptive tail (Tucker and Slack, 1995). A piece of mesoderm was separated and transferred with a cut Gilson tip to another agar-coated Petri dish containing NAM/2 + 20 µg/ml of trypsin inhibitor (Sigma bovine pancreas). In a host embryo, a piece of mesoderm in the position corresponding to the donor was carefully removed. The host embryo was then transferred with a cut Gilson tip to the dish containing the donor mesoderm explant. The host embryo was immobilized in a hole in the agar, with the wounded side up. The donor mesoderm was then implanted into the host embryo. The grafted embryo was allowed to heal for 30 minutes. After healing, the grafted embryo was transferred to a new agar-coated Petri dish filled with NAM/2 + 50 µg/ml gentamicin (Sigma) for culture.

III.2.2 Cell counting in the grafting experiment

A series of transverse cryosections (10 µm thick each) through a GFP labelled tail were prepared and double immunostained with pax7 and GFP antibodies. Muscle satellite cell counting was based on the pax7 antibody staining, which

is a reliable molecular marker for satellite cells in *Xenopus* (see chapter IV for details). Myofibre counting was by morphology. GFP labelled myofibres were counted based on the presence of green fluorescence. Usually one circle of GFP positive area represents one GFP labelled myofibre on a transverse section. The GFP labelled satellite cells were determined by co-localization of GFP and pax7 antibody signals.

To investigate the overall integration and expression of the GFP transgene in CMV-nucGFP donor transgenic tadpoles, we carried out double immunostaining on cross sections as described above. Cell counting was performed on every other section to avoid counting a cell twice. In total we counted eleven different tails of similar size, and for each individual we counted cells on five sections from each tails. Total nuclei within the myofibres were counted by the blue DAPI signal and satellite cells were determined by pax7 antibody labelling. GFP labelled nuclei within the myofibres were counted by green GFP signals. GFP labelled satellite cells were determined by co-localization of GFP and pax7 antibody signals. For calculation, the number of GFP labelled myonuclei=(number of GFP^+ cells)-(number of $pax7^+$:GFP^+) cells. Number of total myonuclei= (number of $DAPI^+$ cells)-(number of $pax7^+$ cells).

III.2.3 Tadpole myofibre isolation and myonuclei counting

To find out the normal number of myonuclei in each myofibre of a stage 49 tadpole, we isolated individual myofibres. The tail of a stage 49 tadpole was fixed in Zamboni's fixative for 1 hour and washed in PBSAT three times for 10 minutes each. After washing, the tail was incubated in 300 µl of L15 medium

(Invitrogen) containing 0.3 % (w/v) collagenase (Sigma, type I) for 40 minutes at 37°C. Collagenase is used to digest muscle connective tissue and release muscle satellite cells. After 40 minutes digestion, the tail is still visible but it is soft and loose. It was transferred to a slide and immersed in several drops of 1 µg/ml DAPI solution for nuclear staining. A cover slip was then put onto the tail and pressure was applied to spread the tail underneath. At this stage, some of the myofibres were physically freed from the tail. The number of myonuclei was counted using a Leica DMRB microscope. Five tails were used in this assay.

III.3 Results

III.3.1 Three types of neurula-stage mesoderm grafting

To identify the origin of muscle satellite cells before somitogenesis, we labelled the mesoderm of stage 15 stage *Xenopus* embryos by grafting. For donor, we used CMV-nucGFP transgenic embryos, in which all the cells are supposed to be constitutively expressing GFP in their nuclei. Stage 15 was chosen for this assay because this is a stage between gastrulation and somitogenesis in *Xenopus* embryonic development. Moreover, mesoderm of neurula stage embryos is easily isolated and purified by trypsin treatment.

We did three types of mesoderm grafting as shown in the figure 3.1. We raised the grafted embryos to stage 49 tadpoles, and checked the whole mount GFP expression before preparing transverse sections from the tadpoles. The GFP expression domain resulting from each type of grafting was then investigated with GFP antibody staining on sections.

Among the three types of mesoderm grafting, we found that only type I and type II grafts end up within the skeletal muscles of host tadpole tails at stage 49. Based on the observation from serial sections through the GFP labelled region, the type III grafts often go to the body wall or the gut wall of the host tadpoles (100%, n=15). This is consistent with the cell fate map of lateral plate mesoderm that is the cell nature of the type III mesoderm. Therefore, we excluded the type III as origin of satellite cells and expected to locate the mesoderm origin of satellite cells from the type I and/or the type II grafting.

III.3.2 Origin of satellite cells in *Xenopus laevis* using Gargioli's method

Initially, we followed the criteria set by Cesare Gargioli, who had previously performed similar presomitic mesoderm grafting in the lab, to decide the origin of satellite cells (Gargioli and Slack, 2004). When the grafted embryos grew up to tadpole stage, he amputated their tails at the middle of the GFP labelled region. Since the regenerated muscle comes from the muscle satellite cells, he reasoned that if GFP re-expresses in these regenerating tails, the original tails near the amputation site must contain the GFP labelled satellite cells. Therefore, it is possible to find out which type of mesoderm graft contains satellite precursor cells.

This approach, however, turned out to be in vain. We got 58 type I grafted embryos and 40 type II grafted embryos. But only 45 type I embryos and 24 type II embryos were able to survive until stage 49. We amputated their tails and recorded them by photographing each day after amputation until the appearance of GFP fluorescence in the regenerating tails. To observe the expression of GFP and take photographs every day, we immobilized each tail-

amputated tadpole by immersing it in 0.2% MS222 solution for 5-10 minutes. Possibly due to repeated exposure to the MS222 solution, or to the amputation procedure itself, most of the tadpoles died before we could clearly see any GFP expression. From the limited remaining tadpoles, we could not get a conclusive answer.

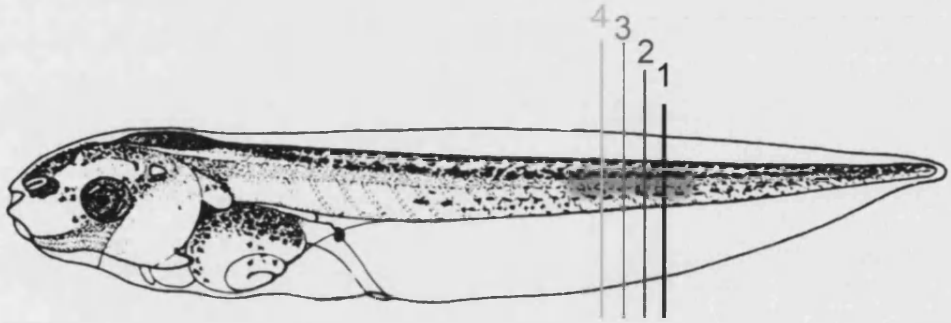

Figure 3.2 Four times tail amputation in a tadpole from type I mesoderm grafting

This tadpole is developed from a type I grafting and subject to 4 amputations. No GFP+ muscle cell was observed in the No.1-3 amputation through the GFP region in the trunk. However, GFP positive muscle fibres appear in the tail regenerate after the fourth amputation. The amputation level is consecutively closer to the anterior of the tadpole trunk.

However, we noticed an interesting case, which is illustrated in Fig. 3.2. We amputated a type I tail at the middle of the GFP expression region. The tail regenerated but without GFP expression in it. Then we cut out its tail at a position a bit further to the original GFP expression region. Again it regenerated without GFP signals. We repeated the tail amputation for another twice. Only when the tail regenerated the fourth time, did we see the GFP fluorescence in the regenerates. It seems that the expression of GFP in the regenerating tails depends on the exact position of cutting site. Regenerated myofibres must have originated from the satellite cells within a certain

distance from the amputation site. If GFP labelled satellite cells are within this distance, we are able to see the GFP expression in regenerates, and vice versa. So the negative GFP expression in the regenerating tails does not necessarily mean that there are no satellite precursor cells in the original grafts.

III. 3.3 Identification of satellite cell origin in *Xenopus laevis* by a new method

Since the Gargioli's method was not reliable in our hands, we figured out another way to decide the origin of satellite cells in the developing embryos. The new method involves a reliable muscle satellite cell marker to label the satellite cells in *Xenopus laevis*. In this experiment, we choose pax7 as the marker. The details of characterization of pax7 as a reliable *Xenopus* satellite cell marker are discussed in chapter IV.

Figure 3.3 shows the strategy of the new method. Briefly, we performed the mesoderm grafting and then raised the grafted embryos to stage 49. At this stage, we used GFP and pax7 antibodies to double immunostain a series of sections through the GFP positive tail. The origin of the satellite cells was decided by the co-localization of pax7 and GFP antibody signals.

Using this method, we found that GFP labelled satellite cells are not evenly distributed along the A-P axis in type I tail. Fig. 3.4 shows a diagram of one example of the distribution of satellite cell along the anterior-posterior axis in a type I grafted tadpole tail. The number of pax7 positive satellite cells in the tail muscle region varies in each section. On average there are about 30 satellite

cells in grafted side of the tail muscle on each 10μm thick section. In the 1250 μm long graft, we only found 12 GFP labelled satellite cells. The distance between the two neighbouring GFP labelled satellite cells varies from 10-350 μm. Usually, at most one GFP positive satellite cell is found per section. So if a satellite cell with GFP signal does not locate close enough to the tail amputation site, it is highly possible that we cannot see GFP expression in regenerates.

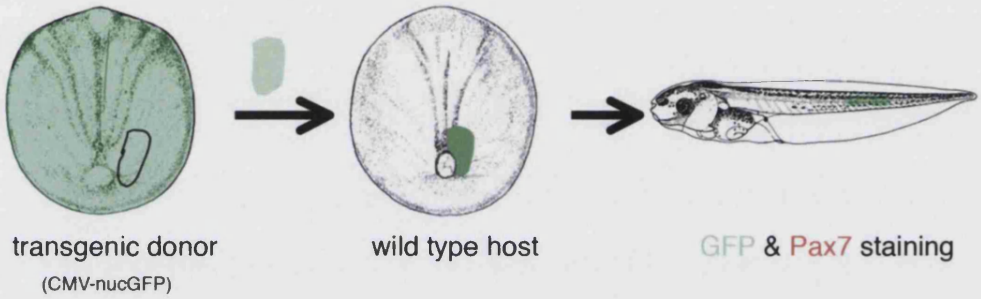

Figure 3.3 Diagram of mesoderm grafting experiment

The diagram shows the procedure of mesoderm grafting experiment. The black circle line indicates the position of mesoderm taken from a CMV driven nuclear GFP transgenic embryo of neurula stage. The isolated mesoderm was then grafted into the same position of a wild type host embryo. When the embryo grows up to tadpole stage, we isolated the green tail region and performed series of cross sections. We used GFP and Pax7 antibodies to double immunostain these sections and counted the number of cells with co-localized antibody signals.

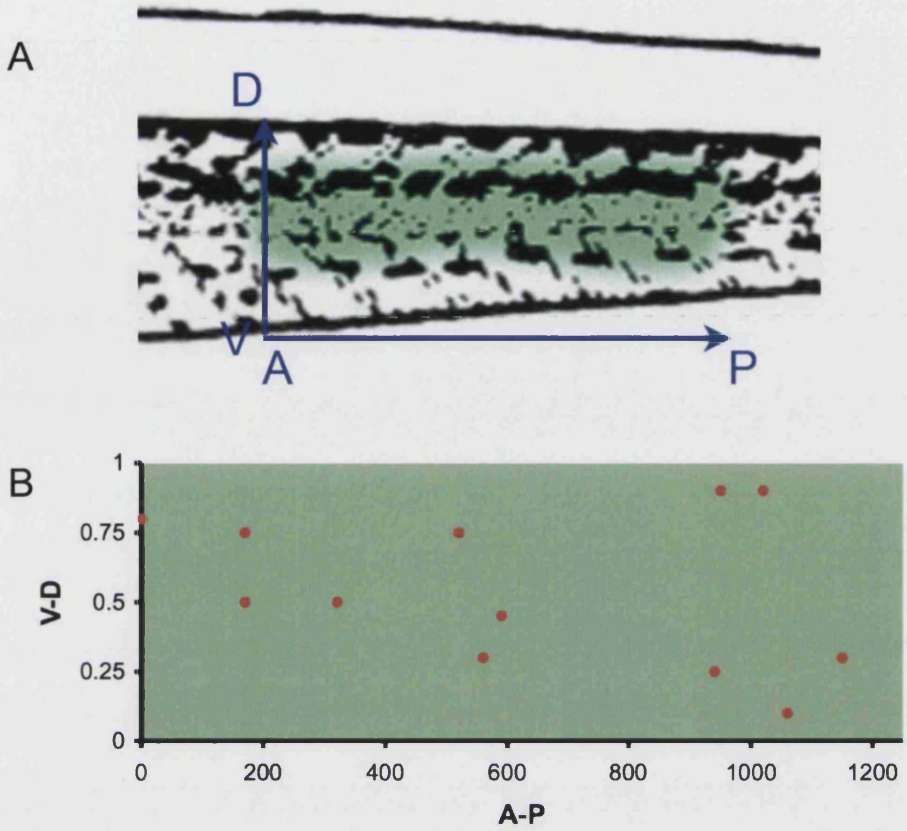

Figure 3.4 Distribution of GFP labelled satellite cells in a type I mesoderm grafted tadpole tail

(A) GFP labelled satellite cells were counted on cross sections based on co-localization of GFP and pax7 immunostaining signals, in a 1250 μm length of GFP+ tail region. (B) Cross sections through this region were analysed according to their position in the anterior-posterior axis of the tail. The first anterior section with GFP+:Pax7+ cell is designated as 0 of the A-P axis. Along the D-V axis in each cross section, 1 stands for the dorsal edge of the muscle block, and 0 stands for the ventral edge of the muscle block. GFP+:Pax7+ satellite cell (red dot) was then plotted with its position in the A-P and D-V axis.

The new method is more reliable to determine the origin of muscle satellite cells. Using this method, we checked all the transverse sections through the GFP+ tails. GFP labelled satellite cells were identified by co-localization of the

pax7 and GFP antibody signals within myofibres on the grafted side. The total number of satellite cells was counted based on the presence of pax7 antibody signals on the grafted side. The GFP labelled myofibres was counted by the presence of green fluorescence in the fibres. As GFP protein diffuses through the cytoplasm, it is possible that not all the nuclei in a green myofibre carry the GFP transgene. This is especially true for fibres near the border of the graft, that are more likely to contain unlabelled nuclei form the host. To correct for this effect, we counted nuclei in *Xenopus* myofibres taken from the same stage as the end point of the satellite cell labelling studies. We found that most myofibres at this stage are mononuclear and some fibres contain at most two nuclei. We assume that each myofibre has an average of 1.5 myonuclei at this stage. So if 50% of myoblasts are expressing GFP in the donor, then 75% of myofibres might be expected to do so. Although this correction cannot accurately reflect an exact GFP labelling situation *in vivo*, it is incorporated in the following cell counting study.

In type I grafts, it is very difficult to find cells with pax7 and GFP positive signals. When we count the number of satellite cells in every 100μm length of the tail (10 sections), at most 1 satellite cell is found to be GFP labelled (Table 3.1, red column). To avoid wasting time, we only counted cells in sections with GFP labelled satellite cell. Based on the quantification from 8 type I tails, we found about 70.2 ± 3.2 % of myofibres in each section are GFP labelled (Table 3.1). The real number of GFP labelled myonuclei is less considering the correction figure described above. In the same sections about 2.0 ± 0.2% of satellite cells are labelled with GFP (Table 3.1).

Table 3.1 Summary of type I mesoderm grafting experiment

	percentage of green myofibres per positive section	percentage of green myonuclei per section after correction	percentage of green satellite cells per positive section	number of green satellite cells per 100μm
Sample 1	85.4%	56.9%	1.0%	1
Sample 2	60.2%	40.1%	2.0%	0.4
Sample 3	70.0%	46.7%	2.0%	0.5
Sample 4	60.3%	40.2%	2.6%	0.5
Sample 5	73.1%	48.7%	1.7%	0.4
Sample 6	74.9%	49.3%	2.0%	0.6
Sample 7	61.4%	40.9%	2.7%	0.6
Sample 8	76.6%	51.1%	1.7%	0.5
Mean	70.2%	46.8%	2.0%	
Standard Error	3.2%	1.2%	0.2%	

In the case of type II grafted tails, it is quite easy to locate GFP positive satellite cells in almost every section through the tail (7.3-14.7 GFP+ satellite cell per 100 μm, table 3.2 red column). The percentage of GFP positive satellite cells in type II grafts is about 5.6 ± 0.8 % in each section and the percentage of the GFP positive myofibres goes down to 33.0±1.2% (Table 3.2). Although the number of GFP positive satellite cells in type II grafts is comparatively much more than that in type I grafts, it is still lower than what we might expect if all satellite cells are entirely derived from region II. Fig. 3.5 represents the typical labelling situation in type I and type II grafts.

Table 3.2 Summary of type II mesoderm grafting experiment

	percentage of green myofibres per positive section	percentage of green myonuclei per section after correction	percentage of green satellite cells per positive section	number of green satellite cells per 100μm
Sample 1	38.8%	25.8%	10.4%	14.7
Sample 2	31.1%	20.7%	5.3%	9.4
Sample 3	34.4%	22.9%	3.9%	8.8
Sample 4	32.4%	21.6%	5.3%	8.2
Sample 5	28.2%	18.8%	5.0%	7.3
Sample 6	34.2%	22.8%	4.1%	10
Sample 7	31.9%	21.2%	5.3%	10
Mean	33.0%	22.0%	5.6%	
Standard Error	1.2%	0.4%	0.8%	

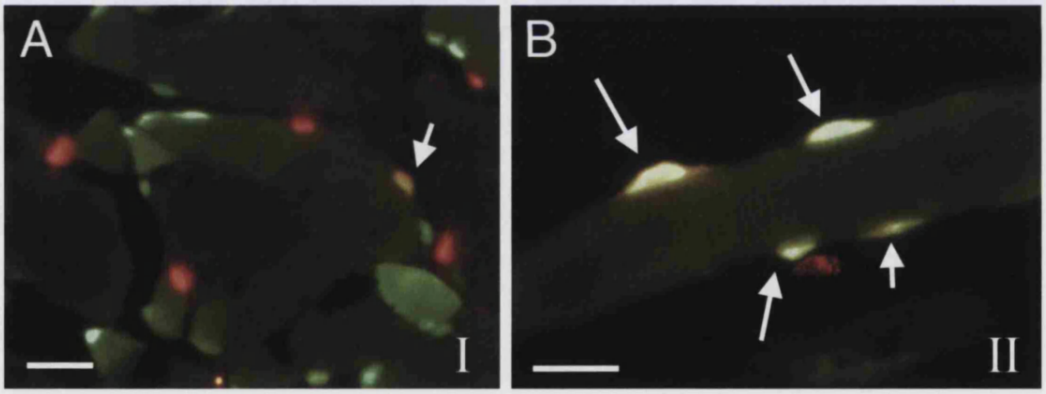

Figure 3.5 Representative immunostaining views of type I and type II grafted muscle

Both sections show the expression of GFP (green) and Pax7 (red) in tail muscle region. The white arrows indicate the cells co-localized with GFP and Pax7 antibody signals. (A) A view of type I grafted muscle. (B) A view of type II grafted muscle. Scale bar: 10 μm.

We thought that the low percentage labelling of satellite cells might be because some satellite cells in tails would come from the anterior mesoderm, since we just grafted the posterior mesoderm. Then we tried a new type of mesoderm grafting which not only combined type I and type II together, but also encompassed anterior mesoderm. This grafted mesoderm is approximately 200 μm wide and 600 μm long which is about half length of a whole neurula embryo. We expected that this larger piece of mesoderm would contain more satellite precursor cells and accordingly increase the percentage of GFP positive satellite cells in host tadpoles.

Grafting a large piece of mesoderm is a very challenging job, because it may cause damage that the embryos are not capable of healing. So most of the grafted embryos did not survive after grafting. Finally, we only got three tadpoles alive. In these tadpoles, the GFP labelled region is about 2/3 length of the whole tail and the percentage of GFP positive myofibres was about 91.7%±1.5%. It is still easy to find the satellite cells with GFP expression in each section. The percentage of GFP positive satellite cells is about 6.9%±0.6%, which remained similar to that of type II grafts (Table 3.3). Moreover, we did not find significant difference in the number of GFP positive satellite cell every 100 μm between type I+II and type II grafts.

Therefore, we reckon that the GFP positive satellite cells in these larger grafts mainly come from the mesoderm of the type II region and their progenitors must be evenly distributed along anterior to posterior type II mesoderm.

Table 3.3 Summary of type I+II mesoderm grafting experiment

	percentage of green myofibres /positive section	percentage of green myonuclei/section after correction	percentage of green satellite cells per positive section	number of green satellite cells per 100 μm
Sample 1	90.1%	60.1%	6.5%	9
Sample 2	90.3%	60.2%	8.2%	8.2
Sample 3	94.8%	63.2%	6.1%	12.8
Mean	91.7%	61.1%	6.9%	
Standard Error	1.5%	0.6%	0.6%	

III.3.4 Detection of overall integration and expression of GFP transgene in the CMV-nucGFP transgenic donor tadpoles

The relatively small percentage of GFP+ satellite cells detected in the grafts raised our suspicion that GFP expression, despite being driven by the supposedly ubiquitous CMV promoter, might get silenced in some of the satellite cells. To test this possibility, we checked the expression of GFP and pax7 on cross sections of CMV-nucGFP transgenic tadpoles, similar to those used as donors. The human cytomegalovirus immediate/early (CMV) promoter is supposed to remain active in all tissues. Surprisingly, we found this is not the case.

Based on cell counting from 11 transgenic tadpoles, we found GFP expression has a tissue preference pattern. We did not count the exact number of GFP positive cells in each tissue or organ except muscle. But it is quite obvious that GFP is not uniformly expressed in spinal cord and intestine. Rarely, a GFP positive cell is detected the mesenchyme in the interstitial space of skeletal muscle. In skeletal muscle, we counted the number of GFP

positive myonuclei and satellite cells. The result is that 89.1%±2.0% myonuclei are GFP positive and 43.0%±4.0% satellite cells are GFP positive. (Table 3.4).

Table 3.4 Cell counting of CMV-nucGFP transgenic tadpole tails

	number of GFP+ myonuclei	number of GFP+ / pax7+ cells
Case 1	91.5%	47.7%
case 2	89.2%	18.8%
case 3	80.4%	74%
case 4	76.3%	48.7%
case 5	98.5%	40.7%
case 6	91.8%	46.3%
case 7	88.4%	42.5%
case 8	92%	32%
case 9	88%	41.7%
case 10	98%	41.7%
case 11	86%	38.4%
Average	89.1%	43.0%
Standard Error	2.0%	4.0%

Taken together, these data shows that GFP expression in transgenic donor embryos has a mosaic pattern even though it is driven by the CMV promoter. The low GFP labelling rate in the muscle satellite cells of CMV-nucGFP transgenic donor could partly account for the low percentage of GFP positive satellite cells from the grafts.

Considering this, the real number of GFP positive satellite cells in the type I or the type II will be more than what we observed. So we corrected the number

of GFP positive satellite cells by dividing the crude figure from the type II grafting with a coefficient. Here, the coefficient is 43.0% which is the mean of the percentage of GFP labelled satellite cells obtained from the cell counting in the GFP donor tadpoles. After correction, the number of green satellite cells in every 100 μm length of the type I tails is about 0.9-2.3. The average percentage of GFP positive satellite cells in the type II tails is 13.0% and there will be about 17.0-34.2 GFP labelled satellite cells in every 100 μm length of the type II tails.

However this is still well short of 100%. Based on our observation on the GFP transgenic donor tadpoles, we noticed that the variation of GFP labelling in satellite cells is very big, from 18.8% to 74%. In most cases, the GFP labelling rates are below 50%. It is highly likely that the donor embryos we used for grafting fall on this situation. Although we correct the labelling figures by a correction coefficient, it still cannot reflect the true labelling situation in each case because it really is a random thing. In addition, we guess the grafting procedure itself will kill a lot of satellite cell precursors, or that some satellite cells come from elsewhere. But we cannot prove these possibilities.

III.4 Discussion

iII.4.1 Gene expression in transgenic tadpoles

The transgenic method developed by Kroll and Amaya is an effective way of introducing genes into *Xenopus* embryos (Kroll and Amaya, 1996). It involves integration of exogenous DNA into sperm nuclei and then injection of these modified sperm nuclei into unfertilised eggs. Since it was developed, this method has been widely used for labelling of specific tissue or organs using

GFP as a marker, in study of the regulation of gene promoters, and especially usefully, in the investigation of later developmental events during *Xenopus* organogenesis. One of the advantages of this gene delivery system is that a transgene is integrated into the male genome before fertilization. So embryos generated by this method are supposed to inherit the transgene in every single cell.

We have taken advantage of this technique to label mesoderm using CMV-nucGFP grafts to investigate the origin of satellite cells in tail muscle. Compared with other cell labelling methods, such as injection of GFP mRNA or vital dyes, in which the injected RNA or dyes will be degraded or diluted within 2-3 days after injection, the transgenic method allows GFP driven by CMV promoter to be constitutively expressed in all cells from gastrula to tadpoles, if the transgene integration occurs before the first embryo cleavage.

However, our findings in CMV-nucGFP transgenic donor tadpoles did not fit this expectation. We checked the GFP expression of 11 CMV-nucGFP transgenic tadpoles that are randomly selected from three separate batches of transgenics by antibody staining on tissue sections. The result shows that GFP is not uniformly expressed at all. There are few GFP+ cells in the interstitial space of skeletal muscle. These cells could be blood cells, fibroblasts and schwann cells suggested by our EM study in chapter IV. In skeletal muscle, the situation is much better, but still only 89.1%±6.6% of myonuclei are GFP+ and less than 50% of the satellite cells are labelled with GFP.

This mosaic expression pattern of GFP in transgenic tadpoles does not result from delayed DNA integration after the first cleavage. This sometimes occurs, but is easily detected because the GFP is expressed on either left or right side. Mosaic expression of transgene could be caused by insertion-site effects, which is caused by the inactivation of a gene in some cells through its abnormal juxtaposition with heterochromatin (position effect variegation) (Dobie et al., 1997). But this does not explain the situation in the cells located in the interstitial space between muscle fibres where no expression of GFP was seen at all. So far, we do not have a satisfactory explanation, although it seems that there is some selectivity of expression based on cell type, some random silencing, and some variation between individual tadpoles perhaps dependent on insertion site.

Based on our observations, we can draw a conclusion that GFP can be silenced even if CMV promoter drives its expression. The silencing frequency is relevant to the cell types. In skeletal muscles, about 10% of myonuclei are GFP negative, whereas about 57% of the satellite cells are GFP negative. Our previous study has shown that there are two types of satellite cells in skeletal muscle during development, the quiescent satellite cells and the activated satellite cells. The quiescent satellite cells are transciptionally less active than the activated one, and perhaps more liable to silencing of GFP transcription. The satellite cells with GFP signals in muscle could be the activated ones that released from the silencer and re-entering cell cycles. As to the myonuclei, the difference of gene transcription between myonuclei within a myofibre has been observed before. Newlands et.al detected that genes are not uniformly

expressed in all the myonuclei within each myofibre by detection of muscle specific endogenous genes, muscle specific transgenes and a ubiquitously expressed transgene. They also noticed that he number of myonuclei expressing the genes of interest declines as muscle matures (Newlands et al., 1998).

In all, the CMV promoter is not as ubiquitous as we thought, and the CMV-nucGFP transgenic technique is not ideal for labelling of satellite cells. We had considered using the Cre-lox system to permanently label mesoderm cells. However, that will require a suitable promoter which is able to label all myogenic mesoderm cells in neurula stage embryos. Unfortunately we still cannot find such a promoter. Taking everything into account, the method we used seems to be the only currently available way to find out the origin of muscle satellite cells in *Xenopus laevis*, although it is not perfect.

III.4.2 Satellite cell origin in *Xenopus laevis*

In spite of the low efficiency of satellite cell labelling by the transgenic method, we were able to show that the muscle satellite cells are predominately derived from type II mesoderm rather than type I mesoderm before somitogenesis.

In *Xenopus laevis*, most cells in the somite constitute the myotome that gives rise to skeletal muscle (Chanoine and Hardy, 2003). Figure 3.6 shows a diagram of the distribution of the neurula stage type I and type II mesoderm at stage 32. Cells within the type I mesoderm populates about 2/3 of cells in somites. These cells constitute the dorsal and middle region of mature somites (stage 32) as shown in Figure 3.6 A and B. Cells in type II mesoderm

accounts for about 1/3 of cells in the somites. They mostly are located at the ventral part of somites (Fig.3.6 C-E). In addition, we observed 66.7% cases of type II mesoderm cells go to the dorsomedial lip of the somite (see Fig. 3.6 C and D). These cells are reminiscent of the *pax7* expressing cells in the dorsomedial lip of somites at this stage, which will be described in chapter IV. At stage 16, we also found *pax7* transcripts in the type II mesoderm. If *pax7* expression is really related to satellite cell formation, the cells located in the region II mesoderm and subsequently in the dorsomedial lip of somites are probably the source of satellite cells. But we do not claim this is the only source of satellite cells.

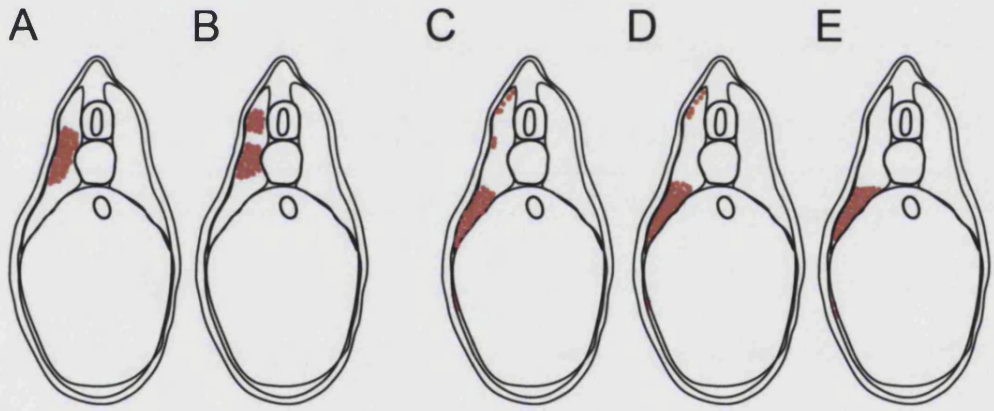

Figure 3.6 Diagram of labelling pattern of Type I and Type II mesoderm at stage 32

(A-E) Reconstruction of labelling pattern on transverse sections of stage 32 embryos. The drawing was based on observations of the type I and type II grafted embryos and the C3/C4 blastomere injections with RDA (chapter V). Red dots indicate the labelling distribution. (A and B), two typical labelling patterns of the type I mesoderm at stage 32. (C-E), three typical labelling patterns of the type II mesoderm at stage 32.

In mouse and chick, muscle satellite cells are derived from the pax3/pax7 positive cells in the central dermomyotome (Gros et al., 2005; Relaix et al., 2005). But the authors of those studies were not able to locate this cell population in the presomitic mesoderm, since pax3 and pax7 are not expressed before somitogenesis in mouse and chick mesoderm. The dermomyotome in *Xenopus* embryo is a sheet of cells on the superficial surface of the somites (Grimaldi et al., 2004). This layer arises shortly after somitogenesis and express pax3. It is suggested that proliferating cells at the dorsomedial and ventrolateral lips of *Xenopus* somite will contribute to dermomyotome, as this is what occurs in the chick somite (Grimaldi et al., 2004; Ordahl et al., 2001). Our type II mesoderm can label the dorsomedial and ventrolateral lips of the somites, which means that the cells within type II mesoderm might constitute the dermomyotome in *Xenopus* embryos. Based on these observations, we propose a process for the developmental origin of satellite cells in *Xenopus laevis*. Before somitogenesis, the precursors of satellite cells in *Xenopus* originate from the lateral presomitic mesoderm. As somitogenesis takes place, these cells will go to the dermomyotome. Later, they will migrate to fully differentiated myofibres and become satellite cells resting on myofibres.

IV. Characterization of *pax7* expression in *Xenopus laevis*

IV.1 Introduction

Muscle satellite cells are located in dentations between the basement membrane and plasma membrane of myofibres, while myonuclei lie within the plasma membrane of myofibres (Mauro, 1961). Although the muscle satellite cells were first discovered in frogs, no molecular markers specific to *Xenopus* satellite cells have been reported yet. Most of the satellite cell markers identified so far are used in mammals and some of them are applied to avian and fish. Shortage of reliable satellite markers hinders our *in vivo* study of this cell population in *Xenopus* tadpoles. To trace the origin of the satellite cells in *Xenopus* development, we felt it is necessary to find a reliable molecular marker of the muscle satellite cell in *Xenopus*. Once we have verified a suitable marker of muscle satellite cells in *Xenopus* by electron microscopy, we will be able subsequently to identify the satellite cells by antibody labelling in the light microscope.

One of the important satellite cell markers used in mammals is pax7. Pax7 belongs to a paired-box (Pax) family of transcription factors. It was first isolated as a gene product specifically expressed in cultured myoblasts derived from muscle satellite cells. The expression pattern study shows that it is exclusively expressed in the muscle satellite cells in adult mice (Seale et al., 2000). Luckily, there is a pax7 antibody available from DSHB and it works on *Xenopus* laevis. Cesare Gargioli had used this antibody, but did not prove

that it would label the satellite cells. Thus, we first used Immuno-electron microscopy with pax7 antibody to check whether it is a reliable marker of muscle satellite cells in *Xenopus* tadpoles. Then we cloned the homologue of *pax7* in *Xenopus* and used it to carry out expression studies by *in situ* hybridisation.

IV.2 Materials and Methods

For the Immuno-Electron Microscopy (IEM) study, stage 49 tadpoles were first fixed in Zamboni's fixative containing 0.5% Glutaraldehyde (Sigma) overnight at 4°C, washed in PBSA and embedded in 5% low melting agarose (Sigma). 100 µm transverse sections were cut with a Leica vibratome and then immunostained by the ABC method as described in chapter II except using 0.05% Triton X-100 in PBSA for permeabilization. Following this, the vibratome sections were washed in PBSA three times for 15 minutes each, and post-fixed in osmium tetroxide (1% w/v) in 0.1M Sodium Cacodylate buffer (pH7.6.) for 1 hour. The post-fixed sections were dehydrated in a series of ethanols, embedded in Epon resin (TAAB) and incubated in an oven at 70°C for 7 hours. The resulting polymerized resin blocks were trimmed and transversely sectioned with a Reichert Ultracut-E ultramicrotome (Leica, Vienna, Austria). 100 nm thick sections were collected onto copper grids, some being stained with uranyl acetate and lead citrate, and examined under a JEOL JEM1200EX transmission electron microscope (JEOL, Tokyo, Japan). Normally the diameter of one nucleus is about 5-6 µm long. Due to the narrow spacing between each section (100 nm), we counted nuclei only in one

section from each resin block. In total we examined 5 tadpole tails, with 2 sections from each tail.

IV. 3 Muscle satellite cell markers in *Xenopus laevis*

IV.3.1 Pax7 is a reliable marker of muscle satellite cells in *Xenopus* tadpoles

We performed immuno-electron microscopy (IEM) with pax7 antibody. The morphological criteria described above enable us to distinguish between the nuclei of satellite cells and the myonuclei by transmission electron microscopy.

Fig. 4.1 A and B show muscle satellite cells that are squeezed between the basal lamina (indicated by arrows in Fig 4.1C and D) and the plasma membrane. The positive Pax7 antibody signals visualized by black electron dense dots concentrate in the nuclei of the satellite cells. In contrast, no pax7 antibody reactivity is detected in the myonuclei (Fig. 4.1E). Among 25 muscle satellite cells from five individual tails, 22 cells were found positive for pax7 (88%, n=25); by contrast all the myonuclei identified are negative for pax7 (0%, n=41; table 4.1). As negative control, tadpole tail sections stained by the same procedure but omitting the pax7 antibody do not show any electron dense granules in the nucleus (data not shown). Thus, we are able to consider pax7 as a reliable muscle satellite cell marker in the tail of *Xenopus* tadpole.

Occasionally the pax7 antibody positive signals are also found in some other cell types in tadpole tail, outside of the muscle fibres. These cells are

identified based on their characteristic structures as described in the Boston University ultrastructure website (http://www.bu.edu/histology/m/t_electr.htm). The pax7 antibody signal is present in the nucleus of Schwann cells whose cell membrane forms myelin coils around the axon (Fig. 4.1F). A lymphocyte that is characterized by its nucleus filling virtually the entire volume of the cell is also found to be positive (Fig. 4.1G). Moreover, a faint pax7 positive signal is located in the nucleus of a fibroblast surrounded with collagen fibrils (Fig. 4.1H). This shows that not every pax7 positive cell in the tail is necessarily a satellite cell.

Table 4.1 Summary of Immuno-electron microscopy study with pax7 labelling

	pax7		
	+	-	Number
Satellite cell	22 (88%)	3 (12%)	25
Myonucleus	0	41 (100%)	41

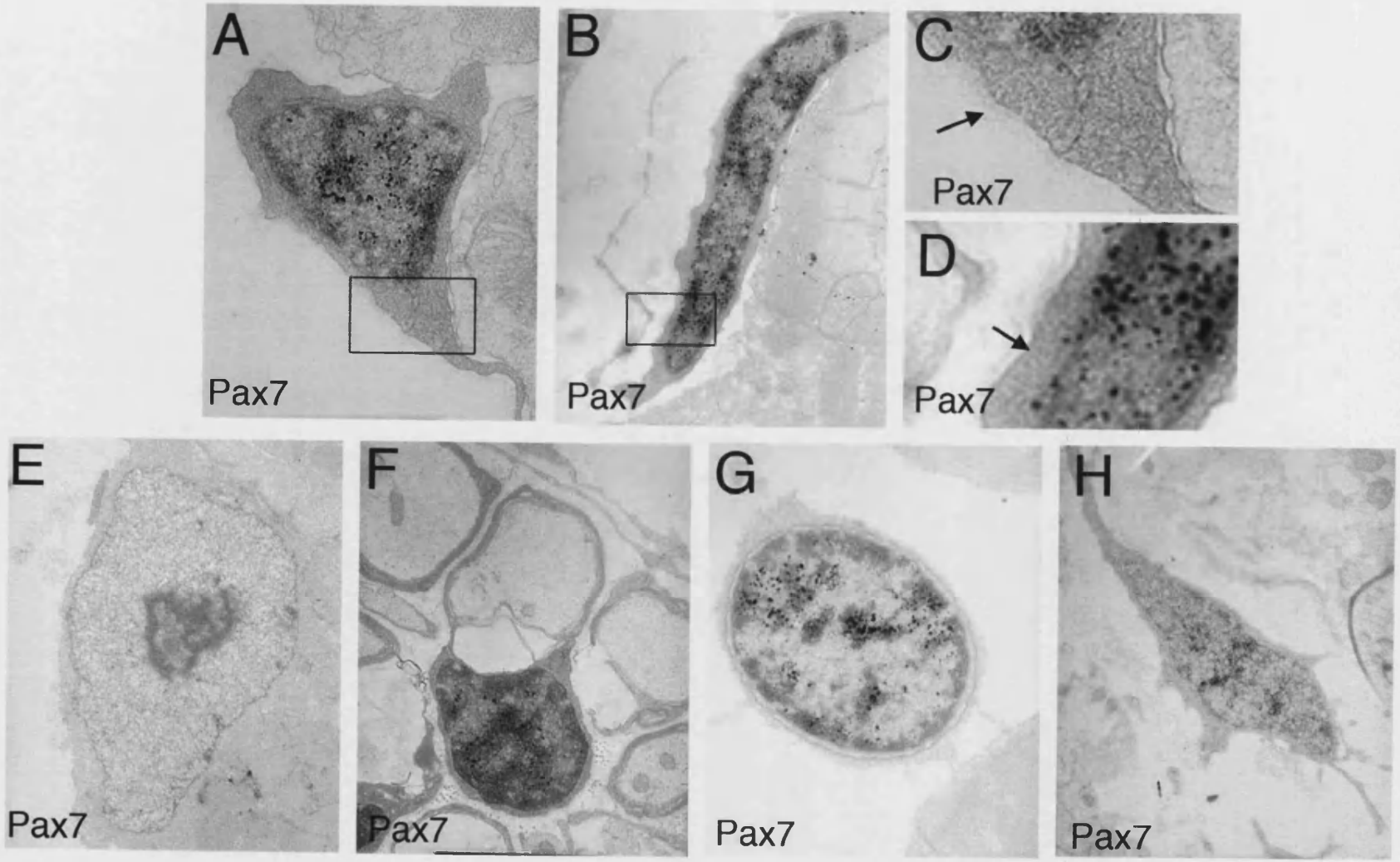
A
Pax7
B
Pax7
C
Pax7
D
Pax7
E
Pax7
F
Pax7
G
Pax7
H
Pax7

Figure 4.1 Immuno-Electron microscopy study of pax7 labelling in tadpole tail

(A,B) Satellite cells with pax7 antibody labelling in the nucleus. Magnification ×20,000

(C,D) High-power views of black box regions of A and B, respectively. The basement membrane is indicated by arrows in C and D.

(E) A myonucleus negative for pax7 signal. Magnification ×15,000

(F) A Schwann cell with pax7 antibody labelling in the nucleus. Magnification × 20,000

(G) A lymphocyte located between myofibres is positive for pax7 labelling signals. Magnification × 6,000

(H) A fibroblast in the muscle connective tissues has a faint signal. Magnification ×20,000

IV.3.2 NCAM is a marker of muscle satellite cells in tadpole tail

Several other molecules, including neural cell adhesion molecule (NCAM), c-met, m-cadherin, pax3 and myf5, have also been used to identify satellite cells in various experimental approaches (Chargé and Rudnicki, 2004), so we also checked the expression of these candidates in *Xenopus*.

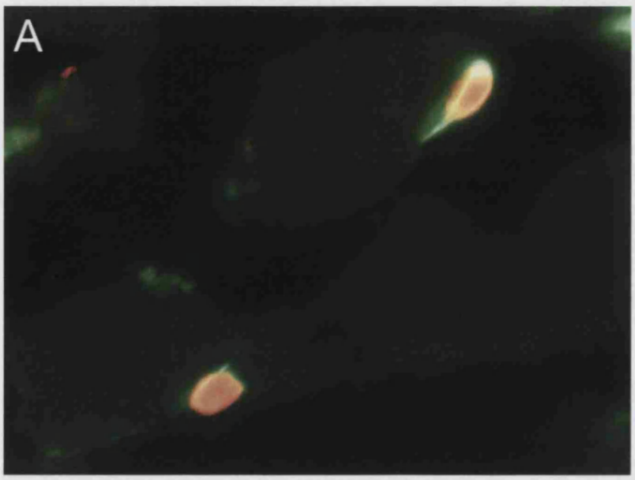

Figure 4.2 Double immuno-staining of tadpole muscle with NCAM and pax7 anti-bodies

(A) A muscle section of tadpole tail was double immunostained with NCAM (green) and Pax7 (red) antibodies.

Two different NCAM antibodies have been tested on tadpole tail sections. One is a monoclonal antibody purchased from DSHB and the other is a polyclonal antibody produced in rabbit from Chemicon™. The results show that there are very few cells labelled with the NCAM monoclonal antibody. Since pax7 and NCAM monoclonal antibodies are both of mouse origin, we are not able to determine whether the NCAM antibody labelled cell is a muscle satellite cell by double immunostaining. However, when the NCAM polyclonal antibody was used, we found there are more cells with cell membrane staining in the muscle region. By co-immunostaining them with pax7 antibody, we have confirmed that these cells are muscle satellite cells

(Fig. 4.2). We also tested c-met (Santa Cruz), m-cadherin (Abcam), pax3 (DSHB) and myf5 (Santa Cruz) Antibodies. But all these antibodies do not work on *Xenopus laevis* tissue. Therefore, the polyclonal NCAM antibody is another useful reagent for our study on the satellite cells in *Xenopus laevis*.

IV. 3.3 Discussion

We need a good molecular marker for *Xenopus* satellite cells, because it is impossible to reliably identify a satellite cell under light microscope by morphology alone. We have established the suitability of pax7 as a satellite cell marker by combining nuclear pax7 antigen expression with morphological observations of satellite cells by electron microscopy. As shown in Fig. 4.1 and our statistical analysis, the immuno-electron microscope result proves that pax7 is a very good satellite cell marker. The observation that 88% of morphologically identified satellite cells express pax7 would allow us to pick up most of satellite cells in a cell population. The minority of negative cells are presumably those that have commenced differentiation to myoblasts. Despite the occasional expression of pax7 in other cell types, expression of pax7 in myonuclei is never found, providing a very clear discrimination between the satellite cells and myofibres themselves.

The NCAM polyclonal antibody from Chemicon™ is the only other satellite cell marker antibody that works in *Xenopus* tissue. But its efficiency at recognising satellite cells is slightly lower than pax7, because about 10% of pax7 expressing satellite cells are negative for NCAM staining. Furthermore, morphologically muscle satellite cells are characterised by a high nuclear to cytoplasmic ratio. Therefore it is preferred to detect nuclear staining of

satellite cells by pax7 antibody than cytoplasmic or cell membrane staining with NCAM antibody. For these reasons, we consider pax7 is the most reliable marker of muscle satellite cells in *Xenopus*.

III. 4 Expression pattern of *pax7* in *Xenopus laevis*

III. 4.1 Cloning of *Xenopus pax7* gene

The above studies confirmed that pax7 is the best satellite cell maker available in *Xenopus laevis*. Together with what we know about pax7 in the mouse, this also suggests that pax7 may play an important role in satellite cell development. To further study its function, we decided to isolate a *pax7* homologue in *Xenopus laevis*. Since the coding sequence of *Xenopus laevis pax7* was available in the NCBI database (NCBI: AY 725267), we designed a pair of primers that specifically target the sequence. Using cDNA of stage 25 embryos as DNA template, we obtained a 2kb DNA fragment containing the whole coding region of *Xenopus pax7* by PCR.

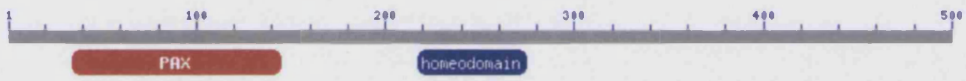

Figure 4.3 Diagrams of *Xenopus laevis* pax7 protein sequence.

Xenopus pax7 contains 500 amino acids. The position of the Pax domain and the homeodomain are illustrated by red and blue respectively.

Xenopus pax7 encodes a protein of 500 amino acids. At the amino-terminal end, it contains a conserved DNA-binding domain, the paired-box (Pax) domain. In addition, it has a homeobox DNA binding domain (Fig 4.3). At the amino acid level, *Xenopus* pax7 is 90% identical to chicken pax7, 89% to mouse pax7 and 82% to human pax7 (Fig 4.4). This high identity suggests pax7 has a conserved function in evolution.

```
Pax7_human        MAALPGTVPRMMRPAPGQNYPRTGFPLEVSTPLGQGRVNQLGGVFINGRPLPNHIRHKIV 60
Pax7_mouse        MAALPGAVPRMMRPGPGQNYPRTGFPLEVSTPLGQGRVNQLGGVFINGRPLPNHIRHKIV 60
Pax7_chick        MAALPGTVPRMMRPAPGQNYPRTGFPLEVSTPLGQGRVNQLGGVFINGRPLPNHIRHKIV 60
Pax7_Xenopus      MAALPGTIPRMMRPAPGQNYPRTGFPLEVSTPLGQGRVNQLGGVFINGRPLPNHIRHKIV 60
                  ******::******.**************************************************

Pax7_human        EMAHHGIRPCVISRQLRVSHGCVSKILCRYQETGSIRPGAIGGSKPRQVATPDVEKKIEE 120
Pax7_mouse        EMAHHGIRPCVISRQLRVSHGCVSKILCRYQETGSIRPGAIGGSKPRQVATPDVEKKIEE 120
Pax7_chick        EMAHHGIRPCVISRQLRVSHGCVSKILCRYQETGSIRPGAIGGSKPRQVATPDVEKKIEE 120
Pax7_Xenopus      EMAHHGIRPCVISRQLRVSHGCVSKILCRYQETGSIRPGAIGGSKPR-VATPDVEKKIEE 119
                  ********************************************** ************

Pax7_human        YKRENPGMFSWEIRDRLLKDGHCDRSTVPS--VSSISRVLRIKFGKKEEEDEADKKEDDG 178
Pax7_mouse        YKRENPGMFSWEIRDRLLKDGHCDRSTVPS--VSSISRVLRIKFGKKEDDEEGDKKEEDG 178
Pax7_chick        YKRENPGMFSWEIRDRLLKDGHCDRSTVPS--VSSISRVLRIKFGKKEEEEDCDKKEEDG 178
Pax7_Xenopus      YKRENPGMFSWEIRDRLLKDGHCDRSSVPSGLVSSISRVLRIKFGKKEEDDDCDKKEEDG 179
                  ***************************:***  *****************:::: ****:**

Pax7_human        EKKAKHSIDGILGDKGNRLDEGSDVESEPDLPLKRKQRRSRTTFTAEQLEELEKAFERTH 238
Pax7_mouse        EKKAKHSIDGILGDKGNRLDEGSDVESEPDLPLKRKQRRSRTTFTAEQLEELEKAFERTH 238
Pax7_chick        EKKAKHSIDGILGDKGNRLDEGSDVESEPDLPLKRKQRRSRTTFTAEQLEELEKAFERTH 238
Pax7_Xenopus      EKKAKHSIDGILGDKGNRIDEGSDVESEPDLPLKRKQRRSRTTFTAEQLEELEKAFERTH 239
                  ******************:*********************************************

Pax7_human        YPDIYTREELAQRTKLTEARVQVWFSNRRARWRKQAGANQLAAFNHLLPGGFPPTGMPTL 298
Pax7_mouse        YPDIYTREELAQRTKLTEARVQVWFSNRRARWRKQAGANQLAAFNHLLPGGFPPTGMPTL 298
Pax7_chick        YPDIYTREELAQRTKLTEARVQVWFSNRRARWRKQAGANQLAAFNHLLPGGFPPTGMPTL 298
Pax7_Xenopus      YPDIYTREELAQRTKLTEARVQVWFSNRRARWRKQAGANQLAAFNHLLPGGFPPTGMPAL 299
                  ************************************************************:*

Pax7_human        PPYQLPDSTYPTTTISQDGGSTVHRPQPLPPSTMHQGGLAAAAAAADTSSAYGARHSFSS 358
Pax7_mouse        PPYQLPDSTYPTTTISQDGGSTVHRPQPLPPSTMHQGGLAAAAAAADTSSAYGARHSFSS 358
Pax7_chick        PPYQLPDSTYPTTTISQDGGSTVHRPQPLPPSTMHQGGLAAAA-AADSSSAYGARHSFSS 357
Pax7_Xenopus      PHYQLPDSSYSAASLGQDVGSTVHRPQPLPPSSMHQGGLS----AADTGSAYGARHSFSS 355
                  * ******:*.:::::.** ************:******:    ***:.***********

Pax7_human        YSDSFMNPAAPSNHMNPVSNGLSP----------------------QVMSILGNPSAVPP 396
Pax7_mouse        YSDSFMNPGAPSNHMNPVSNGLSP----------------------QVMSILSNPSAVPP 396
Pax7_chick        YSDSFMNAAAPANHMNPVSNGLSPQKQGAQNKMQCSRWNLTIALNNQVMSILSNPSGVPP 417
Pax7_Xenopus      YSDTFINPGGPSNHMNPVNNGLSP----------------------QVMSILNSPGGVGP 393
                  ***:*:*...*:******.*****                       ******..*..* *

Pax7_human        QPQADFSISPLHGGLDSATSISASCSQRADSIKPGDSLPTSQAYCPPTYSTTGYSVDPVA 456
Pax7_mouse        QPQADFSISPLHGGLDSASSISASCSQRADSIKPGDSLPTSQSYCPPTYSTTGYSVDPVA 456
Pax7_chick        QPQADFSISPLHGGLDTTNSISASCSQRSDSIKSVDSLPTSQSYCPPTYSTTSYSVDPVA 477
Pax7_Xenopus      QSQSDFSISPLHGGLETSNSLSASCSQRSDSIKSVDSLSTSQSYCAPTYSSSGYSMDPVA 453
                  *.*:************:::.*:*******:****. ***.***:**.****::.**:****

Pax7_human        GYQYGQYGQSECLVPWASPVPIPSPTPRASCLFMESYKVVSGWGMSISQMEKLKSSQMEQ 516
Pax7_mouse        GYQYSQYGQT-AVDYLAKNVSLSTQR-----------RMKLGEHSAVLGLLPVETGQAY- 503
Pax7_chick        GYQYGQYGQT-AVDYLTKNVSLSTQR-----------RMKLGEHSAVLGLLPVETGQAY- 524
Pax7_Xenopus      SYQYGQYGQT-AVDYLAKNVSLSTQR-----------RMKLGDHSAVLGLLPVETGQAY- 500
                  .***.****: .:   :. *.:.:             ::  *   ::  :  :::.*

Pax7_human        FT 518
Pax7_mouse        --
Pax7_chick        --
Pax7_Xenopus      --
```

Figure 4.4 ClustalW alignment of pax7 homologues

Pax7 protein sequences of mouse, human, chick and *Xenopus laevis* were aligned online with ClustalW program. "*" denotes identical residues in all four sequences. ":" indicates conserved substitutions. "." means semi-conserved substitutions.

IV.4.2 Expression pattern study of *Xenopus pax7*

Although the *Xenopus laevis pax7* gene sequence had been published online for several years, its expression pattern and function in *Xenopus laevis* remained unknown. Thus we first carried out an expression pattern study of *Xenopus pax7* by whole mount *in situ* hybridization. In the *Xenopus* embryo, *pax7* transcripts are first detectable at stage13 as two bilateral stripes in the neural plate (Fig. 4.5A). At stage 16, *pax7* is expressed in the neural folds with the highest intensity in the anterior (Fig. 4.5B). Transverse sections of the anterior region show that the expression domain is in the sensorial layer of the neural ectoderm and the dorsal lateral somitic mesoderm (inset in Fig. 4.5B). As the neural folds fuse, *pax7* transcripts become restricted to the future brain (Fig. 4.5C). At tailbud stage, *pax7* expression in the head extends from the forebrain to the hindbrain and by stage 35 to the whole spinal cord. The transcripts in the spinal cord are all concentrated on the dorsal side (Fig. 4.5G, J, L). From the early tailbud stage, two semi-circles of *pax7* expression in head mesenchyme cells are evident surrounding the eye (Fig. 4.5D-F). Cross and horizontal sections show that it is expressed in the mesenchyme cells in the dorsal and anterior region of the developing eye (Fig. 4.5H, M, N). Moreover, *pax7* transcripts are also detected in the pituitary anlage (Fig. 4.5F inset and Fig. 4.5I) and in the pronephric anlage (Fig. 5.5E and J). A horizontal section through the pronephric anlage shows that two strips of *pax7* transcripts are present in the posterior region (Fig. 4.5 J, K).

The segmented expression pattern of *pax7* is obvious in anterior dorsal lateral somites starting from stage 19 (inset in Fig.4.5 C). A series of faint chevrons

of *pax7* expression appear in the trunk region of early tailbud stage embryo (Fig. 4.5D), and intensify as embryo develops (Fig. 4.5D-F). Para-sagittal section shows that *pax7* is expressed in scattered cells at the anterior and posterior edges of individual somites (Fig. 4.5N) and a slight random scatter of cells in the undifferentiated presomitic mesoderm of the tail bud (Fig. 4.5O).

At later tadpole stages, *in situ* probes are unable to penetrate the tadpole skin, rendering detection of *pax7* expression impractical by whole mount *in situ* hybridization. Therefore we used an anti-pax7 monoclonal antibody to detect expression of pax7 protein on paraffin sections. Consistent with our *in situ* results, the immunohistochemistry study shows that high levels of pax7 expression are present in the forebrain (data not shown), midbrain (Fig. 4.6A), hindbrain (Fig. 4.6B), and dorsal spinal cord (Fig. 4.6C). Moreover, pax7 is expressed in the eye muscle and pituitary gland (Fig. 4.6D, A). The cells with pax7 positive signals in the tadpole trunk and tail muscle are flat, peripheral, and squeezed beneath the basement membrane as revealed by laminin antibody staining (Fig. 4.6E). This is consistent with EM study that shows the satellite cell with pax7 expression is located beneath the basement membrane.

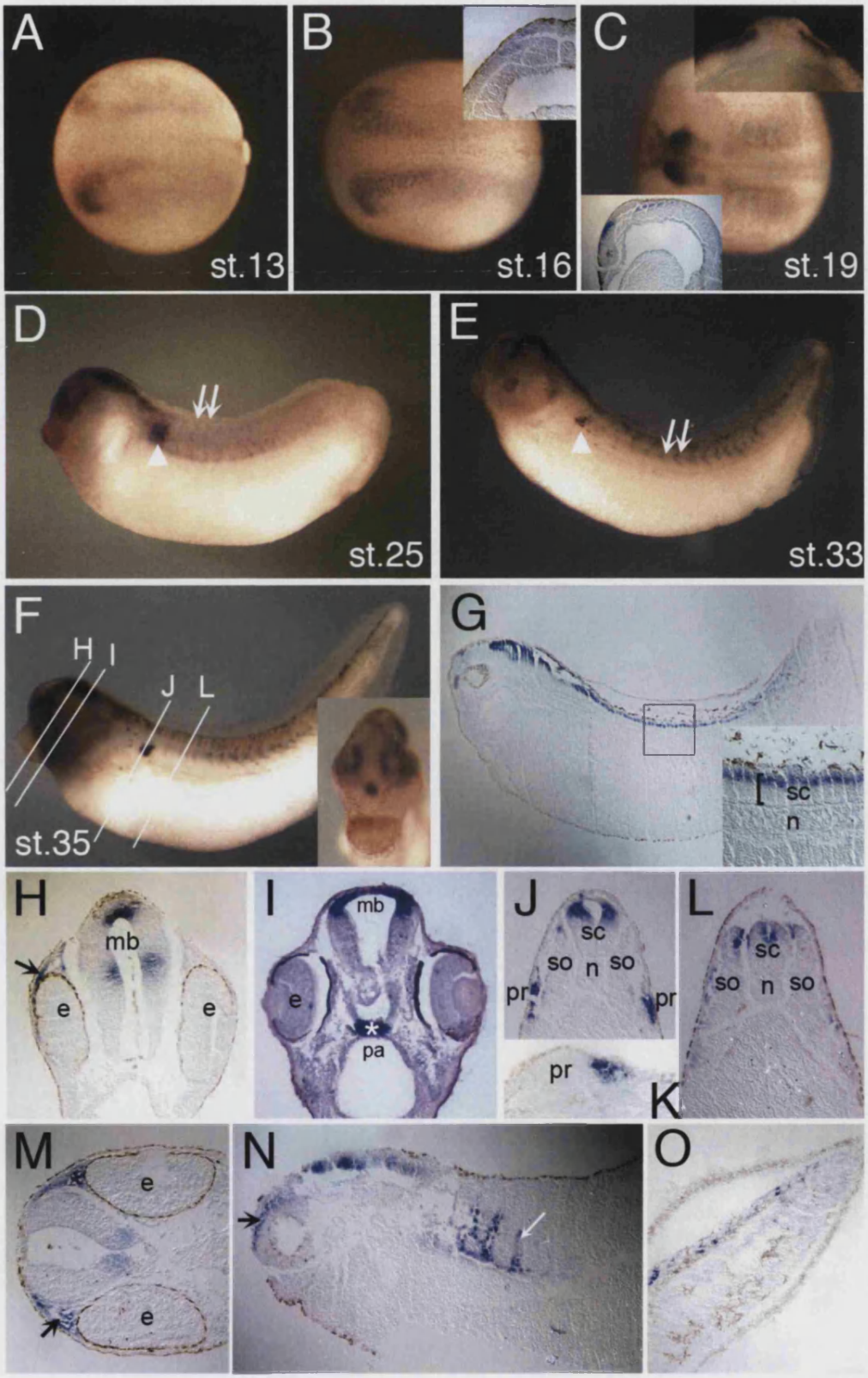
A
st.13
B
st.16
C
st.19
D
st.25
E
st.33
F
H
I
J
L
st.35
G
sc
n
H
mb
e
e
I
mb
e
pa
J
sc
so
n
so
pr
pr
pr
K
L
sc
so
n
so
M
e
e
N
O

Figure 4.5 Expression pattern of *pax7* in *Xenopus* early development.

Whole mount in situ hybridization was performed with the *pax7* antisense RNA probe.

(A-C) Dorsal view of stage 13 (A), stage 16 (B) and stage 19 (C) embryos, anterior to left. The inset in (B) is an anterior transverse section of a stage 16 embryo, showing that *pax7* is expressed in the sensorial layer of neural ectoderm and in the lateral plate mesoderm. The inset at the bottom left corner in (C) shows the segmented pattern of *pax7* expression in stage 19 embryo. The inset on the top right corner is a view of an anterior transverse section.

(D-F) Lateral view of stage 25, 33, 35 embryos, anterior to left. The arrowheads in (D, E) mark the expression domain of *pax7* in the pronephros. Arrows in (D, E) show the chevron pattern of *pax7* expression in somites. The inset in (F) is an anterior view of stage 35 embryo. The lines in (F) indicate the relative position of cross section planes in (H-J, L). (G) Sagittal section of stage 35 embryos. The inset indicates the transcripts of *pax7* in spinal cord concentrated on the dorsal side. *Pax7* expression in the pituitary anlage is marked by an asterisk in (I).

(K) Para-sagittal section of stage 35 embryo showing *pax7* transcripts in posterior pronephric anlage. (M) Horizontal section of stage 35 embryo head. (N) Parasagittal section of stage 35 embryo. The black arrow in (H,M and N) indicates the mesenchyme cells with *pax7* expression anterior to the eye. The white arrow in (N) indicates that *pax7* transcripts locates in the edges of myotomes. (O) Para-sagittal view of the tail of stage 35 embryo. Abbreviations: e, eye; mb, midbrain; n, notochord; pa, pituitary anlage; pr, pronephros; sc, spinal cord; so, somite.

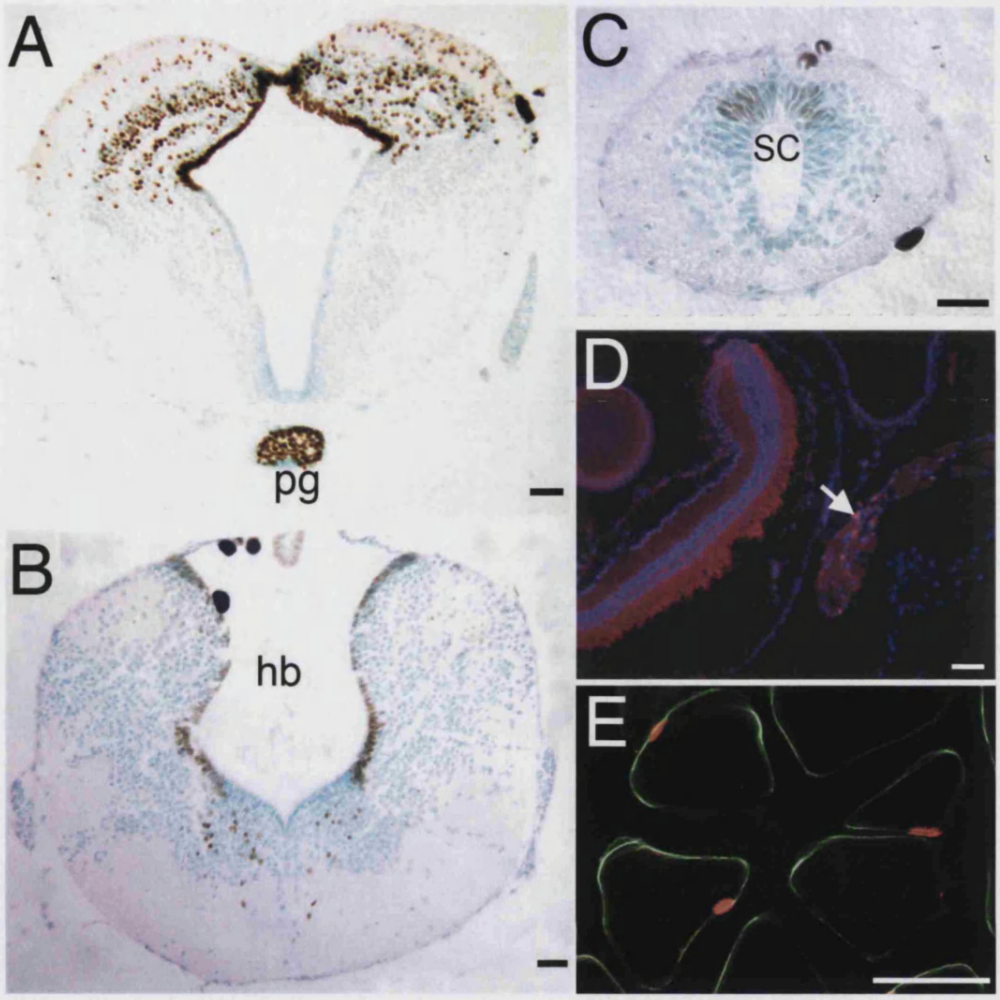

Figure 4.6 Pax7 antibody detection in stage 46 tadpole.

Immunostaining with anti-pax7 monoclonal antibody was carried out on transverse sections of stage 46 tadpoles. (A, B and C) Detection of pax7 with DAB staining (brown). The tissues were counter stained with 0.5% methyl green solution. (A) midbrain; (B) hindbrain; (C) spinal cord. (D) Immunostaining of pax7 (red) and DAPI (blue) on cross section of tadpole head. The arrow in (D) indicates expression of pax7 in eye muscle. (E) Co-immunostaining of pax7 (red) and Laminin (green) on cross section of tadpole tail muscle. Abbreviations: hb, hindbrain; mb, midbrain; pg, pituitary gland; sc, spinal cord. Scale bars, 20 μm.

Furthermore, we checked the expression of *pax7* in different tissues or organs of *Xenopus* adults by RT-PCR. As shown in Fig. 4.7, *pax7* continues to be expressed in adult brain and muscle. Apart from that, *Xenopus pax7* is also expressed in froglet kidney and adult testis.

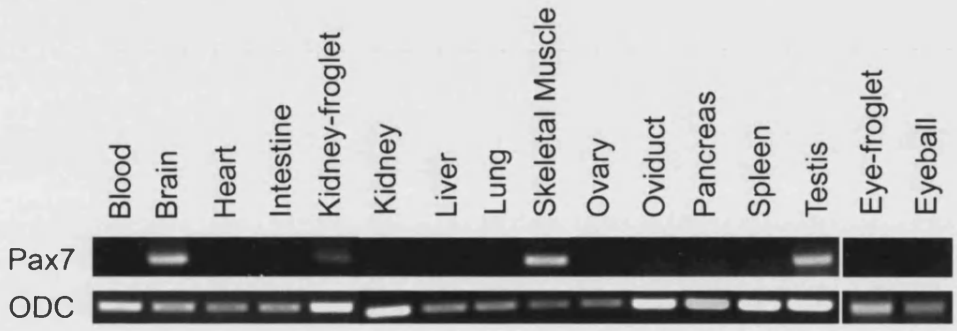

Figure 4.7 Detection of *pax7* expression in *Xenopus* adult by RT-PCR

Xenopus pax7 transcripts maintain in the froglet kidney, adult brain, skeletal muscle, and testis. Abbreviation: ODC, ornithine decarboxylase.

In summary, the expression studies demonstrate that *Xenopus pax7*, like its homologues in other species, is mainly expressed in the central nervous system and muscle.

IV.4.3 Expression pattern comparison of *pax7* and other myogenic regulatory factors in *Xenopus* embryonic myogenesis

The expression of *Xenopus pax7* in embryonic muscle precursor cells suggests its involvement in myogenesis. Myogenesis is a multi-step process. It initiates from the determination of myogenic precursor cells and is followed by myoblast proliferation, cell fusion and terminal differentiation of myofibres (Chanoine and Hardy, 2003). These steps are coordinated by several myogenic regulatory factors (MRFs), including myf5 and myoD. Myf5 and myoD are essential activators of the myogenic lineage that are needed for almost all striated muscles (Pownall et al., 2002).

Even thought mice lacking *myf5* or *myoD* have normal formation of skeletal muscle, *myf5* and *myoD* double mutant mice completely lose skeletal muscle (Kaul et al., 2000; Rudnicki et al., 1992; Rudnicki et al., 1993). The other somitic mesoderm derived tissues such as vertebrae, ribs and dermis develop normally in the double mutant mice. This shows that myf5 and myoD have redundant and important roles in the specification of the myogenic lineage.

Apart from the MRFs, pax3, another member of Pax gene family, has been demonstrated to be involved in the proliferation and mobility of myogenic cells in embryonic myogenesis (Pownall et al., 2002). Recently, a population of pax3/pax7 positive cells in the central dermomyotome region of somite was shown to be the source of muscle satellite cells in mice and chicks (Gros et al., 2005) (Relaix et al., 2005). This unveils the new function of pax3 in the specification of the muscle satellite cells.

To gain insight of possible functions of pax7 in myogenesis, we first compared the expression pattern of *pax7* with *myf5*, *myoD* and *pax3* in *Xenopus* embryos by whole mount *in situ* hybridization. *Myf5* and *myoD* are the first activated muscle specific genes in *Xenopus* myogenesis. Their transcripts increase during gastrulation. After gastrulation, *myoD* is expressed in paraxial mesoderm along the entire anterior-posterior axis (Fig.4.8A), whereas the expression of *myf5* is restricted to the posterior mesoderm of the embryo (Fig.4.8D). Later on, *myoD* is predominately expressed in the differentiating myotome, as shown by the chevron shaped staining (Fig.4.8B and C). The expression of *myf5* is intense in the posterior unsegmented mesoderm and in somites it becomes restricted to the dorsomedial and ventrolateral lips where muscle progenitors are maintained (Fig.4.8E and F).

In the case of pax7, *pax7* is expressed later than *myf5* and *myoD*. And the intensity of its transcripts in somitic mesoderm is comparatively lower than those of *myoD* and *myf5*. At stage 16, *pax7* are expressed mainly in the neural plate (Fig.4.8G). Very faint expression of pax7 is found in the anterior mesoderm, which is located laterally to the somitic mesoderm (inset in the Fig.4.5B). At later stages, the *pax7* transcripts are clearly seen in the anterior somites (Fig.4.8H). In well-formed somites of tailbud stage embryos, some pax7 expressing cells are located in the dorsomedial lip of the somite (Fig.4.5L) and others are randomly scattered throughout the somites (Fig.4.8 I).

Pax3 and pax7 constitute a subfamily within the Pax gene. Both *pax3* and *pax7* transcripts are located in the neural plate, but the intensity of *pax3*

expression is comparatively higher than that of *pax7*. No *pax3* transcripts were detected in the mesoderm region at stage 16 (Fig.4.8J). Afterwards, its expression in mesoderm increases (Fig.4.8K). As the somite matures, the *pax3* transcripts clearly outline a chevron shape for each somite (Fig.4.8L). Sections through the somite shows that it is in the superficial layer of the somite, the dermomyotome. The higher intensity of *pax3* expression is also found in the undifferentiated presomitic mesoderm of the tail bud (Fig.4.8L).

On the whole, *pax7* expression is not as strong as *myf5*, *myoD* and *pax3* in myogenesis. It initially has a distinct expression domain in the anterior somite region where overlaps the *pax3* expression domain. Later on some of the *pax7* expressing cells are at the dorsomedial lip of the somite region and the others are randomly located throughout the somites.

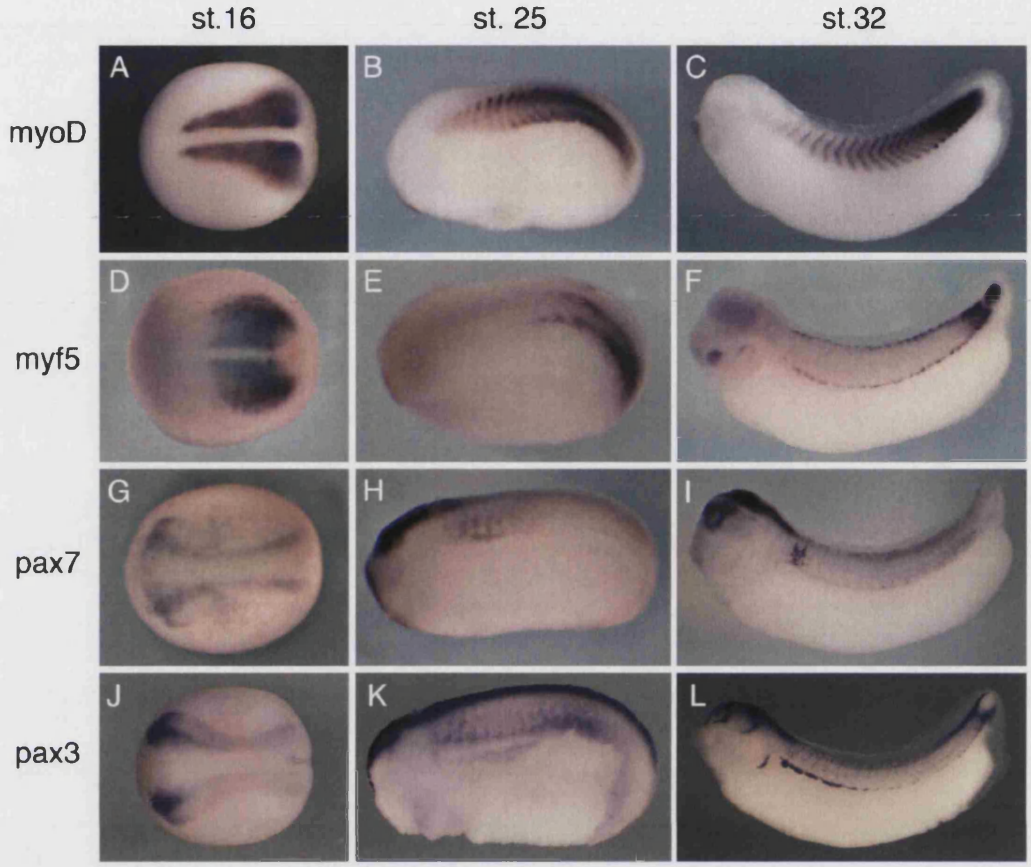

Figure 4.8 Comparison of expression pattern of *myf5*, *myoD*, *pax3* and *pax7* in early embryonic development of *Xenopus laevis*

Whole mount *in situ* hybridization was performed with *myf5*, *myoD*, *pax3* and *pax7* antisense probes. (A, D, G and J) Dorsal view of stage 16 embryos. Anterior is to the left. (B, E, H and K) Lateral view of stage 25 embryos. Anterior is to the left. (C, F, I and L) Lateral view of stage 32 embryos. Anterior is to the left. (A-C) Expression pattern of *myf5*. (D-F) Expression pattern of *myoD*. (G-I) Expression patter of *pax3*. (J-L) Expression pattern of *pax7*. Abbreviations: st16, stage 16; st26, stage 25; st32, stage 32.

IV.4.4 Discussion

The expression pattern of *pax7* gene in mouse and chick has been well documented (Halevy et al., 2004; Horst et al., 2006; Otto et al., 2006; Seale et al., 2000). In mammals or birds, *pax7* begins to be expressed within the ectoderm of the neural folds after gastrulation. Afterwards, its expression domain spreads cranially and caudally. It is expressed in discrete domains of the central nervous system, including dorsal midbrain, dorsal ventricular zone of the whole spinal cord and cranial neural crest cells. The first sign of *pax7* expression in developing muscle in mouse and chick appears at E9 and HH8 respectively, coincident with somitogenesis (Horst et al., 2006; Otto et al., 2006). The transcripts are located in the central region of the dermomyotome, which will give rise to dermatome and myotome. During later stage of myogenesis in mouse and chick, pax7 positive cells are distributed irregularly along the differentiated myofibres. These pax7 expressing cells are muscle satellite cells.

Our *in situ* hybridization and immunohistochemistry studies shows that *pax7* expression is highly conserved in vertebrates. As in mouse and chick, *pax7* transcripts in *Xenopus* are mainly found in the central nervous system and the embryonic and adult muscle. Pax7 expression in embryonic brain and spinal cord shows high regional specificity, as indicated by its dorsal expression in midbrain and the whole spinal cord, with ventral expression in a subpopulation of neural cells in the hindbrain (Figs. 4.5, 4.6). This *pax7* expression pattern is similar to that in mouse and chick. During embryonic myogenesis, the chevron pattern observed in *Xenopus* somites is very similar to the pax7 expression

pattern in the E12.5 mouse myotome (Horst et al., 2006). Expression of pax7 is also observed in a subset of muscle cells, with the position and appearance of satellite cells. This similar expression pattern suggests a conserved involvement of pax7 in embryonic myogenesis and specification of muscle progenitor cells (Gros et al., 2005; Halevy et al., 2004; Kassar-Duchossoy et al., 2005; Relaix et al., 2005; Seale et al., 2004).

However, there exist minor differences of pax7 expression profile between the species. Pax7 expression is found in the melanocyte lineage in chick and quail, but not in the melanocyte lineage in *Xenopus* tadpoles, mouse and rat (Lacosta et al., 2005). Expression of pax7 in the head mesenchyme is also different in *Xenopus* and mouse. As shown in Fig. 4.5H, M, N, pax7 transcripts in *Xenopus* appear earlier and stronger in the head mesenchyme than that in the anterior somites. But in mouse, pax7 expression in the head mesenchyme is not detectable until E11.5, when pax7 has been intensively expressed in the somites (Horst et al., 2006).

Pax3 and *pax7* have distinct and overlapping embryonic expression domains in myogenesis as shown by *in situ* hybridization study in *Xenopus* embryos. Just before or at the onset of somitogenesis, very faint *pax7* expression was observed at the anterior mesoderm region. At this stage, we did not observe *pax3* transcripts in the mesoderm region. But afterwards *pax3* is quickly upregulated and the expression intensity is higher than that of *pax7* in the presomitic mesoderm. During somitogenesis, *pax7* expression domain is initially restricted to the anterior somite region, overlapping with the expression domain of *pax3*. Later on at tailbud stage, *pax3* and *pax7* have

their distinct expression domains: *pax3* is expressed in the dermomyotome and pax7 is in the dorsomedial lip of somite region. This expression profile is different from that in mouse and chick where *pax3* and *pax7* are both expressed in the central dermomyotome and myotome (Horst et al., 2006; Otto et al., 2006). In addition, the order of *pax7* and *pax3* gene expression in the mesoderm of *Xenopus* embryos is opposite to that in mouse and chick, in which *pax3* is expressed slightly earlier than *pax7*.

Notably, the *pax3/pax7* positive cells in the dermomyotome are the origin of muscle satellite cells in mouse and chick (Gros et al., 2005; Relaix et al., 2005). In *Xenopus* embryo, the dermomyotome in *Xenopus* is a superficial layer of somite cells, which is outlined by the expression of *pax3*, but not *pax7* (Grimaldi et al., 2004). We do not know whether the *pax3* positive cells in the dermomyotome will become muscle satellite cells in *Xenopus*, or whether pax3 is expressed in *Xenopus* satellite cells. But our IEM study shows that pax7 is a reliable marker of muscle satellite cells in *Xenopus laevis*. Given that, we reckon that the pax7 expressing cells in the mesoderm are the probable source of muscle satellite cells in *Xenopus*.

V. Role of pax7 in the specification of muscle satellite cells in *Xenopus* embryos

V.1 Introduction

The expression profile of a gene is relevant to its function in animal development. The expression studies of pax7 in several organisms all confirm that it is specifically expressed in the muscle satellite cells. Our grafting experiments (see chapter III) show that the type II mesoderm at neurula stage represents the origin of at least a proportion of the satellite cells. We also noticed that *pax7* is expressed in this domain at stage 16 (inset in Fig. 4.5B). This coincidence suggests that pax7 plays a role in the specification of satellite cells lineage during *Xenopus* embryonic development.

For gene function analysis in *Xenopus* embryos, mRNA injection is the most popular way to express gene of interest in the desired place *in vivo*. To gain insight into the potential biological activity of pax7 in specifying satellite cells, we wanted to over-express pax7 ectopically, or to down-regulate its activity in the type II mesoderm and then check the number of muscle satellite cells on the injected side.

Before this functional assay, we performed a lineage tracing experiment using lysinated Rhodamine Dextran Amine (RDA) injection at 32-cell stage, trying to find a suitable injection site that could delivery mRNA more precisely to the type I or type II mesoderm.

V.2 Materials and Methods

V.2.1 Microinjections

RNAs or Rhodamine dextran amine (RDA) were injected into early *Xenopus* embryos using a Nanoject injector (Drummond Scientific company). Injection needles were prepared with 31/2 Drummond 300-203-G/X glass capillary (Drummond Scientific company). A glass capillary was pulled with a Flaming/ Brown Micropipette Puller (Sutter Instrument P-97) using the same condition for transgenic injection needles. Before injection, it was clipped with forceps to produce a bevelled tip of 20-30 μm in diameter. Then the needle was backfilled with mineral oil (Sigma), put onto the injector and filled with the solution of interest. The embryos were in NAM/2 +3% Ficoll during injection. The Ficoll assists the embryos to heal up the injection holes. After injection, they were kept in the medium for 2-3 hours before transferred to a new agar-coated Petri dish containing fresh NAM/10. The next day, all dead embryos were removed. The rest of the embryos were transferred to a new petri dish and cultured in NAM/10.

V.2.1.1 Rhodamine-dextran injections

Lysinated rhodamine dextran amine (RDA) powder (Molecular Probes, D3312) was dissolved in H_2O to make up 10mg/ml stock. 2.3 nl of 1mg/ml RDA was injected into blastomere C3 or C4 at the 32-cell stage (Fig. 5.1B).

V.2.1.2 pax7 mRNA injections

For pax7 over-expression in brain, 500 pg of *Xenopus pax7* mRNA and 80 pg of *GFP* mRNA were injected into one side of dorsal animal pole at 4-cell stage (Fig. 5.1A).

For pax7 over-expression in muscle, 1 ng of *Xenopus pax7* mRNA was injected into one side of blastomere C3 or C4 at the 32-cell stage (Fig. 5.1B).

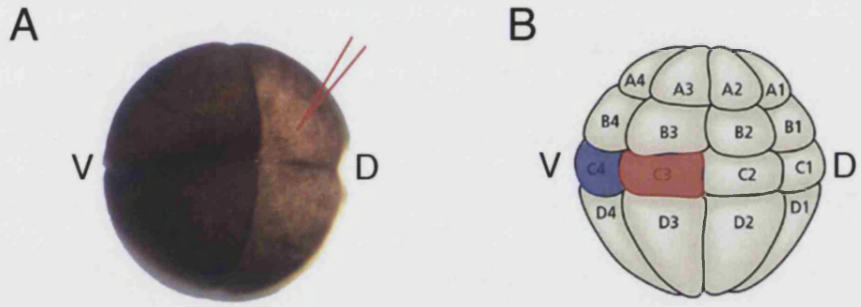

Figure 5.1 Illustration of microinjection sites in early stage *Xenopus laevis* embryo.
(A) An animal view of a 4- cell stage embryo. The red lines point out the mRNA injection site. (B) A diagram of a 32-cell stage embryo with nomenclature of each blastomere. Blastomere C3 and C4 are shown in red and blue respectively. Abbreviations: D, dorsal side; V, ventral side

V.2.1.3 pax7EnR mRNA injections

For pax7EnR overexpression in brain, 200 pg of *pax7EnR* mRNA and 80 pg of *GFP* mRNA were injected into one side of dorsal animal pole at 4-cell stage. For rescue, 500 pg of *pax7* mRNA and 200 pg of *pax7EnR* mRNA were co-injected into one side of dorsal animal pole at 4-cell stage (Fig. 5.1A).

For pax7EnR overexpression in muscle, 500 pg of *pax7EnR* mRNA was injected into one side of blastomere C4 at the 32-cell stage (Fig. 5.1B).

V.2.2 Satellite cell counting in pax7/pax7EnR overexpressing tadpoles

To count the number of satellite cells in tadpoles after overexpression of pax7 or pax7EnR in embryos, a series of 10 µm thick cross sections were prepared from the injected tadpole tails at stage 45. These sections were then double immunostained with NCAM and pax7 antibodies. Satellite cell counting was based on the NCAM staining signals. Cell counting was performed on every other section to avoid counting a cell twice. In total ten different tails of similar size were used in each group and five sections were counted from each tail. Statistical analysis was performed using Student's *t*-test.

V.3 Results

V.3.1 RDA injection in C3 and C4 blastomere could label type I and type II mesoderm respectively

According to the existing fate map developed by Dale and Slack, C2, C3 and C4 blastomeres at 32-cell stage will give rise to most muscle (Dale and Slack, 1987). We injected RDA into these three different blastomeres. RDA is a non-diffusible dye, so that it will normally stay in the injected blastomere and its progeny. Fig. 5.2 A and C shows that C3 RDA injection could label type I mesoderm at stage 16 and 84% of the injected embryos have this labelling pattern (Table 5.1). RDA in the remaining 16% of the injected embryos is found in type I and type II mesoderm. Compared to C3 injection, RDA by C2

injection does not exclusively label type I mesoderm. It always labels spinal cord or notochord as well. Therefore, we chose the C3 blastomere as injection site to target type I mesoderm. Moreover, we observed that 68% of C4 injections resulted in RDA labelling in type II mesoderm (Fig.5.2.B and D). The C4 injection also can label some cells at the lateral plate mesoderm with RDA. In spite of this, RDA by C4 injection never goes to the type I mesoderm and type III mesoderm alone (Table 5.1). So we decided that C4 blastomere was a suitable injection site to target type II mesoderm.

To check the distribution of C3 and C4 progeny in the developing somite, we looked at the RDA labelling pattern in stage 32 embryos, when somitogenesis is still going on. We found that all the RDA by C3 injection is located in the dorsal and central parts of the somites (Fig. 5.2 E and F, table 5.1), while RDA by C4 injection has two different cell labelling patterns. RDA in 33.3% of the injected embryos is only located in the cells of ventral somite. In the other 66.7% embryos, RDA signals are also present in a few cells of the dorsomedial lip of somites (Fig. 5.2.G, table 5.1). In all, the lineage tracing experiment shows that the cells in type I and type II mesoderm regions are mainly derived from C3 and C4 blastomere at 32-cell stage.

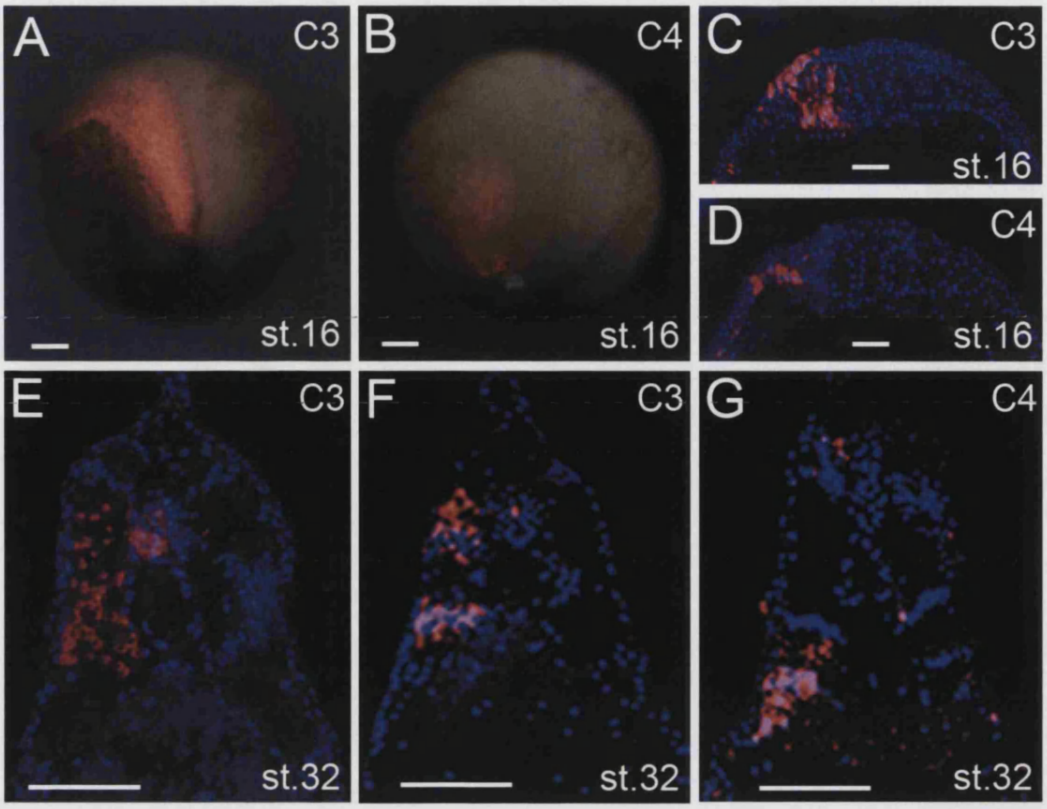

Figure 5.2. Lineage tracing of mesoderm by RDA injection at 32-celll stage

2.3 nl of 1mg/ml RDA was injected into blastomere C3 or C4 at the 32-cell stage. (A, C, E and F) blastomere C3 injection. (B, D and G) blastomere C4 injection. (A and B) dorsal view of stage 16 embryos receiving RDA labelling. Anterior is to the top. (C and D) sections of stage 16 embryos with RDA injection. (E-G) sections of stage 32 embryos with RDA injection. (E) is an anterior section of a C3 injected embryo and (F) is its more posterior section. (G) shows the presence of RDA both in the ventral somite and the dorsomedia lip of the somite. The sections were counter-stained with DAPI dye. Scale bar: 100 mm. Abbreviation: st., stage.

Table 5.1 Distribution of RDA after 32-cell stage injection

		Stage 16				
RDA injection site	N	Type I labelling	Type I+II labelling	Type II labelling	Type II+III labelling	Type III labelling
C3	56	47(84.0%)	9 (16.0%)	0	0	0
C4	50	0	0	34(68.0%)	16(32.0%)	0

		Stage 32			
RDA injection site	N	dorsal & middle somite	middle somite	dorsal most & ventral somite	Ventral somite
C3	43	43(100 %)	0	0	0
C4	30	0	0	20 (66.7%)	10 (33.3%)

Note: For lineage tracing, 2.3 nl of 1mg/ml RDA was injected into blastomere C3 or C4 at the 32-cell stage.

In the C3 blastemere injected embryos, when checked at stage 16, 84% of the embryos contained RDA labellled cells only in the type I mesoderm. At stage 32, RDA positive cells were found in the dorsal and middle part of the somites.

In the C4 injection group, 68% of C4 injections resulted in RDA labelling in the type II mesoderm at stage 16. These embryos showed two different cell labelling patterns at stage 32. One third of the embryos contained RDA positive cells in the ventral somites only. In the other two-thirds embryos, RDA signals are present in the ventral somites and a few cells of the dorsomedial lip of somites.

V.3.2 pax7EnR is a dominant negative form of pax7

To investigate the role of pax7 in *Xenopus* development, we needed a dominant negative form of pax7 to perform loss of function studies. Therefore, we generated a domain-swapped construct pax7EnR, in which the C-terminal

region of *Xenopus* pax7 was replaced with the transcriptional repression domain of Drosophila engrailed (Han and Manley, 1993).

This method has been used many times to generate transcription factor domain swaps, but we felt it important to confirm that it really had the predicted biological activity: namely that it can inhibit normal pax7 function. To do this we over-expressed pax7EnR in the brain region, which is rich in endogenous expression of pax7. We injected 200 pg of *pax7EnR* mRNA, together with 80 pg of *gfp* mRNA, into the left side of the dorsal animal hemisphere of four cell stage embryos. The injected neurulae show defects in the anterior neural fold on the left (Fig. 5.3A) and later on in the developing left eye (Fig. 5.3C and table 5.2). These defects become obvious at advanced stages. The left eye is absent or smaller, while the right eye has fully developed (Fig. 5.3C, D and F). The GFP fluorescence on the injected side indicates that it still has a small lens underneath the epidermis (inset in Fig. 5.3C). Moreover, we checked a series of transcription factors related to eye field specification after *pax7EnR* injection by *in situ* hybridization. We found that *rx1*, *krox20* and *tll* are down-regulated by *pax7EnR* injection. But the other factors such as *pax6* and *en2* are not affected (Fig. 5.4).

To test the specificity of Pax7EnR, we co-injected *pax7EnR* mRNA together with 500 pg of wild type *pax7* mRNA. As shown in fig. 5.3B, E and table 5.2, the *pax7* RNA is able to rescue these eyes back to approximately normal size.

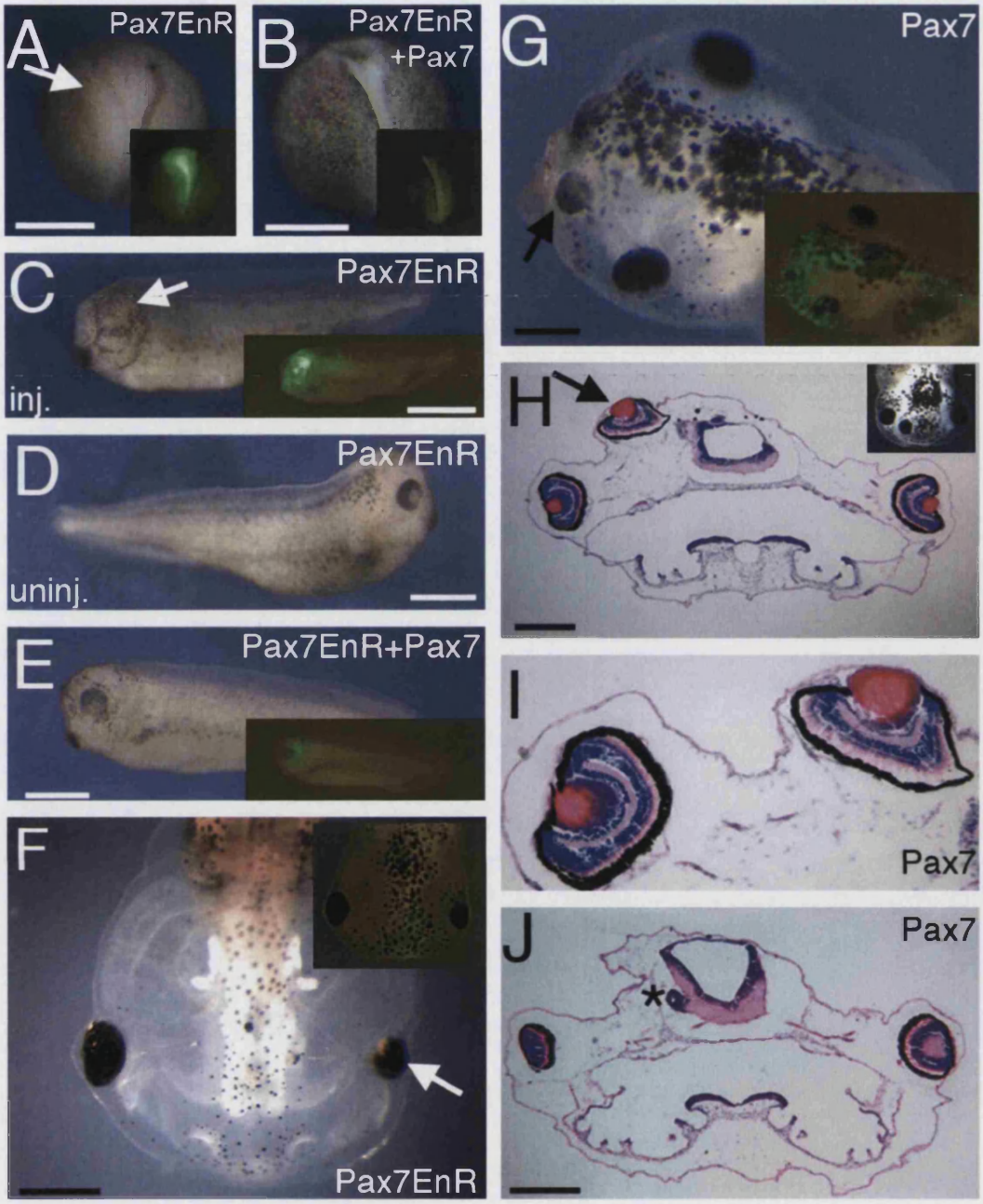

Figure 5.3 Pax7EnR functions as a dominant negative form of Pax7.

(A, C, D, F) embryos injected with 200 pg *pax7EnR* mRNA and 80 pg *GFP* into left side of dorsal animal hemisphere at four cell stage. (A) A stage16 embryo, the arrow indicates the anterior neural fold defect on left side. (C) Left side of pax7EnR injected embryo, the arrow indicates the developing eye. The fluorescence in the inset shows a small lens underneath the epidermis. (D) Eye development on the un-injected side. (F) A tadpole with a smaller left

eye. (B, E) Co-injection of 500 pg *pax7* mRNA, 200 pg *pax7EnR* mRNA and 80 pg *gfpP* is able to rescue the defective eyes to normal size. (G) Injection of 500 pg *pax7* and 80 pg *gfp* mRNA into one side of the dorsal animal hemisphere results in an ectopic eye in the forebrain of stage 43 tadpoles. The GFP fluorescence in the insets indicates the injected region. (H-J) Transverse sections through ectopic eye of injected tadpole (showed in inset) were stained with hematoxylin and eosin. The arrows in (G) and (H) point out the extra eyes. (I) is a magnified view of the ectopic eye and one normal eye. The asterisk in (J) highlights the tube protruding from the ventral midbrain. Scale bars, 300 μm. Abbreviations: inj., injected; uninj., uninjected.

Table 5.2 Summary of eye development in pax7/pax7EnR injected embryos

Constructs	Two normal eyes and one extra eye	Two normal eyes	One small eye and one normal eye	Single eye
Pax7EnR	0	43 (48.8%)	32 (36.4%)	13 (14.8%)
Pax7EnR+Pax7	0	37 (94.9%)	2 (5.1%)	0
Pax7	15 (10.0%)	135 (90.0%)	0	0

Note: 200 pg *pax7EnR* or 500 pg *pax7* capped mRNA, or both, were injected into one of the dorsal animal hemispheres of 4 cell stage embryos. Eye development was measured at stage 46.

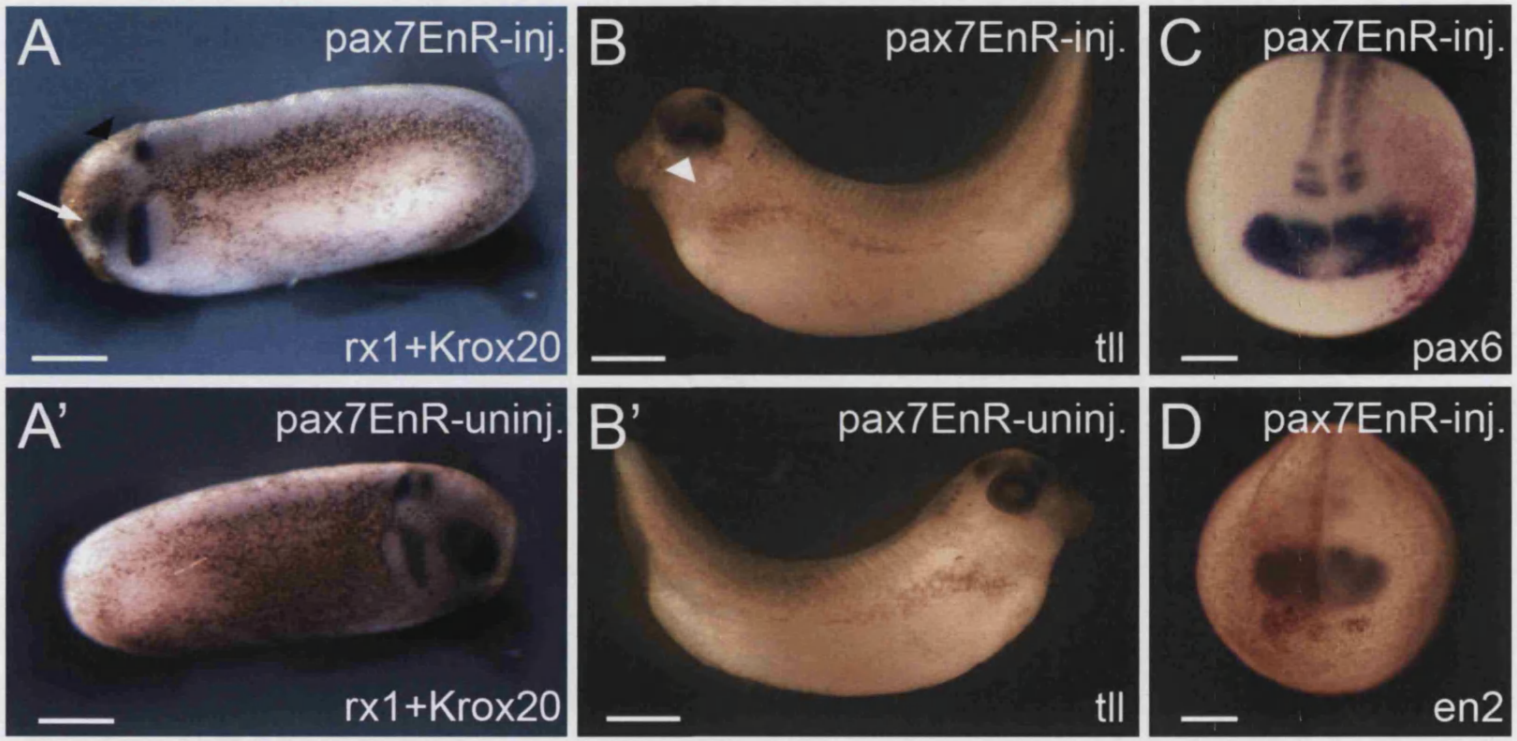

Figure 5.4 Detection of the expression of eye field transcription factors by whole mount *in situ* hybridization after overexpression of pax7EnR

200 pg *pax7EnR* mRNA was injected into left side of dorsal animal hemisphere at four cell stage. (A) Left side view of a stage 28 embryo. *rx1* and *krox20* are down-regulated by pax7EnR. The black arrowhead indicates the absence of *krox20* expression. The white arrow indicates the downregulation of *rx1* expression at the injected site. (A') Right side view of the same embryo in (A). (B) Left side view of a stage 34 embryo. The white arrow indicates the downregulation of tll expression in the left eye. (B') Right side view of the embryo in (B'). (C and D) Anterior view of stage 19 embryos. (C) Expression of pax6 is not affected. The red-gal signals points out the injected site. (D) Expression of *en2* is not affected by pax7EnR overexpression. Scale bar: 200 µm.

The above results suggest an involvement of pax7 in eye development in *Xenopus laevis*. Since pax7EnR inhibits eye development, it is possible that pax7 itself can promote eye development on overexpression. Indeed this is the case. When 500 pg *pax7* and 80 pg of *gfp* mRNA were co-injected into one side of the dorsal animal hemisphere at the four cell stage, some tadpoles developed an ectopic eye at the injected site (Fig. 5.3 G-I, table 5.2). Although only a small proportion of the injected tadpoles developed an ectopic eye, when found it is very well formed, containing a retinal pigmented epithelial layer, outer nuclear layer, inner nuclear layer, ganglion cell layer and lens in a spatial arrangement identical to the endogenous eyes. Detailed examination of these tadpoles shows that the ectopic eye is often accompanied by a tube protruding from ventral midbrain (Fig. 5.3J). No ectopic eyes were seen in tadpoles resulting from embryos injected into the same region with *gfp* mRNA alone.

We are not claiming that pax7 has a normal function in *Xenopus* eye development, but the phenomena described here provide us with a useful bioassay. The experiments show that pax7 promotes eye development, pax7EnR represses it and sufficient pax7 can restore eye development in the presence of pax7EnR. This proves that pax7EnR is able to inhibit the function of pax7 and we can therefore use pax7EnR as a dominant negative form of pax7 to in vestigate the function of pax7 in muscle development.

V.3.3 pax7 is able to induce *myf5* and *pax3* in myogenesis

The results presented in chapter III demonstrated that satellite cells mainly come from the type II mesoderm in early neurula stage embryos, and our RDA labelling showed that this type of mesoderm can be effectively targeted by C4 blastomere injection of 32-cell stage embryos. We were tempted to find the effect of ectopic expression of pax7 in the C3 blastomere, whose progeny are expected rarely to give rise to satellite cells. So we first injected *pax7* mRNA into C3 blastomere of the left side with three different concentrations (200 pg, 500 pg and 1 ng). Almost all the injected embryos developed normally until tadpole stage. Three independent batches of injections were performed, but no obvious phenotypes were observed.

We then fixed some injected embryos at stage 16 and stage 32 and checked the expression pattern of three muscle regulatory genes (*myf5*, *myoD* and *pax3*) by *in situ* hybridization. We observed changes of gene expression only following 1 ng *pax7* mRNA injection and not at the lower doses. Pax7 can induce *myf5* and *pax3* mRNA expression, but does not affect the expression level of *myoD*. As shown in Fig. 5.5A, at stage16, *myf5* is ectopically induced in the anterior presomitic mesoderm, which should be negative for endogenous *myf5* expression (see the right side of the embryo). The *myf5* expression domain in the posterior presomitic mesoderm is also expanded laterally. At the same stage, *pax3* transcript is hardly detectable in the presomitic mesoderm in uninjected embryos. But once they have received the *pax7* mRNA injection, 87% the embryos display patches of *pax3* expression in the mesoderm on the injected side (Fig. 5.5.E, table 5.3). The ectopic

expression of *myf5* and *pax3* induced by *pax7* mRNA injection is still maintained until at least stage 32 (Fig.5.5B and F). Both are upregulated in the central dosoventral part of the somites. They are also induced in the anterior lateral plate mesoderm, which is often populated by descendants of C3. Interestingly, we also noticed that some *myf5* expressing cells appear in the dorsal fin in some injected embryos (Fig. 5.5B).

As type II mesoderm of early neurula stage embryo is the bigger contributor of future satellite cells, we also checked the effect of pax7 overexpression in type II mesoderm by C4 injection. 40% of the embryos receiving injection show an enlargement in the ventral region around stage 24. In spite of this, the injected embryos developed normally until tadpole stage. The *in situ* result shows that only pax3 is induced at the lateral plate mesoderm of the injected side (Fig. 5.6). The other two factors, myf5 and myoD are not affected.

Table 5.3 Ectopic gene expression induced by *pax7* mRNA injection at 32-cell stage

	pax7 mRNA c3 injection			*pax7* mRNA c4 injection		
	myf5	*myoD*	*Pax3*	*myf5*	*myoD*	*pax3*
st.16	23 (88.5%)	0	20 (87.0%)	0	0	18 (72%)
st.32	35 (87.5%)	0	31 (88.6%)	0	0	17 (65.4%)

Note: 1ng of *pax7* mRNA was injected into blastomere C3 or C4 at the 32-cell stage. We collected stage 16 and stage 32 injected embryos and check the expression pattern of *myf5*, *myoD* and *pax3* by whole mount *in situ* hybridization. In the C3 blastomere injection group, pax7 could ectopically induce *myf5* expression in 88.5% of the injected embryos and ectopically induce *pax3* expression in 87.0% of embryos at stage 16. 87.5% of embryos

showed ectopic expression of *myf5* and 88.6% of embryos showed ectopic expression of *pax3* at stage 32. Pax7 over-expression did not affect *myoD* expression in both stages. In C4 blastomere injection group, pax7 could not induced *myf5* or *myoD* expression ectopically, but could up-regulate *pax3* expression. 72% of stage 16 embryos and 65.4% of stage 32 embryos showed ectopic *pax3* expression.

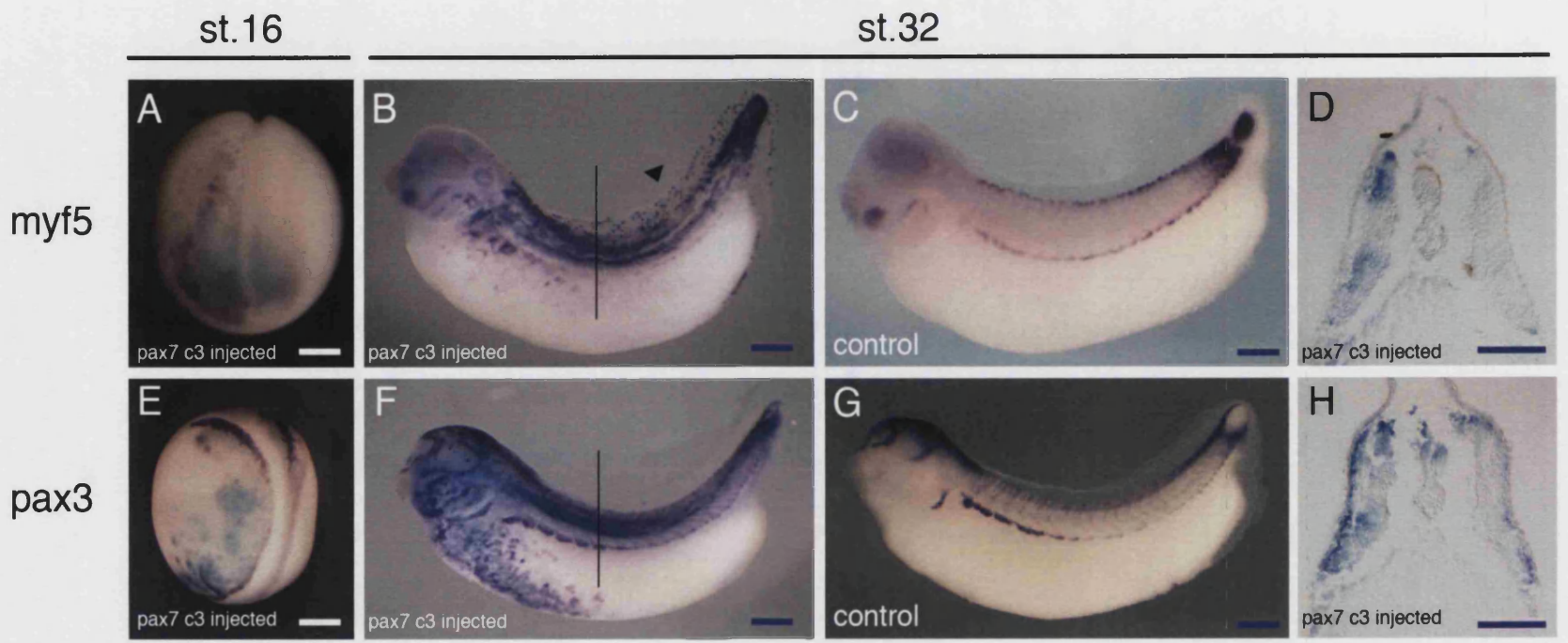

Figure 5.5 *pax7* mRNA injection induces ectopic expression of *myf5* and *pax3*

1ng *Xenopus pax7* mRNA was injected into blastomere c3 of left side at 32-cell stage. (A-D) detection of *myf5* expression by whole mount *in situ* hybridization. (E-H) detection of *pax3* expression by whole mount *in situ* hybridization. (A and B) *myf5* is ectopically expressed at the left side. (E and F) *pax*3 is ectopically expressed at the left side. The black lines in B and F indicate the position of sections in D and H respectively. The black arrow head in B shows the expression of *myf5* in fins. (C and G) control embryos. (A and E) dorsal view of stage 16 embryos. Anterior is on the top. (B, C, F and G) lateral view of stage 32 embryos. Anterior is to the left. Scale bars: 100 mm

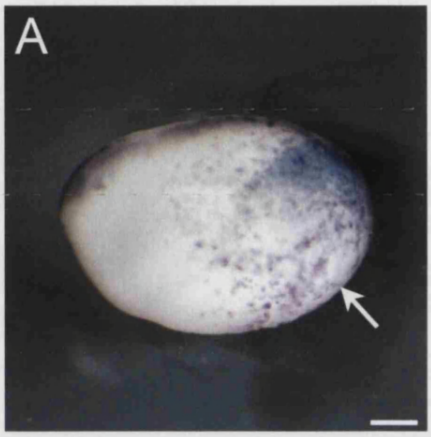

Figure 5.6 *pax3* mRNA expression in C4 blastomere injected embryos

Expression of *pax3* mRNA was detected by *in situ* hybridization in embryos injected with *pax7* mRNA in C4 blastomere at 32-cell stage. (A) Lateral view of a stage 26 embryo. Left is the anterior of the embryos. White arrow indicates ectopic expression of *pax3* induced by pax7 overexpression. Scale bars: 200 mm.

V.3.4 pax7/pax7EnR overexpression does not affect the number of muscle satellite cells

In our assay, *pax3* and *myf5* are both upregulated by pax7 in the somites. This might indicate that there are more myoblasts in the injected side, and thus the somite in the injected side should be bigger than that in the uninjected side. But detailed examination of the injected embryos and their sections did not support this idea (Fig. 5.5). So the elevated expression of the genes in the somite occurs in cells that are already myoblasts, or in the case of the lateral plate cells, the ectopic expression does not make them myogenic.

The lineage analysis from chick and mouse demonstrated that the population of pax3/pax7 positive cells in somites represent the progenitors of embryonic and fetal myoblasts and satellite cells. So an alternative hypothesis is that the cells with *pax3* expression induced by pax7 overexpression in the somite represent the progenitors of muscle satellite cells, as they do in mammals and birds. If this is the case, we should find more satellite cells in the injected side at later tadpole stages. To test this, we made a series of sections of the C3 injected tadpoles (stage 45) and performed double immunostaining on them with pax7 and NCAM antibodies (As explained in chapter IV, NCAM is another satellite cell marker). Looking through the stained sections, we did not find any patches of pax7 expression on the injected side. We think that pax7 protein generated by the mRNA injection itself has already been degraded before the stage of fixation. Counting of NCAM+ cells showed no obvious increases in the number of satellite cells on the injected side (Fig. 5.7). We

also checked the number of satellite cells in the tadpoles receiving pax7 injection in the C4 blastomere. Again, no patches of pax7 expression were found in the injected muscle. The number of satellite cells on the injected side still remained similar to that on the uninjected side (Fig.5.7). These date suggests that pax7 alone, or together with the induced pax3, is not sufficient to specify myogenic or satellite lineage during *Xenopus* embryonic development.

In the previous sections, we have shown that pax7EnR is a dominant negative form of pax7 and it is able to inhibit the function of pax7 in eye development. Therefore, we use it to test the effects by loss of pax7 function in somites. Again we injected 100 pg *pax7EnR* mRNA into C4 blastomere of one side embryos. Most embryos developed normally and no change of expression of *myf5*, *myoD* and *pax3* was detected by *in situ* hybridization. Moreover, the number of satellite cells was not affected by inhibition of pax7 on the injected side (Fig. 5.7).

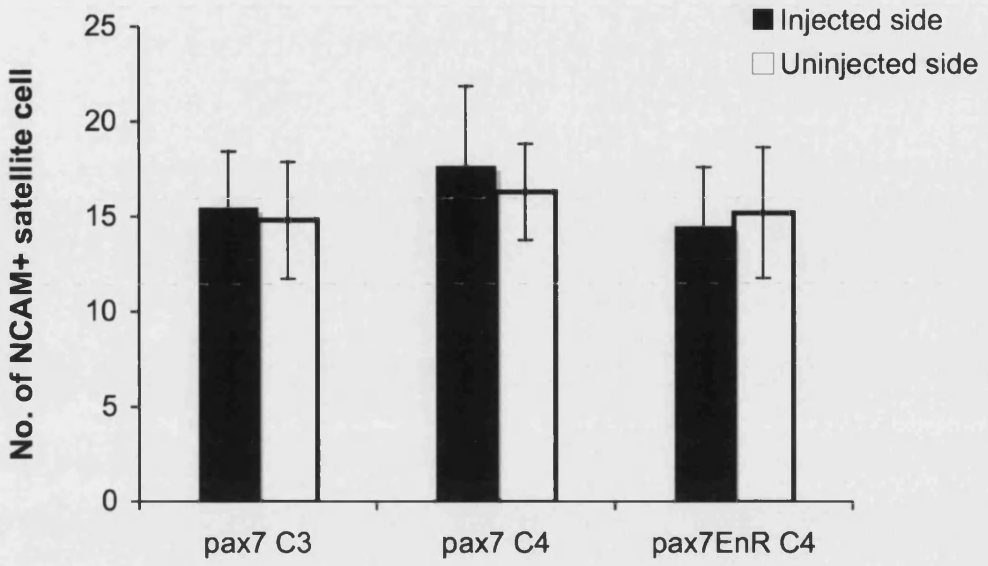

Figure 5.7 Counting of satellite cells in C3/C4 blastomere injected embryos.

Counting of satellite cells was based on NCAM antibody immunostaining. Only NCAM positve cells in the muscle were counted. Ten samples of each kind of injection were counted, with 5 section of each sample counted. Statistic analysis with Student's *t*–test indicates no significance between the number of satellite cells of injected and uninjected side, within each injection.

V.4 Discussion

V.4.1 Pax7 in eye development

Our testing of the function of pax7 and pax7EnR constructs by injecting them into the dorsal side of 4-cell stage embryos resulted in a quite surprising phenotype: the induction of a well-formed extra eye. This phenotype is reproducible despite the low frequency of occurrence (10% of cases). In an elegant manner this overexpression phenotype is the "opposite" of the

pax7EnR phenotype, which involves reduction of the normal eye. The eye-reduction phenotypes of pax7EnR can be rescued by co-injection of pax7. An overexpression phenotype does not, of course, prove that the gene in question is involved in the normal development of the affected structure. In our case pax7 is probably not directly involved since it is not normally expressed in the eye field itself. However it is expressed in the region immediately anterior to the eye and so the overexpression effects may indicate an indirect function of pax7 in eye development involving signals from the surrounding tissues.

Consistent with this, pax7 is expressed in chick optic tectum and mouse superior colliculus, one of the major visual targets in brain (Nomura et al., 1998; Thomas et al., 2004; Thompson et al., 2004; Ziman et al., 2001). When misexpressed, pax7 can induce ectopic formation of superior collicular tissue, with characteristic laminae innervated by retinal ganglion cell axons (Matsunaga et al., 2001; Thompson et al., 2004). Interestingly, among the tadpoles with an extra eye developed by the overexpression of pax7, we very often observed formation of an extra tube-like structure protruding from the midbrain (asterisks in Fig.5.3J). Detection of a series of transcription factors related to eye field specification shows that some of the transcription factors, such as *rx1*, *krox20* and *tll*, are downregulated by *pax7EnR* injection (Fig.5.4) Thus, these findings do support a role of pax7 in the development and maturation of the vertebrate visual system, even if it is indirect. It is also possible that the overexpression experiments are interfering in some way with pax6, well known as a master controlling gene in eye development (Gehring

and Ikeo, 1999). However the *in situ* hybridization results do not indicate any effect on *pax6*, at least at the level of mRNA content.

V.4.2 Pax7 in embryonic myogenesis

In our study, we found ectopic expression of pax7 by the C3 blastomere injection could induce *myf5* and *pax3* in neurula and tailbud stage embryos. This induction only occurs upon injection with a high concentration of pax7 mRNA (1ng).

The induced expression of these genes in the somites did not result in enlarged myotomes, which suggested that the cells with elevated expression of *myf5* or *pax3* are already myoblasts. Therefore, we think that the ectopic expression of pax7 in the somites is likely to maintain *myf5* and *pax3* expression in the myoblasts in anterior myotome where muscle will differentiate anyway. But this activity is transient and not strong enough to disturb normal muscle differentiation in later stage embryos as showed by *myoD* and 12/101 staining.

Our overexpression study shows that pax7 is not able to affect *myoD* expression during myogenesis. This result is not consistent with findings in two *in vitro* cell culture studies. One of these studies showed that pax7 acts genetically upstream of myoD. Ectopic expression of pax7 could increase myoD expression in a *pax7-/-* mutant myogenic line. The other study, however, showed downregulation of myoD by overexpression of pax7 in cultured satellite cells. We do not discuss the discrepancy of these two experiments in detail here. But we need to point out that our study of pax7

function is in the context of embryonic myogenesis *in vivo*. Its developmental background is clearly different from that in postnatal muscle growth or *in vitro* cultured myogenic cells, where musculature or myogenic lineage has already been specified. So the molecular regulation mechanisms of these factors may vary in these different contexts.

Moreover, we noticed that some C3 injected embryos displayed ectopic expression of *myf5* in the fins and anterior lateral plate mesoderm. These expression domains are out of our expectation, since normally the fin and lateral plate mesoderm is not the progeny of the C3 blastomere. But we must point out that the blastomere injections at 32-cell stage sometimes are not precise because the cleavage planes of this stage embryo vary in different batches or even in the same batch. Moreover, it is possible that injected mRNA in one blastomere will diffuse to its neighbouring blastomere because a little bit further injection in a tiny blastomere will break the neighbouring cell membrane. As a result, the injected mRNA will display inconsistent distribution at later stage in some cases.

Given these, we guess that our C3 injection is likely to contaminate the progeny of neighbouring blastomere. We do notice this situation from the RDA injection. The *myf5* expressing cells in the fin probably are neural crest cells derived from the neural tube, which contains descendants of the C2 blastomere, because we noticed that *myf5* was also expressed in the dorsal neural tube and migrating neural crest cells in several transverse sections of *pax7* injected embryos (data not shown). Myogenic cells derived from the neural tube was observed *in vitro* (Tajbakhsh et al., 1994). It is thought that a

small proportion of cells in the neural tube have the myogenic potential *in vivo*, which however is repressed by the surrounding neural tube environment. These cells will be released from the inhibition and underwent myogenic lineage if the neural tube is isolated and cultured *in vitro*. Higher strength of pax7 may be able to release the inhibition *in vivo* and directly induce *myf5* expression.

V.4.3 Pax7 in the specification of satellite cell lineage in *Xenopus* embryos

Seale et.al showed that pax7 is necessary and sufficient for the myogenic specification of CD45+:Sca1+ adult stem cells during muscle regeneration (Seale et al., 2004). However, we did not find this lineage specification ability in the early development of *Xenopus* embryos. The specification of muscle satellite cell is closely related to embryonic myogenesis. Although we find that pax7 can induce two muscle regulatory factors, myf5 and pax3, our counting of NCAM+ cells shows no obvious change in the number of satellite cells by *pax7/pax7EnR* mRNA injection. This suggests that pax7 is not sufficient to specify muscle satellite cells during *Xenopus* embryonic development, although it may be necessary to do so. Our results in chapter VI shows that pax7 functions mainly in muscle regeneration rather than the early satellite cell specification.

VI. Role of pax7 in *Xenopus* tail regeneration

VI.1 Introduction

Recent findings suggest that pax7 has functions other than lineage specification in muscle development. This idea first comes from the surprising observation from Braun's lab that *pax7-/-* mice in a mixed C57/BL/Sv129 genetic background do have muscle satellite cells, albeit at a greatly reduced number compared to wild type mice (Oustanina et al., 2004). They suggested a role of pax7 in the renewal and propagation of the satellite cells in postnatal muscle development. This finding was confirmed by Rudnicki's lab using viable pax7-/- mutants in the 129Sv/J genetic background (Kuang et al., 2006). However, they summarized that pax7 is essential for the formation of functional myogenic lineage from the satellite cells. These studies suggest that pax7 functions in a more complex way than we expected.

Our study aimed to further understand molecular functions of pax7 in the satellite cells during muscle regeneration. A cell lineage tracing study on *Xenopus* tail regeneration done by Cesare Gargioli suggests that regenerating myofibres arise from pre-existing muscle satellite cells (Gargioli and Slack, 2004). So we took advantage of this regeneration model to study pax7 function in the satellite cells during muscle regeneration.

VI.2 Materials and Methods

VI.2.1 Heat shock

Xenopus laevis tadpoles were placed into a warmed water bath at 34°C for 30min each day during the period of heat shock experiments.

VI.2.2 Tail amputation

Tadpoles were anaesthetized in 0.02% MS222 and kept in the anaesthetic solution during the operation. About 50% of the tail was removed with a razor blade. For repeated amputation, 50% of the tail was removed first, 10 or 14 days later when the tail regenerated to its full length, the distal 75% of the regenerated tail was amputated again. The tadpoles were allowed to recover from anaesthesia in tap water before returning to aquarium tanks.

VI.2.3 Satellite cell counting in the heat shock experiments

Muscle satellite cell counting was based on the pax7 antibody labelling on tissue cross sections of regenerated tails. Cells were counted on a series of sections comprising the 50 µm length of the tail that is nearest to the first amputation site or near to the second tail amputation site, since the regenerated muscle near the tail tip is too small for any quantification. Ten tails of similar size in each group were examined and statistical analysis was performed using Student's *t*-test.

VI.2.4 TUNEL Assay

For apoptosis detection, paraffin tissue sections were prepared and rehydrated as described above. The TUNEL assay was applied on 7 µm section with an *in situ* cell death detection kit (Roche). The sections were

washed in PBSA for 5 minutes and in 10 mM Tris/HCl (pH 7.4-7.8 for 10 minutes. Then the sections were treated with 10-20 µg/ml Proteinase K in 10 mM Tris/HCl (pH 7.4-8) at 37°C for 20 minutes followed by two washes in PBSA for 10 minutes each. Meanwhile, a TUNEL reaction mixture was set up by adding 50 µl of Enzyme solution to 450 µl of Label Solution. The mixture is mixed well to equilibrate components. At the end of the second PBSA wash, 50 µl of TUNEL reaction mixture was applied to each slide. The slides were covered with parafilm to ensure a homogeneous spread of the mixture and to avoid evaporative loss. The sections were incubated for 1 hour at 37°C in the dark. Once the incubation was done, the slides were washed in PBSA three times for 10 minutes each. At this stage the sections could be analyzed under a fluorescence microscope using the GFP set. For chromogenic detection of the labelling signal, 50 µl of Converter-AP was added to each slide and incubated for 30 minutes at 37°C. After three times washing in PBSA, 50-100 µl of Fast Red substrate solution (tablets from Sigma) was added to each slide and colour development was performed in the dark at room temperature for 10 minutes. Then the stained sections were washed in PBSA to stop the reaction and mounted in gel mounting medium.

For detection of apoptosis in pax7 expressing cells, pax7 immunohisto-chemistry was carried out first, developed with DAB, and then the apoptosis labelling reaction performed and visualized with a GFP filter set. For detection of apoptosis in myoD expressing cells, myoD immunohistochemistry was performed first, and then followed by the apoptosis labelling reaction. For

statistic analysis, apoptotic cells were counted in three series of sagittal sections of 3 days regenerated tails.

VI.2.5 BrdU injection

Stage 49 tadpoles were anaesthetized in 0.02% MS222, and intraperitoneally injected with 2 µl of the thymidine analog 5-Bromo-2'-deoxyuridine (BrdU) labelling reagent from the Cell Proliferation Kit (Amersham, RPN20). The injection was performed 24 hours before fixation.

VI.3 Role of pax7 during muscle regeneration in the *Xenopus* tadpole

VI.3.1 pax7 is upregulated during tail regeneration

Tails of *Xenopus* tadpoles will regenerate fully after amputation (Slack et al., 2004). To test whether pax7 plays a role in this process, we performed RT-PCR assays with regenerating tails 3 days post amputation. To get enough RNA for PCR assay, 10 tails of each experimental group were collected for total RNA isolation. Three independent batches of RT-PCR assays were performed. As shown in Fig. 6.1A, the *pax7* mRNA level is increased in the regenerating tails, compared to that in tails without amputation. We consider that this is due to an increase in number of pax7 positive cells. It is not possible to make a precise quantitative comparison of cell numbers because the structures of mature tail muscle and the regeneration bud are so different. However, at this stage there is a considerable amount of cell proliferation in the regeneration bud, indicated by PCNA antibody staining (Fig. 6.1B), and many pax7 positive cells are found free of the muscle lying close to the

amputation level in the blastema (Fig. 6.1C), which is the undifferentiated region of the regeneration bud.

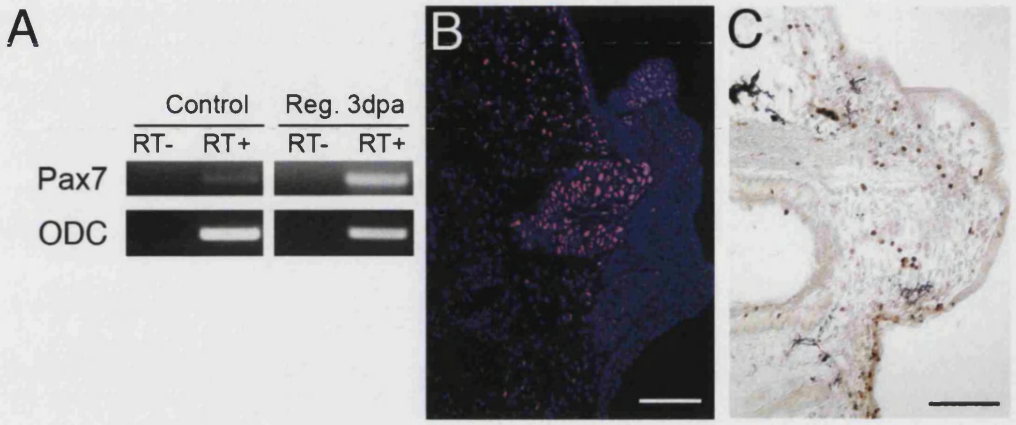

Figure 6.1 Pax7 is upregulated in regenerating tadpole tails.

(A) RT-PCR shows that *pax7* messenger RNA is more abundant in regenerating tails 3dpa, compared to the tails without amputation. (B) PCNA antibody staining (red) on para-sagittal section of regenerating tail. DAPI (blue) shows the nuclei. The dense region in the centre is the notochord tip, with the blastema above and below. (C) Pax7 antibody labelled cells (brown) on para-sagittal sections of regenerating tail. Dorsal side up and anterior left. Scale bars, 100 µm. Abbreviation: dpa, day after amputation.

VI.3.2 The number of muscle satellite cells is decreased in heat shocked *pax7EnR* transgenic tails

Since the RNA experiments showed that over-expression of *pax7EnR* disturbs the early embryonic eye development of *Xenopus laevis*, we generated transgenic tadpoles in which the *pax7EnR* gene is driven by a heat shock promoter in response to a 34°C warm pulse (Fig. 6.2, (Beck et al., 2003)). This means that the gene is inactive through development and only activated when the temperature is raised.

We performed RT-PCR analysis on four groups of tadpole tails to test the effect of activating *pax7EnR*. They are: 1) wild type tails regenerated for 7 days without heat shock; 2) *pax7EnR* transgenic tails regenerated for 7 days without heat shock; 3) wild type tails regenerated for 7 days with one heat shock each day after amputation; 4) *pax7EnR* transgenic tails regenerated for 7 days with one heat shock each day after amputation. Again 10 tails of each group were collected and the expression profiles of *pax7EnR, pax7* and *pax6* were then examined. The primers of *pax7EnR* were designed by targeting its sequence across the fusion region. The primers of *pax6* and *pax7* used for PCR are able to distinguish these two different transcripts. As shown in Fig. 6.3A, *pax7EnR* is only induced in the case of *pax7EnR* transgenic tails with heat shock, and no leaking expression of *pax7EnR* is detected in tails without heat shock. The PCR results also show that the endogenous *pax7* mRNA is reduced in the regenerating tails with *pax7EnR* expression. By contrast activating *pax7EnR* has no effect on the expression level of *pax6* messenger RNA, which is also present in the regenerating tail (Fig. 6.3A).

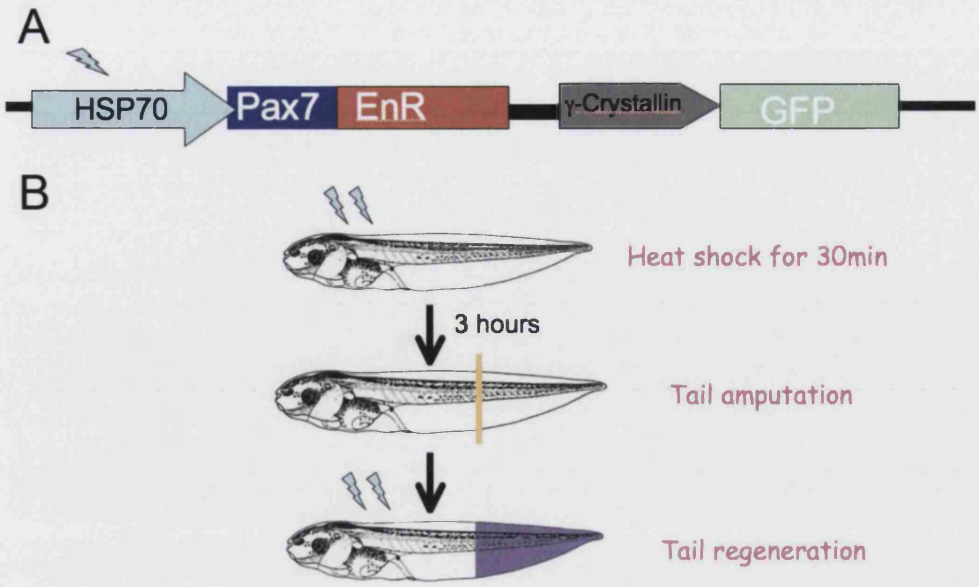

Figure 6.2 Diagram of heat shock experiment

(A) The diagram illustrates a transgenic version of *pax7EnR* construct. The construct contains two cassettes. One cassette is a heat shock promoter70 driven *pax7EnR* gene. The other is a GFP marker gene driven by r-crystallin promoter, which is accordingly expressed in lens of a transgenic tadpole

(B) Flowchart of a heat shock experiment. Tadpoles were immersed in a 34°C warm water bath for 30 minutes. Three hours after heat shock when a transgenic gene begins to express, the tadpole tails were amputated. The yellow line shows the position of tail amputation. During tail regeneration, the heat shock was performed each day for 30 minutes.

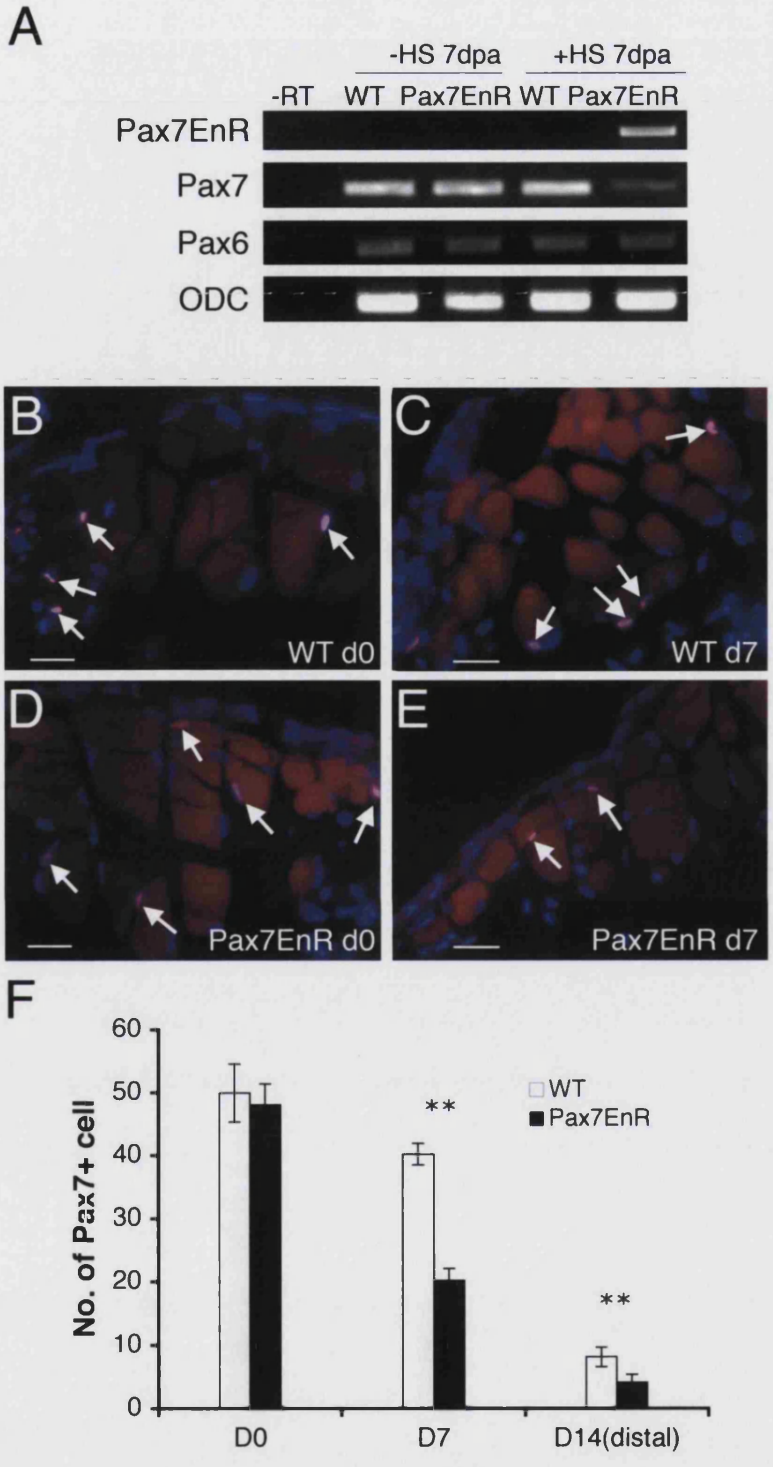
A
-HS 7dpa
+HS 7dpa
-RT
WT
Pax7EnR
WT
Pax7EnR
Pax7EnR
Pax7
Pax6
ODC
B
WT d0
C
WT d7
D
Pax7EnR d0
E
Pax7EnR d7
F
No. of Pax7+ cell
60
50
40
30
20
10
0
WT
Pax7EnR
**
**
D0
D7
D14(distal)

Figure 6.3 The number of muscle satellite cells is reduced in the heat shocked *pax7EnR* transgenic tails.

(A) RT-PCR detection of *pax7*, *pax6* and *pax7EnR* in wild type and *pax7EnR* transgenic tadpoles with or without heat shock treatment. (B-E) show the expression of pax7 (red) in transverse sections of the tails. (B) Wild type tail. (C) Wild type regenerating tail with daily heat shock for seven days after amputation. (D) *pax7EnR* transgenic tail. (E) *pax7EnR* transgenic regenerating tail with daily heat shock for seven days after amputation. (F) The histogram shows the number of satellite cells quantified by pax7 antibody staining. Ten tails of similar size were examined in each case. ** indicates $p<0.05$. The d7 bars refer to 7 day regenerates. The d14 bars refer to 14 day regenerates amputated at a more distal level to provoke a second regeneration. Because of the more distal position the absolute cell numbers per section are lower, but the wild type still has about twice the number of satellite cells compared to the heat-shocked *pax7EnR*. Scale bars, 20 μm.

The reduction of *pax7* level might arise from repression of transcription or from a reduction in the number of cells expressing *pax7*. To investigate these possibilities we compared the number of muscle satellite cells in wild type and *pax7EnR* regenerates. Both wild type and *pax7EnR* transgenic tadpoles were given the first heat shock three hours before tail amputation. Then the distal 50% of the tail was cut off and sectioned to generate the samples: WT d0 and *Pax7EnR* d0. During tail regeneration, a heat shock was administered once every day. Seven days later, the regenerating tails were fixed as the samples WT d7 and *Pax7EnR* d7. We counted the number of muscle satellite cells in the 50 μm long tail region that is nearest to the amputation surface. Based on Pax7 antibody staining of ten tails of each group, we found the number of satellite cells in WT d0 and *Pax7EnR* d0 is similar (Fig. 6.3B, D, F). After 7 days of regeneration, the number of satellite cells falls a little in the wild type regenerates but falls substantially in the *pax7EnR* regenerates (Fig. 6.3C, E, F). After 14 days of regeneration, the number of satellite cells in the *pax7EnR* tadpoles was still about half the number in wild type (Fig.6.3F). The 14 day sections are from a more distal level of the regenerate corresponding to the level of a second amputation (see below), and so the absolute cell numbers per section are much reduced due to the smaller area. For all the specimens the level of pax7 protein in the satellite cells appears approximately similar, indicating that the reduction of *pax7* mRNA level by pax7EnR arises from a reduction in the number of satellite cells.

VI.3.3 pax7EnR causes cell death during muscle regeneration

The reduction of the number of muscle satellite cells in *pax7EnR* transgenic tails might arise from a reduction in the normal proliferation or from promotion of cell death of satellite cells during muscle regeneration. We examined cell proliferation by PCNA antibody staining in three day regenerating tails of wild type and *Pax7EnR* transgenic tadpoles, but this showed no obvious difference (Fig. 6.4).

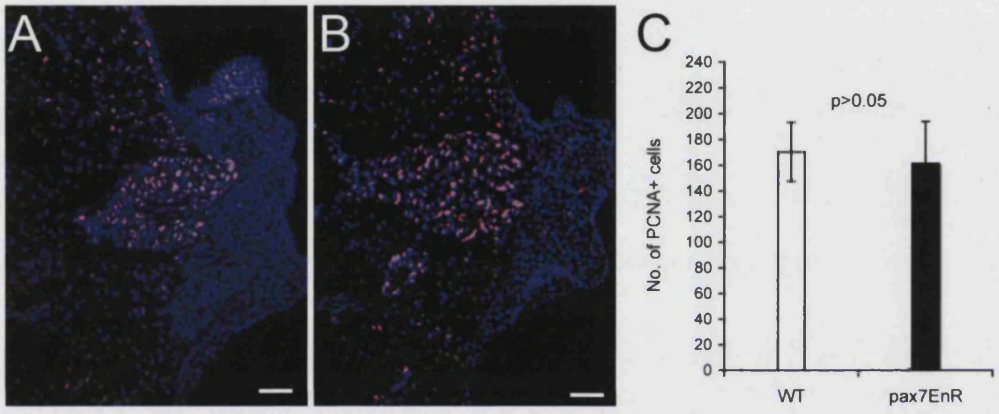

Figure 6.4 Cell proliferation detection by PCNA staining in regenerating tail

(A, B) PCNA staining on para-sagittal sections of 3 dpa wild type (A) and *pax7EnR* (B) tadpole tails are shown in red. Nucleus are counterstained with DAPI and shown in blue. (C) Number of PCNA+ cells were counted on 5 samples in each group and analysed with student's *t*-test.

Then Gufa Lin (my colleague) performed TUNEL staining to test apoptosis in the regenerating tails, and the results are shown in Fig. 6.5. In the case of *pax7EnR* transgenic tails, most apoptotic cells are present in the blastema region, the same location that muscle satellite cells are found freed from the myofibres (Fig. 6.5 A, B, C). In the wild type tails, the number of apoptotic

cells is smaller than that in the *pax7EnR* transgenic tails (Fig. 6.5 E). Moreover, in many clusters of cells, possibly indicating small clones, those with low level of pax7 expression are often entering apoptosis (red arrows in Fig. 6.5 D), while those with high level of pax7 expression are not. Given that the heat shock promoter is expected to have a similar activity in all cells, it may be that the cells with lower content of pax7 are more vulnerable to the effect of the pax7EnR. Quantification of cell death shows that cell death in mesenchyme and blastema of *pax7EnR* transgenic tails is more severe than that in wild type tails, whereas cell death in the regenerating spinal cord and notochord is unaffected (Fig. 6.5 E).

To further investigate apoptosis of muscle satellite cells during regeneration, we used the myoD antibody (Hopwood et al., 1992) to label the activated satellite cells (Zammit et al., 2004) and then performed a TUNEL assay (Fig. 6.5 F-H). The cell quantification result demonstrates that over 60% of myoD-labelled cells in the mesenchyme and blastema region of *pax7EnR* transgenic tails are undergoing apoptosis, whereas only 25% of myoD positive cells are undergoing apoptosis in wild type tails (Fig. 6.5 H). This result confirms a protective role of Pax7 in cell survival, something that has also been noticed in mammalian studies (Relaix et al., 2006). In other words, pax7EnR reduces the number of satellite cells not by reducing their proliferation rate but by increasing their rate of cell death.

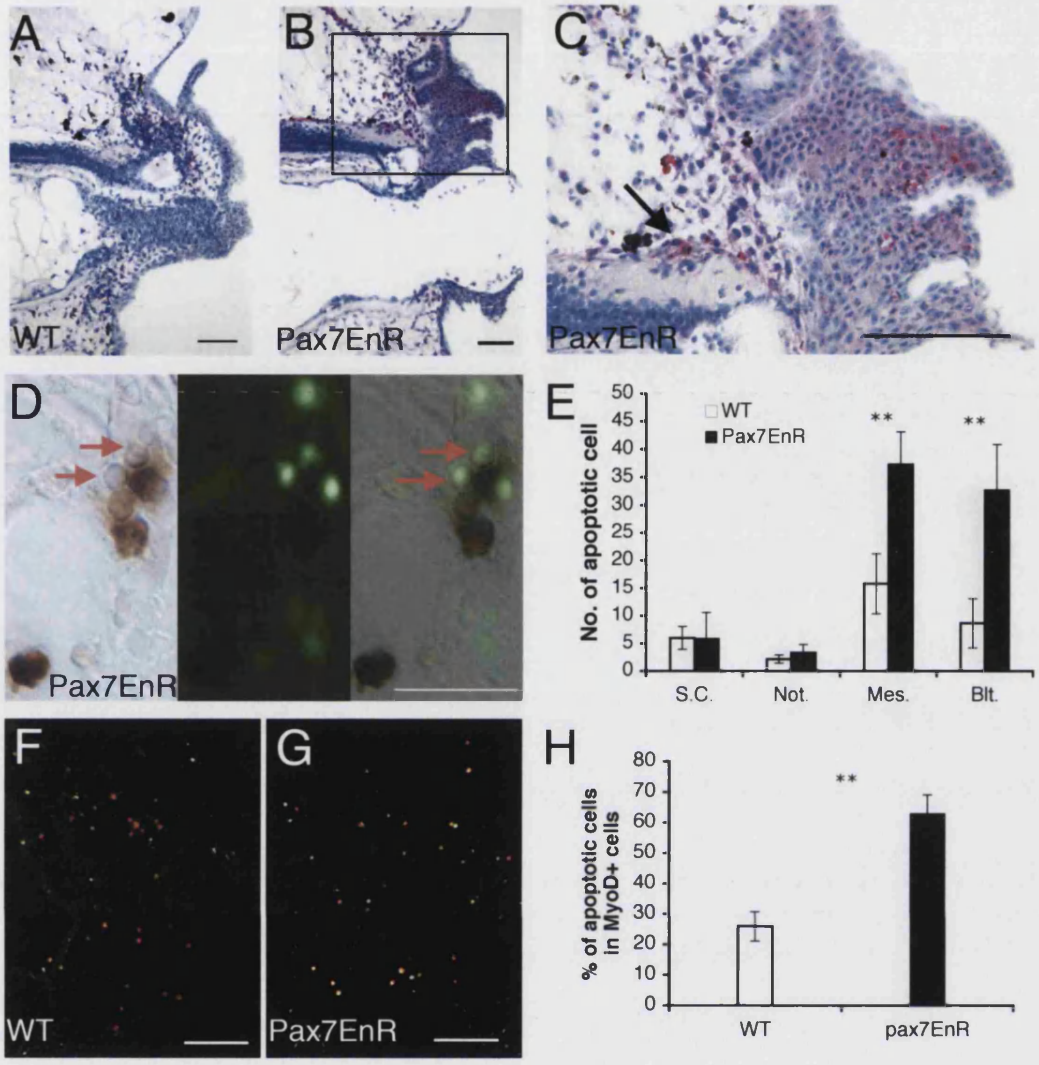

Figure 6.5 Pax7EnR promotes satellite cell apoptosis during tail regeneration.

(A-C) TUNEL assays were performed on para-sagittal sections of regenerated tail 3 dpa, the colour was developed with a Fast Red tablet and counterstained with Mayor's Hematoxylin. (A) Wild type regenerated tail. (B) Heat-shocked *pax7EnR* transgenic regenerated tail. (C) Higher power view of (B). TUNEL signals in the blastema region arrowed. (A-C) Dorsal side up, anterior to left. (D) Detection of pax7 with DAB staining (left panel) and apoptosis with fluorescein labelling (middle panel), in a cluster of cells in *pax7EnR* transgenic tail. The right panel is the merged view. Red arrows: two TUNEL positve/pax7 low expression cells. (E) Quantification of the number of apoptotic cells in the two groups of tails. (F and G) Detection of myoD (red) and cell death (green) on para-sagittal sections of regenerated tails 3dpa. (F) Blastema region of wild type tail. (G) Blastema region of heat chocked *pax7EnR* tails. (H) Quantification of the percentage of apoptotic cells among the myoD positive cells in the two groups of tails. Ten tails of similar size were examined in each group. ** in (E and H) indicate

$p<0.01$. Scale bars, 100 μm. Abbreviations: S.C., spinal cord; Not., notochord; Mes., mesenchyme; Blt., blastema. (A-E is contributed by Dr. Gufa Lin)

VI.3.4 Muscle regeneration is inhibited in *pax7EnR* transgenics

The above results show that the number of satellite cells in regenerating tails is sharply decreased when production of pax7EnR is activated by heat shock. So we predicted that less muscle would form in the regenerating *pax7EnR* transgenic tails compared to the wild type, if muscle satellite cells are the sole source of muscle regeneration. However, after fourteen days' heat shock treatment, when muscle in wild type tail has terminally differentiated, we did not find a significant reduction of muscle in the transgenic *pax7EnR* tails. As shown in Fig. 6.6 B and C, the staining strength of 12/101, a marker of muscle differentiation, is similar in *pax7EnR* and in wild type tails.

However, we know that the first regenerate is depleted of satellite cells and this raises the question of whether it can regenerate yet more muscle following a second amputation. To investigate this, we followed the procedure as depicted in Fig. 6.6 A. The *pax7EnR* expression is induced with a daily heat shock throughout the regeneration period. The first regenerate is allowed to grow for 14 days and then the distal 75% of the primary regenerated tail is re-amputated and allowed to regenerate for another 14 days. After the second regeneration, we performed 12/101 immunostaining on both regenerates. As shown in Fig. 6.6 B, D and G, the muscle in both first and second regenerates of wild type tails was well formed. In contrast, for the case of *pax7EnR* heat shocked tadpoles, 61% of the second tail regenerates showed substantially reduced differentiated muscle, and another 11% had no muscle at all (Fig. 6.6 E, F, table 6.1). In these individuals the spinal cord and the notochord do

regenerate fully in the second regenerate, so even though pax7 is expressed in some spinal cord cells it is presumably not necessary for regeneration (Fig. 6.6H). This experiment clearly shows that the regeneration of muscle depends on the presence of a population of satellite cells in the amputated tail.

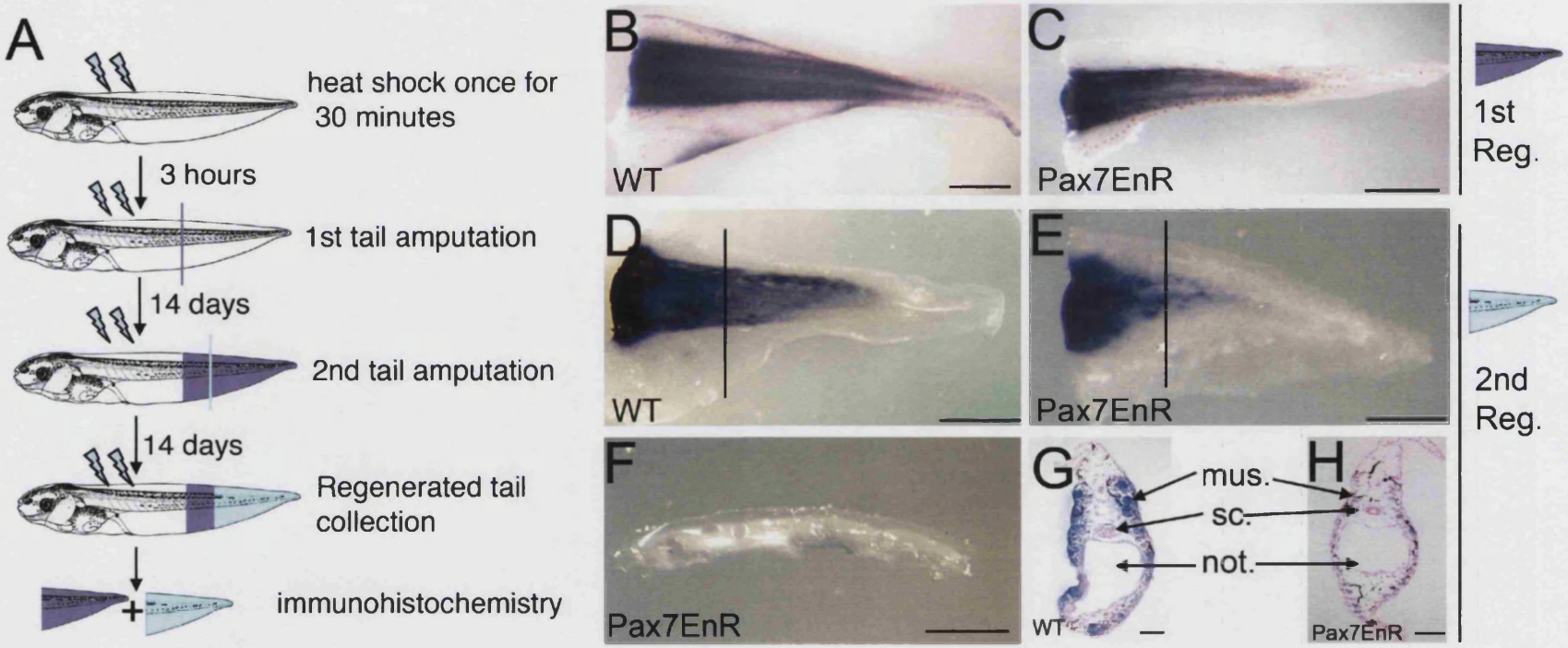
A
heat shock once for 30 minutes
3 hours
1st tail amputation
14 days
2nd tail amputation
14 days
Regenerated tail collection
immunohistochemistry
B
WT
C
Pax7EnR
1st Reg.
D
WT
E
Pax7EnR
2nd Reg.
F
Pax7EnR
G
mus.
sc.
not.
WT
H
Pax7EnR

Figure 6.6 12/101 staining of regenerating tails in wild type and *pax7EnR* transgenic tadpoles.

(A) The flowchart in the experiment of repeated tail amputation. The first heat shock is given 3 hours before the first amputation and heat shocks are given daily thereafter. The distal 50% tail was cut in the first tail amputation. The second tail amputation was performed 14dpa at the site of distal 75% of the first regenerated tail. The purple and blue tails indicate the primary and secondary regenerated tail respectively. (B-F) 12/101 antibody staining of the regenerated tails. (B) Wild type tails 14 days post first amputation. (C) *pax7EnR* transgenic tails 14 days post first amputation. (D) Wild type regenerated tails, 14 days after second amputation. (E, F) *pax7EnR* regenerated tails 14 days after second amputation. (G, H) Transverse section of second regenerated tail in wild type (G) and *pax7EnR* transgenic tadpoles (H). Section level is indicated by the black lines in (D) and (E). Scale bars in (B-F), 500 μm. Scale bars in (G and H), 50 μm. Abbreviations: sc, spinal cord; not. notochord; mus, muscle.

Table 6.1 Muscle regeneration in WT and *pax7EnR* transgenic tadpole tails

	HS 1st amputation				*HS 2nd amputation*			
Transgene	None	Partial	Complete	N	*None*	*Partial*	*Complete*	*N*
WT control	0	0	40 (100%)	40	*0*	*0*	*32 (100%)*	*32*
pax7EnR	0	0	35 (100%)	35	*3 (11)%*	*17 (61)%*	*8 (28)%*	*28*

Wild type and pax7EnR transgenic tadpoles were subjected to heat shock once a day after tail amputation. Myofibers were showed by 12/101 antibody staining. 14 days after first tail amputation, tail muscle in the wild type and *pax7EnR* tadpoles were both completely regenerated. The distal 75% of the primary regenerated tail was re-amputated and allowed to regenerate for another 14 days. All the second regenerates in the wild type group could fully regenerate muscle. But in the *pax7EnR* group, 11% of the second regenerates contained no muscle, 61% of the regenerates contained less muscle and only 28% of the regenerates could fully regenerate muscle.

VI. 4 Role of pax7 in the normal growing tadpole tail

VI.4.1 Muscle satellite cells are proliferating in the growing tail

Previously, we observed many BrdU labelled cells in the muscle of the growing tadpoles (Gargioli and Slack, 2004). To find whether these are, in fact, satellite cells, we injected BrdU into stage 49 tadpoles and fixed the tadpole tails one day after injection. They were processed for immuno-electron microscopy, using antibody to BrdU. We found that 60% of satellite cell nuclei are labelled with anti-BrdU (Fig. 6.7A, table 6.2). In contrast, almost all the myonuclei examined from four tails are negative for BrdU (Fig. 6.7B and table 6.2). Only one myonucleus was detected with a faint BrdU antibody signal. This is perhaps due to DNA repair synthesis, or to recent incorporation of a satellite cell in the fibre.

Muntz's group had also reported that mitotic division of myonuclei does not occur in *Xenopus laevis* by tritiated thymidine labelling experiment (Boudjelida and Muntz, 1987). And they observed the number of satellite cells does increase with time although they did not detect the satellite cells incorporated tritiated thymidine. This could be because of competition by endogenous thymidine. In our assay, the BrdU labelling mix contains 5-fluoro-2'-deoxyuridine, an inhibitor of thymidilate synthetase, and this is able to increase BrdU incorporation by lowering competition by endogenous thymidine. Therefore, we believe our results truly reflect the *in vivo* DNA synthesis situation. Since satellite cells are multiplying and myonuclei are not, it seems highly likely that the satellite cells are the source of the new fibres, or

contributes to fibre expansion during growth, as they do in mammals (Moss and Leblond, 1971).

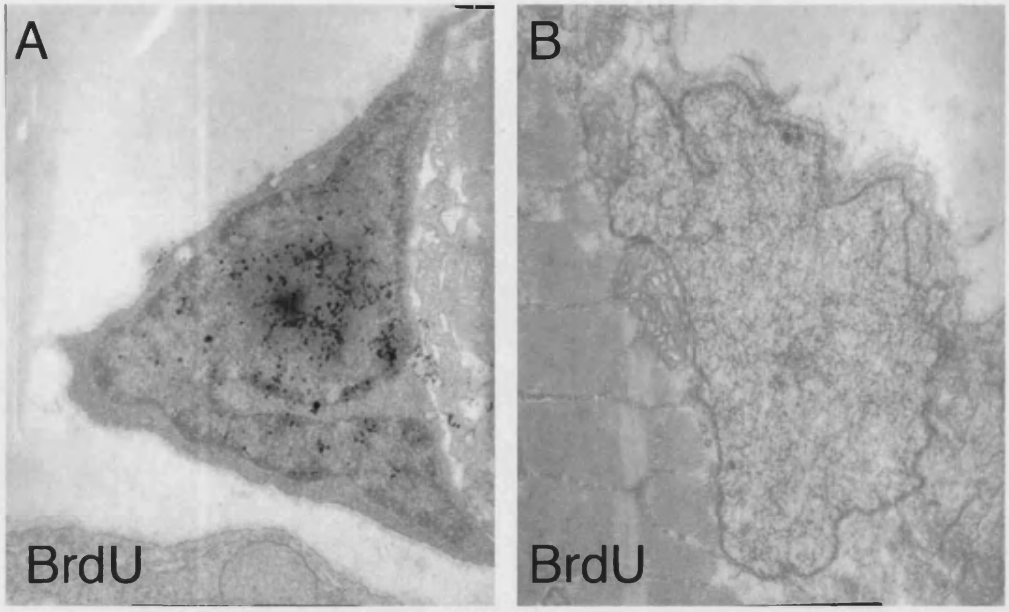

Figure 6.7 Immuno-Electron microscopy study of BrdU labelling in normal growing tadpole tails

(A) A satellite cell with BrdU labelling in the nucleus. Magnification ×20,000.

(B) A myonucleus negative for BrdU. Magnification ×15,000.

Table 6.2 Summary of Immuno-electron microscopy study with BrdU labelling

	BrdU		
	+	-	Total Number
Satellite cell	12 (60%)	8 (40%)	20
Myonucleus	1(3.3%)	30 (96.7%)	31

VI.4.2 The number of satellite cells is reduced by pax7EnR in normal growing tadpole tails

In mammals, postnatal muscle growth relies on functional muscle satellite cells. Stimulated by certain growth signals, the quiescent satellite cells residing on a myofibre are activated to become adult muscle progenitor cells contributing to muscle growth. Relaix et al. demonstrated that the postnatal muscle growth depends on pax7 to maintain survival of the activated satellite cells (Relaix et al., 2006). In *Xenopus* tadpole muscle regeneration, we have shown that pax7 has the same protective function as it does in mammalian adult muscle growth. Given that 60% of the satellite cells are activated in the normal growing tail, we expect that pax7 plays the same role in enabling normal muscle growth in *Xenopus* tadpole.

To test this, we generated *pax7EnR* transgenic tadpoles first and then sorted out similar sized tadpoles into two groups. One group of tadpoles was heat shocked for 30 minutes each day for 4 days as described before, while the other group of transgenic tadpoles did not receive heat shock treatment at all. Afterwards, we fixed each tail from both groups, sectioned, and counted the number of satellite cells based on pax7 antibody staining. As shown in Fig.6.8, in the heat shock treated group, the number of satellite cells in the tail is reduced to 62% of the cell number in non-heatshocked group. Therefore, our results further support the idea that pax7 is able to protect activated satellite cells from dying both in muscle growth and regeneration.

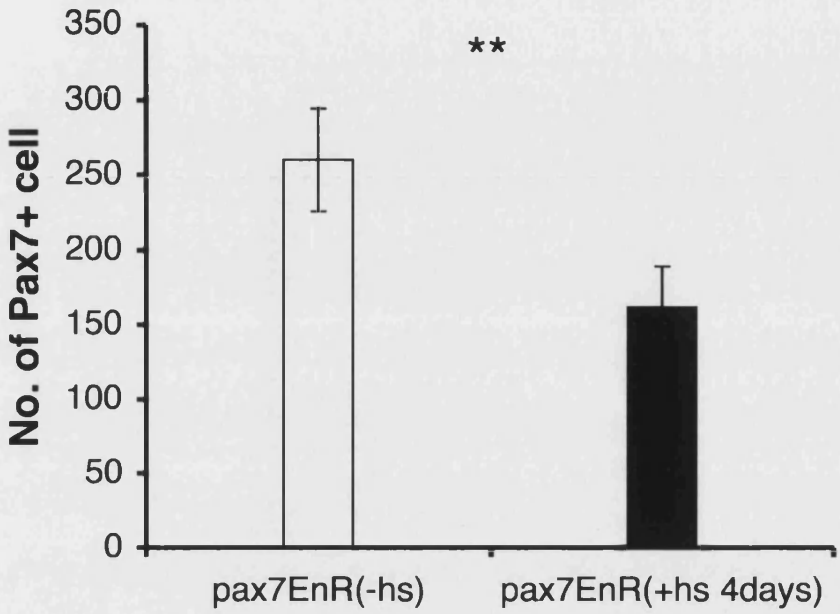

Figure 6.8 The number of muscle satellite cells in growing tadpole tails

The histogram shows the number of satellite cells quantified by pax7 antibody staining on sections of growing *pax7EnR* transgenic tadpole tails with (black bar) or without (white bar) heat shock for 4 days. Ten tails of similar size were examined in each case. ** indicates $p<0.05$. Abbreviations: hs, heat shock; pax7+, pax7 positive.

VI.5 Discussion

VI.5.1 Cellular origin of muscle regeneration in *Xenopus* tadpoles

Our results supports the previous conjecture that satellite cells residing in the tail muscle fibres are the origin of muscle regeneration in *Xenopus* tadpoles. Firstly, additional expression of pax7 in the regenerating tail suggests that satellite cells are activated to divide after tail amputation. In regenerating tails 3 days post amputation, a large number of pax7 positive cells appears in the region where muscle fibres are undergoing degeneration, and many pax7 positive cells are visible in the growing blastema (Fig. 6.1). Secondly, our experiments show that inhibition of pax7 action by pax7EnR causes apoptosis of muscle satellite cells, and reduces the number of satellite cells in regenerating tails. The tails that are depleted of satellite cells do still regenerate, but especially the second regenerates contain little or no muscle (Fig. 6.6 and table 6.1). Thus our results demonstrate that muscle regeneration in *Xenopus* tails is similar to muscle repair in mammals, where it has been generally accepted that satellite cells are adult muscle precursor cells and contribute to repair of damaged muscle (Wagers and Conboy, 2005).

Our experiments do not support the view that myofibres regenerate from resident or circulating stem cells of the side population (SP) type (Chargé and Rudnicki, 2004). As discussed above, these stem cells should be available to reconstitute the muscle fibres in *pax7EnR* tadpoles but do not do so. Our results also differ from the previous findings on limb regeneration in newts and axolotl, in which it has been well documented that de-differentiation and re-

differentiation of multinucleate muscle fibres occurs (Echeverri et al., 2001; Echeverri and Tanaka, 2002; Kumar et al., 2000; Lo et al., 1993). We see no particular reason to doubt the results from the urodele species but consider that the mode of *Xenopus* tail muscle regeneration to be much closer to the regeneration of damaged muscle in mammals. Interestingly a recent paper on newt regeneration has also highlighted a role for satellite cells (Morrison et al., 2006) .

IV.3.3 Role of pax7 in muscle regeneration and muscle growth

The actual requirement for pax7 function must be in the survival of the proliferating satellite cells rather than in their differentiation into muscle, as the ability to form a first regenerate is not significantly impaired. This is consistent with the observed loss of pax7 expression on differentiation (Seale and Rudnicki, 2000).

Recent studies have demonstrated that pax7 has an important role in cell survival of adult muscle satellite cells in postnatal muscle growth (Relaix et al., 2006). They found that activated caspase3 was immediately detectable after birth of *pax7-/-* mutant mice. Consistent with this, our detection of cell death with TUNEL assay during the tadpole muscle regeneration suggest that cells with low level of pax7 tend to go to apoptosis while those with high level of pax7 expression can be protected from dying in muscle regeneration. Moreover, we found the same situation when pax7EnR was induced in the normal growing tadpole tail. Notably, the anti-apoptotic role of pax7 occurs only at the activated state. Once the activated satellite cells differentiate, expression of pax7 will be turned off. The cells that retain pax7 expression

exit the cell cycle and replenish the satellite cell pool. In the regenerating tails of *pax7EnR* tadpoles, the number of cells undergoing apoptosis was increased (Fig. 6.5) and accordingly the satellite pool decreased. This ultimately resulted in the failure of regeneration of muscles in *pax7EnR* transgenic tails. Therefore, pax7 must also be required in the self-renewal process of satellite cells.

In mice it was found that pax3, which is expressed both in quiescent and activated muscle satellite cells in mammals, has a partially redundant function with Pax7 in satellite cells (Relaix et al., 2006; Relaix et al., 2005). Since the pax3 antibody from DSHB does not work on *Xenopus* tissue, we do not know whether pax3 is expressed in the *Xenopus* satellite cells. We do not obtain 100% suppression of muscle regeneration with *pax7EnR*. It is possible that this is because of the presence of a redundant component such as pax3, but it is also possible that we do not obtain 100% inhibition of pax7 function.

Taken together, our experiments demonstrated that Pax7 is required for the survival of the proliferating satellite cells in muscle and hence the maintenance of the satellite cell pool during muscle regeneration, as well as in normal muscle development in *Xenopus laevis*.

VII. Conclusions

In our study we have explored the embryonic origin of muscle satellite cells in *Xenopus laevis*. To do this, we identified a reliable satellite cell marker in *Xenopus* system and modified the method developed by Cesare Gargioli to more accurately trace the origin of satellite cells. We expected to get a clear-cut conclusion by taking advantage of transgenics and grafting techniques. However, we found that CMV-nucGFP expression itself in transgenic donor tadpoles does not label all the cells in the grafts.

Although the method is not perfect, we believe that the type II mesoderm (the dorsal-lateral presomitic mesoderm) rather than the type I (the presomite plate, immediately adjacent to the notochord) mesoderm contains the progenitors of at least some of the tail muscle satellite cells. Because of the way that the somite forms in the late neurula and tailbud stages, the type II mesoderm will end up as the outer part of the myotomes. We do not currently know whether the progenitors within the type II mesoderm are already committed to satellite cell lineage at the neurula stage. But the satellite cells derived from this region are found all through the myotomes indicating that they have some stable commitment which is retained as they move to their final positions.

When a correction is made to account for incomplete labelling of donor cells, still only a minority of satellite cells are labelled in type II grafts. It may be that the donors used for these grafts had significantly lower labelling levels than those we counted. Alternatively, it may be that the labelling is incomplete

because there is an additional source of satellite cells in *Xenopus laevis*. The satellite cells might come from ectoderm, for instance, the neural crest, or from the circulatory system, as suggested by the work of Cossu's group (De Angelis et al., 1999). To label these cells, we could use Cre-lox system to label neural crest cells with *slug* promoter (Vallin et al., 2001) or inject suitable dyes such as DiI-LDL into the heart to label the embryonic circulatory system. There was not time to undertake these experiments within the time limit of the thesis period.

In addition to the study of developmental origin of satellite cells, we put some effort into the functional analysis of the *pax7* gene during embryonic development and tadpole tail regeneration. Although pax7 is specifically expressed in the region where the progenitors of satellite cells locate, the mRNA injection study suggested that pax7 is not sufficient on its own to specify the satellite cell lineage.

We were able to demonstrate a real function for pax7 at a stage when the satellite cells are activated. According to our results, pax7 is able to prevent the activated satellite cells from apoptosis and hence maintain a persistent pool of satellite cells. Our finding not only can explain the continuous loss of satellite cells and impaired muscle regeneration in pax7-/- mice, but also provides evidence that pax7 acts as a novel apoptosis inhibitor in satellite cells.

Furthermore, the study proves that the satellite cells residing in the tail muscle fibres are the origin of muscle regeneration in *Xenopus* tadpoles. The cellular source of regenerated muscle has been controversial for some time.

It is well established that in urodele amphibians muscle regeneration involves dedifferentiation of multinucleated skeletal muscle fibre, which re-enter the cell cycle to proliferate and then re-fuse to form new fibres (Carlson, 2003). The cellular component of mammalian muscle regeneration is more complex. In mammals, non-muscle-derived and muscle-derived stem cells, other than satellite cells, have been demonstrated to be capable of myogenic differentiation and integrate into the regenerating musculature *in vivo* (Asakura et al., 2002; Bittner et al., 1999; Ferrari et al., 1998; Gussoni et al., 1999; Jankowski et al., 2002; Qu-Petersen et al., 2002). Moreover, mammalian myotubes stimulated by msx1 are capable of dedifferentiation *in vitro* (Odelberg et al., 2000). In spite of this complexity, compelling evidence proves that the satellite cell population is a principal contributor to mammalian regenerating muscle (Chargé and Rudnicki, 2004).

Our study shows for the first time that satellite cells in the anuran amphibian, *Xenopus laevis,* can not only form new muscle fibres, but can also form the entire muscle masses of a regenerating appendage. In *Xenopus* regeneration there is no de-differentiation of myofibres and we have seen no evidence of other cell population reconstituting the myofibres. Compared with the urodele limb regenerate, where de-differentiation of multinucleate muscle fibres is an important mechanism, the muscle regeneration in tadpole tails is more akin to the tissue regeneration found in mammals. We therefore believe that the

Xenopus tadpole provides us a new muscle regeneration model and that the results should also be relevant to the mechanisms in higher vertebrates.

VIII. Bibliography

Amaya, E. and Kroll, K. L. (1999). A method for generating transgenic frog embryos. *Methods Mol Biol* **97**, 393-414.

Armand, O., Boutineau, A. M., Mauger, A., Pautou, M. P. and Kieny, M. (1983). Origin of satellite cells in avian skeletal muscles. *Arch Anat Microsc Morphol Exp* **72**, 163-81.

Asakura, A., Seale, P., Girgis-Gabardo, A. and Rudnicki, M. A. (2002). Myogenic specification of side population cells in skeletal muscle. *J Cell Biol* **159**, 123-34.

Austin, L., Bower, J., Kurek, J. and Vakakis, N. (1992). Effects of leukaemia inhibitory factor and other cytokines on murine and human myoblast proliferation. *J Neurol Sci* **112**, 185-91.

Austin, L., Bower, J. J., Bennett, T. M., Lynch, G. S., Kapsa, R., White, J. D., Barnard, W., Gregorevic, P. and Byrne, E. (2000). Leukemia inhibitory factor ameliorates muscle fiber degeneration in the mdx mouse. *Muscle Nerve* **23**, 1700-5.

Barnard, W., Bower, J., Brown, M. A., Murphy, M. and Austin, L. (1994). Leukemia inhibitory factor (LIF) infusion stimulates skeletal muscle regeneration after injury: injured muscle expresses lif mRNA. *J Neurol Sci* **123**, 108-13.

Beauchamp, J. R., Heslop, L., Yu, D. S., Tajbakhsh, S., Kelly, R. G., Wernig, A., Buckingham, M. E., Partridge, T. A. and Zammit, P. S. (2000). Expression of CD34 and Myf5 defines the majority of quiescent adult skeletal muscle satellite cells. *J Cell Biol* **151**, 1221-34.

Beck, C. W., Christen, B. and Slack, J. M. W. (2003). Molecular pathways needed for regeneration of spinal cord and muscle in a vertebrate. *Dev Cell* **5**, 429-39.

Bittner, R. E., Schofer, C., Weipoltshammer, K., Ivanova, S., Streubel, B., Hauser, E., Freilinger, M., Hoger, H., Elbe-Burger, A. and Wachtler, F.

(1999). Recruitment of bone-marrow-derived cells by skeletal and cardiac muscle in adult dystrophic mdx mice. *Anat Embryol (Berl)* **199**, 391-6.

Boudjelida, H. and Muntz, L. (1987). Multinucleation during myogenesis of the myotome of Xenopus laevis: a qualitative study. *Development* **101**, 583-90.

Brockes, J. P. and Kumar, A. (2002). Plasticity and reprogramming of differentiated cells in amphibian regeneration. *Nat Rev Mol Cell Biol* **3**, 566-74.

Cairns, J. (1975). Mutation selection and the natural history of cancer. *Nature* **255**, 197-200.

Campion, D. R., Hausman, G. J. and Richardson, R. L. (1981a). Skeletal muscle development in the fetal pig after decapitation in utero. *Biol Neonate* **39**, 253-9.

Campion, D. R., Richardson, R. L., Reagan, J. O. and Kraeling, R. R. (1981b). Changes in the satellite cell population during postnatal growth of pig skeletal muscle. *J Anim Sci* **52**, 1014-8.

Carlson, B. M. (2003). Muscle regeneration in amphibians and mammals: passing the torch. *Dev. Dyn.* **226**, 167-81.

Chanoine, C. and Hardy, S. (2003). Xenopus muscle development: from primary to secondary myogenesis. *Dev Dyn* **226**, 12-23.

Chargé, S. B. and Rudnicki, M. A. (2004). Cellular and molecular regulation of muscle regeneration. *Physiol Rev* **84**, 209-38.

Chen, S. E., Gerken, E., Zhang, Y., Zhan, M., Mohan, R. K., Li, A. S., Reid, M. B. and Li, Y. P. (2005). Role of TNF-{alpha} signaling in regeneration of cardiotoxin-injured muscle. *Am J Physiol Cell Physiol* **289**, C1179-87.

Coletti, D., Moresi, V., Adamo, S., Molinaro, M. and Sassoon, D. (2005). Tumor necrosis factor-alpha gene transfer induces cachexia and inhibits muscle regeneration. *Genesis* **43**, 120-8.

Collins, C. A., Olsen, I., Zammit, P. S., Heslop, L., Petrie, A., Partridge, T. A. and Morgan, J. E. (2005). Stem cell function, self-renewal, and behavioral

heterogeneity of cells from the adult muscle satellite cell niche. *Cell* **122**, 289-301.

Conboy, I. M. and Rando, T. A. (2002). The regulation of Notch signaling controls satellite cell activation and cell fate determination in postnatal myogenesis. *Dev Cell* **3**, 397-409.

Conway, K., Price, P., Harding, K. G. and Jiang, W. G. (2006). The molecular and clinical impact of hepatocyte growth factor, its receptor, activators, and inhibitors in wound healing. *Wound Repair Regen* **14**, 2-10.

Cooper, R. N., Tajbakhsh, S., Mouly, V., Cossu, G., Buckingham, M. and Butler-Browne, G. S. (1999). In vivo satellite cell activation via Myf5 and MyoD in regenerating mouse skeletal muscle. *J Cell Sci* **112**, 2895-901.

Cornelison, D. D., Filla, M. S., Stanley, H. M., Rapraeger, A. C. and Olwin, B. B. (2001). Syndecan-3 and syndecan-4 specifically mark skeletal muscle satellite cells and are implicated in satellite cell maintenance and muscle regeneration. *Dev Biol* **239**, 79-94.

Cornelison, D. D., Wilcox-Adelman, S. A., Goetinck, P. F., Rauvala, H., Rapraeger, A. C. and Olwin, B. B. (2004). Essential and separable roles for Syndecan-3 and Syndecan-4 in skeletal muscle development and regeneration. *Genes Dev* **18**, 2231-6.

Cornelison, D. D. and Wold, B. J. (1997). Single-cell analysis of regulatory gene expression in quiescent and activated mouse skeletal muscle satellite cells. *Dev. Biol.* **191**, 270-83.

Cossu, G. and Biressi, S. (2005). Satellite cells, myoblasts and other occasional myogenic progenitors: possible origin, phenotypic features and role in muscle regeneration. *Semin Cell Dev Biol* **16**, 623-31.

Cossu, G., Molinaro, M. and Pacifici, M. (1983). Differential response of satellite cells and embryonic myoblasts to a tumor promoter. *Dev Biol* **98**, 520-4.

Dale, L. and Slack, J. M. W. (1987). Fate map for the 32-cell stage of Xenopus laevis. *Development* **99**, 527-51.

De Angelis, L., Berghella, L., Coletta, M., Lattanzi, L., Zanchi, M., Cusella-De Angelis, M. G., Ponzetto, C. and Cossu, G. (1999). Skeletal myogenic progenitors originating from embryonic dorsal aorta coexpress endothelial and myogenic markers and contribute to postnatal muscle growth and regeneration. *J. Cell Biol.* **147**, 869-78.

Dent, J. N. (1962). Limb regeneration in larvae and metamorphosing individuals of the South African clawed toad. *J Morphol* **110**, 61-77.

Dobie, K., Mehtali, M., McClenaghan, M. and Lathe, R. (1997). Variegated gene expression in mice. *Trends Genet* **13**, 127-30.

Echeverri, K., Clarke, J. D. and Tanaka, E. M. (2001). In vivo imaging indicates muscle fiber dedifferentiation is a major contributor to the regenerating tail blastema. *Dev Biol* **236**, 151-64.

Echeverri, K. and Tanaka, E. M. (2002). Ectoderm to mesoderm lineage switching during axolotl tail regeneration. *Science* **298**, 1993-6.

Ferrari, G., Cusella-De Angelis, G., Coletta, M., Paolucci, E., Stornaiuolo, A., Cossu, G. and Mavilio, F. (1998). Muscle regeneration by bone marrow-derived myogenic progenitors. *Science* **279**, 1528-30.

Gamble, H. J., Fenton, J. and Allsopp, G. (1978). Electron microscope observations on human fetal striated muscle. *J Anat* **126**, 567-89.

Gangenahalli, G. U., Singh, V. K., Verma, Y. K., Gupta, P., Sharma, R. K., Chandra, R. and Luthra, P. M. (2006). Hematopoietic stem cell antigen CD34: role in adhesion or homing. *Stem Cells Dev* **15**, 305-13.

Gargioli, C. and Slack, J. M. W. (2004). Cell lineage tracing during Xenopus tail regeneration. *Development* **131**, 2669-79.

Garry, D. J., Meeson, A., Elterman, J., Zhao, Y., Yang, P., Bassel-Duby, R. and Williams, R. S. (2000). Myogenic stem cell function is impaired in mice lacking the forkhead/winged helix protein MNF. *Proc Natl Acad Sci U S A* **97**, 5416-21.

Garry, D. J., Yang, Q., Bassel-Duby, R. and Williams, R. S. (1997). Persistent expression of MNF identifies myogenic stem cells in postnatal muscles. *Dev Biol* **188**, 280-94.

Gehring, W. J. and Ikeo, K. (1999). Pax 6: mastering eye morphogenesis and eye evolution. *Trends Genet* **15**, 371-7.

Gibson, M. C. and Schultz, E. (1982). The distribution of satellite cells and their relationship to specific fiber types in soleus and extensor digitorum longus muscles. *Anat Rec* **202**, 329-37.

Gille, J., Khalik, M., Konig, V. and Kaufmann, R. (1998). Hepatocyte growth factor/scatter factor (HGF/SF) induces vascular permeability factor (VPF/VEGF) expression by cultured keratinocytes. *J Invest Dermatol* **111**, 1160-5.

Griffith, C. M., Wiley, M. J. and Sanders, E. J. (1992). The vertebrate tail bud: three germ layers from one tissue. *Anat Embryol (Berl)* **185**, 101-13.

Grimaldi, A., Tettamanti, G., Martin, B. L., Gaffield, W., Pownall, M. E. and Hughes, S. M. (2004). Hedgehog regulation of superficial slow muscle fibres in Xenopus and the evolution of tetrapod trunk myogenesis. *Development* **131**, 3249-62.

Gros, J., Manceau, M., Thomae, V. and Marcelle, C. (2005). A common somitic origin for embryonic muscle progenitors and satellite cells. *Nature* **435**, 954-8.

Gussoni, E., Soneoka, Y., Strickland, C. D., Buzney, E. A., Khan, M. K., Flint, A. F., Kunkel, L. M. and Mulligan, R. C. (1999). Dystrophin expression in the mdx mouse restored by stem cell transplantation. *Nature* **401**, 390-4.

Halevy, O., Piestun, Y., Allouh, M. Z., Rosser, B. W., Rinkevich, Y., Reshef, R., Rozenboim, I., Wleklinski-Lee, M. and Yablonka-Reuveni, Z. (2004). Pattern of Pax7 expression during myogenesis in the posthatch chicken establishes a model for satellite cell differentiation and renewal. *Dev Dyn* **231**, 489-502.

Han, K. and Manley, J. L. (1993). Transcriptional repression by the Drosophila even-skipped protein: definition of a minimal repression domain. *Genes Dev* **7**, 491-503.

Hartley, K. O., Nutt, S. L. and Amaya, E. (2002). Targeted gene expression in transgenic Xenopus using the binary Gal4-UAS system. *Proc Natl Acad Sci U S A* **99**, 1377-82.

Hartley, R. S., Bandman, E. and Yablonka-Reuveni, Z. (1992). Skeletal muscle satellite cells appear during late chicken embryogenesis. *Dev Biol* **153**, 206-16.

Holmdahl, D. E. (1939). Die morphogenese des Vertebratenorganismus vom ormalen und experimentellen gesichtspunkt. . *Wilhelm Roux's Archiv.* **139**, 191-226.

Hopwood, N. D., Pluck, A., Gurdon, J. B. and Dilworth, S. M. (1992). Expression of XMyoD protein in early Xenopus laevis embryos. *Development* **114**, 31-8.

Horst, D., Ustanina, S., Sergi, C., Mikuz, G., Juergens, H., Braun, T. and Vorobyov, E. (2006). Comparative expression analysis of Pax3 and Pax7 during mouse myogenesis. *Int J Dev Biol* **50**, 47-54.

Illa, I., Leon-Monzon, M. and Dalakas, M. C. (1992). Regenerating and denervated human muscle fibers and satellite cells express neural cell adhesion molecule recognized by monoclonal antibodies to natural killer cells. *Ann Neurol* **31**, 46-52.

Jackson, K. A., Mi, T. and Goodell, M. A. (1999). Hematopoietic potential of stem cells isolated from murine skeletal muscle. *Proc Natl Acad Sci U S A* **96**, 14482-6.

Jaffredo, T., Gautier, R., Eichmann, A. and Dieterlen-Lievre, F. (1998). Intraaortic hemopoietic cells are derived from endothelial cells during ontogeny. *Development* **125**, 4575-83.

Jankowski, R. J., Deasy, B. M., Cao, B., Gates, C. and Huard, J. (2002). The role of CD34 expression and cellular fusion in the regeneration capacity of myogenic progenitor cells. *J Cell Sci* **115**, 4361-74.

Jesse, T. L., LaChance, R., Iademarco, M. F. and Dean, D. C. (1998). Interferon regulatory factor-2 is a transcriptional activator in muscle where It regulates expression of vascular cell adhesion molecule-1. *J Cell Biol* **140**, 1265-76.

Jo, C., Kim, H., Jo, I., Choi, I., Jung, S. C., Kim, J., Kim, S. S. and Jo, S. A. (2005). Leukemia inhibitory factor blocks early differentiation of skeletal muscle cells by activating ERK. *Biochim Biophys Acta* **1743**, 187-97.

Kassar-Duchossoy, L., Giacone, E., Gayraud-Morel, B., Jory, A., Gomes, D. and Tajbakhsh, S. (2005). Pax3/Pax7 mark a novel population of primitive myogenic cells during development. *Genes Dev* **19**, 1426-31.

Kaul, A., Koster, M., Neuhaus, H. and Braun, T. (2000). Myf-5 revisited: loss of early myotome formation does not lead to a rib phenotype in homozygous Myf-5 mutant mice. *Cell* **102**, 17-9.

Kroll, K. L. and Amaya, E. (1996). Transgenic Xenopus embryos from sperm nuclear transplantations reveal FGF signaling requirements during gastrulation. *Development* **122**, 3173-83.

Kuang, S., Charge, S. B., Seale, P., Huh, M. and Rudnicki, M. A. (2006). Distinct roles for Pax7 and Pax3 in adult regenerative myogenesis. *J Cell Biol* **172**, 103-13.

Kuang, S., Kuroda, K., Le Grand, F. and Rudnicki, M. A. (2007). Asymmetric self-renewal and commitment of satellite stem cells in muscle. *Cell* **129**, 999-1010.

Kumar, A., Velloso, C. P., Imokawa, Y. and Brockes, J. P. (2000). Plasticity of retrovirus-labelled myotubes in the newt limb regeneration blastema. *Dev Biol* **218**, 125-36.

Kurek, J. B., Bower, J. J., Romanella, M., Koentgen, F., Murphy, M. and Austin, L. (1997). The role of leukemia inhibitory factor in skeletal muscle regeneration. *Muscle Nerve* **20**, 815-22.

Kurek, J. B., Nouri, S., Kannourakis, G., Murphy, M. and Austin, L. (1996). Leukemia inhibitory factor and interleukin-6 are produced by diseased and regenerating skeletal muscle. *Muscle Nerve* **19**, 1291-301.

Lacosta, A. M., Muniesa, P., Ruberte, J., Sarasa, M. and Domâinguez, L. (2005). Novel expression patterns of Pax3/Pax7 in early trunk neural crest and its melanocyte and non-melanocyte lineages in amniote embryos. *Pigment Cell Res* **18**, 243-51.

Lagna, G. and Hemmati-Brivanlou, A. (1998). Use of dominant negative constructs to modulate gene expression. *Curr Top Dev Biol* **36**, 75-98.

Lane, M. C. and Sheets, M. D. (2002). Rethinking axial patterning in amphibians. *Dev Dyn* **225**, 434-47.

Langsdorf, A., Do, A. T., Kusche-Gullberg, M., Emerson, C. P., Jr. and Ai, X. (2007). Sulfs are regulators of growth factor signaling for satellite cell differentiation and muscle regeneration. *Dev Biol* **311**, 464-77.

Lee, S. J. (2004). Regulation of muscle mass by myostatin. *Annu Rev Cell Dev Biol* **20**, 61-86.

Lin, G., Chen, Y. and Slack, J. M. W. (2007). Regeneration of neural crest derivatives in the Xenopus tadpole tail. *BMC Dev Biol* **7**, 56.

Lo, D. C., Allen, F. and Brockes, J. P. (1993). Reversal of muscle differentiation during urodele limb regeneration. *Proc Natl Acad Sci U S A* **90**, 7230-4.

Maier, A. and Bornemann, A. (2004). M-cadherin transcription in satellite cells from normal and denervated muscle. *Am J Physiol Cell Physiol* **286**, C708-12.

Matsunaga, E., Araki, I. and Nakamura, H. (2001). Role of Pax3/7 in the tectum regionalization. *Development* **128**, 4069-77.

Mauro, A. (1961). Satellite cell of skeletal muscle fibers. *J. Biophys. Biochem. Cytol.* **9**, 493-5.

McCroskery, S., Thomas, M., Maxwell, L., Sharma, M. and Kambadur, R. (2003). Myostatin negatively regulates satellite cell activation and self-renewal. *J Cell Biol* **162**, 1135-47.

McCroskery, S., Thomas, M., Platt, L., Hennebry, A., Nishimura, T., McLeay, L., Sharma, M. and Kambadur, R. (2005). Improved muscle healing through enhanced regeneration and reduced fibrosis in myostatin-null mice. *J Cell Sci* **118**, 3531-41.

McPherron, A. C., Lawler, A. M. and Lee, S. J. (1997). Regulation of skeletal muscle mass in mice by a new TGF-beta superfamily member. *Nature* **387**, 83-90.

Mendler, L., Zador, E., Ver Heyen, M., Dux, L. and Wuytack, F. (2000). Myostatin levels in regenerating rat muscles and in myogenic cell cultures. *J Muscle Res Cell Motil* **21**, 551-63.

Milhorat, A. T. (1970). Forward in regeneration of striated muscle and myogenesis. *Amsterdam: Ekcerpta Medica.*

Molofsky, A. V., Pardal, R. and Morrison, S. J. (2004). Diverse mechanisms regulate stem cell self-renewal. *Curr Opin Cell Biol* **16**, 700-7.

Montarras, D., Morgan, J., Collins, C., Relaix, F., Zaffran, S., Cumano, A., Partridge, T. and Buckingham, M. (2005). Direct isolation of satellite cells for skeletal muscle regeneration. *Science* **309**, 2064-7.

Moody, S. A. (1987). Fates of the blastomeres of the 32-cell-stage Xenopus embryo. *Dev Biol* **122**, 300-19.

Morrison, J. I., Loof, S., He, P. and Simon, A. (2006). Salamander limb regeneration involves the activation of a multipotent skeletal muscle satellite cell population. *J Cell Biol* **172**, 433-40.

Moss, F. P. and Leblond, C. P. (1970). Nature of dividing nuclei in skeletal muscle of growing rats. *J Cell Biol* **44**, 459-62.

Moss, F. P. and Leblond, C. P. (1971). Satellite cells as the source of nuclei in muscles of growing rats. *The Anatomical record.* **170**, 421-35.

Namenwirth, M. (1974). The inheritance of cell differentiation during limb regeneration in the axolotl. *Dev Biol* **41**, 42-56.

Neufeld, D. A. and Day, F. A. (1996). Perspective: a suggested role for basement membrane structures during newt limb regeneration. *Anat Rec* **246**, 155-61.

Newlands, S., Levitt, L. K., Robinson, C. S., Karpf, A. B., Hodgson, V. R., Wade, R. P. and Hardeman, E. C. (1998). Transcription occurs in pulses in muscle fibers. *Genes Dev* **12**, 2748-58.

Nieuwkoop, P. D. and Faber, J. (1967). Normal table of Xenopus laevis (Daudin). Amsterdam: North-Holland.

Nomura, T., Kawakami, A. and Fujisawa, H. (1998). Correlation between tectum formation and expression of two PAX family genes, PAX7 and PAX6, in avian brains. *Dev. Growth. Differ.* **40**, 485-95.

Odelberg, S. J., Kollhoff, A. and Keating, M. T. (2000). Dedifferentiation of mammalian myotubes induced by msx1. *Cell* **103**, 1099-109.

Ordahl, C. P., Berdougo, E., Venters, S. J. and Denetclaw, W. F., Jr. (2001). The dermomyotome dorsomedial lip drives growth and morphogenesis of both the primary myotome and dermomyotome epithelium. *Development* **128**, 1731-44.

Osborn, L., Hession, C., Tizard, R., Vassallo, C., Luhowskyj, S., Chi-Rosso, G. and Lobb, R. (1989). Direct expression cloning of vascular cell adhesion molecule 1, a cytokine-induced endothelial protein that binds to lymphocytes. *Cell* **59**, 1203-11.

Otto, A., Schmidt, C. and Patel, K. (2006). Pax3 and Pax7 expression and regulation in the avian embryo. *Anat Embryol (Berl)* **211**, 293-310.

Oustanina, S., Hause, G. and Braun, T. (2004). Pax7 directs postnatal renewal and propagation of myogenic satellite cells but not their specification. *Embo J* **23**, 3430-9.

Peck, D. and Walsh, F. S. (1993). Differential effects of over-expressed neural cell adhesion molecule isoforms on myoblast fusion. *J Cell Biol* **123**, 1587-95.

Potten, C. S., Owen, G. and Booth, D. (2002). Intestinal stem cells protect their genome by selective segregation of template DNA strands. *J Cell Sci* **115**, 2381-8.

Pownall, M. E., Gustafsson, M. K. and Emerson, C. P. (2002). Myogenic regulatory factors and the specification of muscle progenitors in vertebrate embryos. *Annu. Rev. Cell Dev. Biol.* **18**.

Qu-Petersen, Z., Deasy, B., Jankowski, R., Ikezawa, M., Cummins, J., Pruchnic, R., Mytinger, J., Cao, B., Gates, C., Wernig, A. et al. (2002). Identification of a novel population of muscle stem cells in mice: potential for muscle regeneration. *J Cell Biol* **157**, 851-64.

Rapraeger, A. C. (2000). Syndecan-regulated receptor signaling. *J Cell Biol* **149**, 995-8.

Relaix, F., Montarras, D., Zaffran, S., Gayraud-Morel, B., Rocancourt, D., Tajbakhsh, S., Mansouri, A., Cumano, A. and Buckingham, M. (2006). Pax3 and Pax7 have distinct and overlapping functions in adult muscle progenitor cells. *J Cell Biol* **172**, 91-102.

Relaix, F., Rocancourt, D., Mansouri, A. and Buckingham, M. (2005). A Pax3/Pax7-dependent population of skeletal muscle progenitor cells. *Nature* **435**, 948-53.

Rosen, G. D., Sanes, J. R., LaChance, R., Cunningham, J. M., Roman, J. and Dean, D. C. (1992). Roles for the integrin VLA-4 and its counter receptor VCAM-1 in myogenesis. *Cell* **69**, 1107-19.

Rudnicki, M. A., Braun, T., Hinuma, S. and Jaenisch, R. (1992). Inactivation of MyoD in mice leads to up-regulation of the myogenic HLH gene Myf-5 and results in apparently normal muscle development. *Cell* **71**, 383-90.

Rudnicki, M. A., Schnegelsberg, P. N., Stead, R. H., Braun, T., Arnold, H. H. and Jaenisch, R. (1993). MyoD or Myf-5 is required for the formation of skeletal muscle. *Cell* **75**, 1351-9.

Rutishauser, U. and Landmesser, L. (1991). Polysialic acid on the surface of axons regulates patterns of normal and activity-dependent innervation. *Trends Neurosci* **14**, 528-32.

Ryffel, G. U., Werdien, D., Turan, G., Gerhards, A., Goosses, S. and Senkel, S. (2003). Tagging muscle cell lineages in development and tail regeneration using Cre recombinase in transgenic Xenopus. *Nucleic Acids Res* **31**, e44.

Schienda, J., Engleka, K. A., Jun, S., Hansen, M. S., Epstein, J. A., Tabin, C. J., Kunkel, L. M. and Kardon, G. (2006). Somitic origin of limb muscle satellite and side population cells. *Proc Natl Acad Sci U S A* **103**, 945-50.

Schmalbruch, H. and Hellhammer, U. (1977). The number of nuclei in adult rat muscles with special reference to satellite cells. *Anat Rec* **189**, 169-75.

Schubert, W., Zimmermann, K., Cramer, M. and Starzinski-Powitz, A. (1989). Lymphocyte antigen Leu-19 as a molecular marker of regeneration in human skeletal muscle. *Proc Natl Acad Sci U S A* **86**, 307-11.

Schultz, E., Gibson, M. C. and Champion, T. (1978). Satellite cells are mitotically quiescent in mature mouse muscle: an EM and radioautographic study. *J Exp Zool* **206**, 451-6.

Schultz, E. and McCormick, K. M. (1994). Skeletal muscle satellite cells. *Rev Physiol Biochem Pharmacol* **123**, 213-57.

Seale, P., Asakura, A. and Rudnicki, M. A. (2001). The potential of muscle stem cells. *Dev Cell* **1**, 333-42.

Seale, P., Ishibashi, J., Scime, A. and Rudnicki, M. A. (2004). Pax7 is necessary and sufficient for the myogenic specification of CD45+:Sca1+ stem cells from injured muscle. *PLoS. Biol.* **2**, E130.

Seale, P. and Rudnicki, M. A. (2000). A new look at the origin, function, and "stem-cell" status of muscle satellite cells. *Dev Biol* **218**, 115-24.

Seale, P., Sabourin, L. A., Girgis-Gabardo, A., Mansouri, A., Gruss, P. and Rudnicki, M. A. (2000). Pax7 is required for the specification of myogenic satellite cells. *Cell* **102**, 777-86.

Sheehan, S. M. and Allen, R. E. (1999). Skeletal muscle satellite cell proliferation in response to members of the fibroblast growth factor family and hepatocyte growth factor. *J Cell Physiol* **181**, 499-506.

Shefer, G., Van de Mark, D. P., Richardson, J. B. and Yablonka-Reuveni, Z. (2006). Satellite-cell pool size does matter: defining the myogenic potency of aging skeletal muscle. *Dev Biol* **294**, 50-66.

Shi, X. and Garry, D. J. (2006). Muscle stem cells in development, regeneration, and disease. *Genes Dev* **20**, 1692-708.

Shinin, V., Gayraud-Morel, B., Gomes, D. and Tajbakhsh, S. (2006). Asymmetric division and cosegregation of template DNA strands in adult muscle satellite cells. *Nat Cell Biol* **8**, 677-87.

Slack, J. M. W. (2006). Essential Developmental Biology. Oxford: Blackwell publishing company.

Slack, J. M. W., Beck, C. W., Gargioli, C. and Christen, B. (2004). Cellular and molecular mechanisms of regeneration in Xenopus. *Philos Trans R Soc Lond B Biol Sci* **359**, 745-51.

Slack, J. M. W., Lin, G. and Chen, Y. (2007). The Xenopus tadpole: a new model for regeneration research. *Cell Mol Life Sci DOI 10.1007/s00018-007-7431-1.*

Snow, M. H. (1977). The effects of aging on satellite cells in skeletal muscles of mice and rats. *Cell Tissue Res* **185**, 399-408.

Snow, M. H. (1983). A quantitative ultrastructural analysis of satellite cells in denervated fast and slow muscles of the mouse. *Anat Rec* **207**, 593-604.

Stefanelli, A. (1951). I fenomeni rigenerativi e degenerativi del midolo spinale caudale degli anfibi a dei rettili. *Boll. Zool.*

18, 279-290.

Suzuki, J., Yamazaki, Y., Li, G., Kaziro, Y. and Koide, H. (2000). Involvement of Ras and Ral in chemotactic migration of skeletal myoblasts. *Mol Cell Biol* **20**, 4658-65.

Suzuki, M., Angata, K., Nakayama, J. and Fukuda, M. (2003). Polysialic acid and mucin type o-glycans on the neural cell adhesion molecule differentially regulate myoblast fusion. *J Biol Chem* **278**, 49459-68.

Tajbakhsh, S., Vivarelli, E., Cusella-De Angelis, G., Rocancourt, D., Buckingham, M. and Cossu, G. (1994). A population of myogenic cells derived from the mouse neural tube. *Neuron* **13**, 813-21.

Tatsumi, R., Anderson, J. E., Nevoret, C. J., Halevy, O. and Allen, R. E. (1998). HGF/SF is present in normal adult skeletal muscle and is capable of activating satellite cells. *Dev Biol* **194**, 114-28.

Thomas, M., Lazic, S., Beazley, L. and Ziman, M. (2004). Expression profiles suggest a role for Pax7 in the establishment of tectal polarity and map refinement. *Exp. Brain Res.* **156**, 263-73.

Thompson, J., Lovicu, F. and Ziman, M. (2004). The role of Pax7 in determining the cytoarchitecture of the superior colliculus. *Dev. Growth Differ.* **46**, 213-8.

Tosh, D. and Slack, J. M. (2002). How cells change their phenotype. *Nat Rev Mol Cell Biol* **3**, 187-94.

Tschumi, P. A. (1957). The growth of the hindlimb bud of Xenopus laevis and its dependence upon the epidermis. *J Anat* **91**, 149-73.

Tucker, A. S. and Slack, J. M. W. (1995). The Xenopus laevis tail-forming region. *Development* **121**, 249-262.

Vallin, J., Thuret, R., Giacomello, E., Faraldo, M. M., Thiery, J. P. and Broders, F. (2001). Cloning and characterization of three Xenopus slug promoters reveal direct regulation by Lef/beta-catenin signaling. *J Biol Chem* **276**, 30350-8.

Wagers, A. J. and Conboy, I. M. (2005). Cellular and molecular signatures of muscle regeneration: current concepts and controversies in adult myogenesis. *Cell* **122**, 659-67.

Warren, G. L., Hulderman, T., Jensen, N., McKinstry, M., Mishra, M., Luster, M. I. and Simeonova, P. P. (2002). Physiological role of tumor necrosis factor alpha in traumatic muscle injury. *Faseb J* **16**, 1630-2.

Wokke, J. H., Van den Oord, C. J., Leppink, G. J. and Jennekens, F. G. (1989). Perisynaptic satellite cells in human external intercostal muscle: a quantitative and qualitative study. *Anat Rec* **223**, 174-80.

Yang, Q., Kong, Y., Rothermel, B., Garry, D. J., Bassel-Duby, R. and Williams, R. S. (2000). The winged-helix/forkhead protein myocyte nuclear factor beta (MNF-beta) forms a co-repressor complex with mammalian sin3B. *Biochem J* **345 Pt 2**, 335-43.

Zammit, P. S., Golding, J. P., Nagata, Y., Hudon, V., Partridge, T. A. and Beauchamp, J. R. (2004). Muscle satellite cells adopt divergent fates: a mechanism for self-renewal? *J Cell Biol* **166**, 347-57.

Ziman, M. R., Rodger, J., Chen, P., Papadimitriou, J. M., Dunlop, S. A. and Beazley, L. D. (2001). Pax genes in development and maturation of the vertebrate visual system: implications for optic nerve regeneration. *Histol. Histopathol.* **16**, 239-49.